

Aus dem Bereich Medizinische Biochemie und Molekularbiologie

Theoretische Medizin und Biowissenschaften

der Medizinischen Fakultät

der Universität des Saarlandes, Homburg/Saar

**Differential import of proteins across the mitochondrial  
inner membrane via the TIM23 Complex**

**Dissertation zur Erlangung des Grades einer Doktorin  
der**

**theoretischen Medizin**

**der Medizinischen Fakultät der**

**UNIVERSITÄT DES SAARLANDES**

2021

Vorgelegt von: Nilam Yadao

geb. am: 10.08.1987 in Chandrapur

## **Supervisor**

**Prof. Dr. Martin Van  
der Laan**

Center for Molecular Signaling  
(PZMS)

Medical Biochemistry &

Molecular Biology

Universität des Saarlandes

Germany

**Tag der mündlichen Prüfung: 06.07.2021**

**Dekan:** Univ.-Prof. Dr. M.D. Menger

**Prüfungsvorsitzender:** Univ.-Prof. Dr. Daniela Yildiz

**1. Berichterstatter:** Univ.-Prof. Dr. Martin van der Laan

**2. Berichterstatter:** Univ.-Prof. Dr. Barbara Anne Niemeyer-Hoth

# Contents

<b>I. Zusammenfassung</b> .....	<b>6</b>
<b>I. Summary</b> .....	<b>7</b>
<b>II. Introduction</b> .....	<b>8</b>
II.A. Mitochondrial architecture and function .....	8
II.B Biogenesis of mitochondrial precursor proteins .....	12
II.B.1 Mitochondrial precursor protein import pathways.....	15
II.B.2 The general import gate of the outer membrane, TOM complex .....	19
II.B.3 Presequence translocase complex, TIM23 complex .....	21
<b>III. AIM</b> .....	<b>28</b>
<b>IV. Material and Methods</b> .....	<b>29</b>
IV. A Yeast strains and media.....	29
IV.B Spot assay .....	30
IV.C Mitochondria isolation .....	30
IV.D. Steady-state level .....	32
IV.E Solubilization of membrane protein complexes .....	33
IV.F Preparation of Lysate .....	33
IV.G <i>In vitro</i> import experiments.....	34
<b>V. Result</b> .....	<b>38</b>
V.A Characterization of temperature sensitive mutants of Tim17 .....	38
V.B Differential import response of <i>tim17ts</i> mutant .....	43
V.C Conditional release of the laterally sorted precursor protein in <i>tim17ts</i> mutants.....	48
V.D Mgr2 rescues the translocation defect of <i>ts97B</i> mutant.....	51
V.E Absence of Mgr2 retards the lateral release of precursor protein .....	54
V.F Expression of Tim23 alters import precursor protein.....	60
<b>VI. Discussion</b> .....	<b>66</b>
<b>VII. References</b> .....	<b>72</b>
<b>VIII. Acknowledgments</b> .....	<b>82</b>
<b>IX. Curriculum Vitae</b> .....	<b>83</b>

## Abbreviations

$\Delta\psi$	Mitochondrial membrane potential
ADP	Adenosine-5'-diphosphate
ATP	Adenosine-5'-triphosphate
BN-PAGE	Blue native polyacrylamide gel electrophoresis
DHF	Dihydrofolate
DHFR	Dihydrofolate reductase
Hsp	Heat shock protein
IM	Inner membrane
IMP	Inner membrane mitochondrial peptidase
IMS	Intermembrane space
kD	Kilodalton
MIA	mitochondrial import and assembly machinery
MPP	Mitochondrial processing peptidase
MTX	Methotrexate
NADH	Nicotinamide adenine dinucleotide
NADPH	Nicotinamide adenine dinucleotide phosphate reduced form
OD	Optical density
OM	Outer membrane
PAM	Presequence translocase-associated motor
PBD	Presequence binding domain
PK	Proteinase K
SAM	Sorting and assembly machinery
SDS-PAGE	Sodium dodecylsulfate polyacrylamide gel electrophoresis
TM	Transmembrane
TOM	Translocase of the outer membrane
URA	Uracil
YPD	Yeast extract peptone dextrose
YPG	Yeast extract peptone glycerol

# I. Zusammenfassung

Mitochondriale Vorläuferproteine unterscheiden sich in ihrer Struktur, ihrem Ziel und ihrem Signal, was den Importprozess über Membranen durch Translokasekomplexe erleichtert. Der Translokasekomplex der äußeren und inneren Membran, TOM-TIM23 Complex, importiert Präsequenz- und Sortiersignale, die Vorläuferprotein tragen, in die Matrix und wird in die innere Membran integriert. Der Matriximport von Präsequenz tragendem Vorläuferprotein wird durch die Wechselwirkung von TIM23 Complex und Präsequenztranslokase-assoziiertem Importmotor (PAM) durchgeführt. Die Membraninsertion von hydrophoben Segmenten des Vorläuferproteins über den Stop-Transfer-Mechanismus wird durch die direkte physikalische Wechselwirkung von Mgr2 mit dem ankommenden Vorläuferprotein unterstützt. Verschiedene Studien konzentrieren sich auf die Biogenese, Substraterkennung und das Importverhalten des TIM23-Komplexes, während vergleichsweise weniger über die regulatorische Einheit Tim17 untersucht wird. Ortsspezifische Photovernetzungsdaten legen nahe, dass Tim17 und Mgr2 unterschiedlich mit hydrophilen und hydrophoben Vorläuferproteinsegmenten innerhalb des TIM23-Komplexes interagieren.

In dieser Studie werden temperaturempfindliche (ts) Tim17-Mutanten verwendet, um zu verstehen, wie Tim17 und Mgr2 bei der Decodierung von Sortiersignalen der inneren Membran und der Freisetzung von Vorläuferprotein in die Phospholipid-Doppelschicht zusammenarbeiten. In-vitro-Importversuche mit radioaktiv markierten Vorläuferproteinen werden verwendet, um das unterschiedliche Sortierverhalten von Tim17 zu beobachten. Die Studie zeigt, dass Tim17 zusammen mit Mgr2 an der lateralen Sortierung des Vorläuferproteins beteiligt ist. Das Mgr2 bietet Stabilität und rettet den Importdefekt von Tim17 und öffnet sich zusammen analog als Kanal zur inneren Membran nur für das hydrophobe Sortiersignal, das das Vorläuferprotein trägt.

Im zweiten Teil werden *cst6*-Mutanten verwendet, um die Importkinetik als Reaktion auf die Hochregulation von Tim23 zu beobachten. Das *cst6* ist einer der Transkriptionsfaktoren von Tim23, der eine Mutation aushält, um die allotrope Expression des mitochondrialen Gens ATP9 zu unterstützen. Es wird beobachtet, dass die Überexpression von Tim23 einen erhöhten Import von mitochondrialem Vorläuferprotein als Gewinn von Funktionsmutationen zeigt.

## I. Summary

Mitochondrial precursor proteins differ in their structure, destination and signal, which facilitates the import process across membranes through translocase complexes. The outer and inner membrane translocase complex, TOM-TIM23 complex imports presequence and sorting signal carrying precursor proteins into the matrix and integrated into the inner membrane, respectively. Matrix import of presequence carrying precursor proteins are performed by the interaction of TIM23 complex and presequence translocase-associated import motor (PAM). Membrane insertion of hydrophobic segments of the precursor proteins via stop-transfer mechanism is supported by the direct physical interaction of Mgr2 to the incoming precursor protein. Various studies are focused on the biogenesis, substrate recognition, import behavior, of the TIM23 complex, whereas comparatively less is explored about the regulatory unit, Tim17. Site-specific photo-crosslinking data suggest that Tim17 and Mgr2 differentially interact with hydrophilic and hydrophobic precursor protein segments within the TIM23 complex.

In this study, Tim17 temperature-sensitive (*ts*) mutants are used to understand how Tim17 and Mgr2 cooperate in the decoding of inner membrane sorting signals and the release of precursor proteins into the phospholipid bilayer. *In vitro* import experiments performed with radiolabelled precursor proteins are used to observe differential sorting behavior of Tim17. The study shows that Tim17 is involved in the lateral sorting of precursor proteins along with Mgr2. Mgr2 provides stability and rescues the import defect of Tim17 and together opens analogously as a channel towards the inner membrane only for hydrophobic sorting signal carrying precursor proteins.

In the second part, *cst6* mutants are used to observe import kinetics in response to upregulation of Tim23. The *cst6* is one of the transcriptional factors of Tim23, which endures mutation to support the allotropic expression of the mitochondrial gene, ATP9. It is observed that the overexpression of Tim23 displays increased import of mitochondrial precursor proteins as the gain of function mutations.

## **II. Introduction**

### **II.A. Mitochondrial architecture and function**

Various organelles present inside the cell represent its diverse nature and capability to manage multiple functions. A prominent and distinguishing feature between eukaryotic and prokaryotic cells is the presence and absence of cellular organelles, especially those with membrane-bound structures. In eukaryotic cells, mitochondria are one of the dual membrane-bound organelle (Ernster & Schatz, 1981). The morphological feature of mitochondria depends on cell type, tissue, and organism (Anderson et al., 2019). One of the first detailed analyses about the structure of mitochondria was performed using high-resolution electron micrographs in 1952, and mitochondrial architecture is intensively studied till date (Palade, 1953; Tucker & Park, 2019). The elementary architecture shows that it is a dual membrane-bound organelle where the inner membrane appears to be folded up in ridges. Dual membrane structure forms the basis to differentiate different compartments of mitochondria. First two compartments are the outer membrane (OM), inner membrane (IM) composed of proteins and phospholipid bilayer. The narrow separation space between these two membranes is termed the intermembrane space (IMS). Also, the inner membrane holds an enclosed space called matrix and has folded invaginations named cristae as illustrated in figure 1 (Frey et al., 2002; Lane, 2011).

The mitochondrial outer membrane is similar to the cellular membrane and represents a homogenous structure harboring lower composition of protein to phospholipid ratio (1.0-1.5  $\mu\text{g}/\mu\text{g}$ ) (Schenkel & Bakovic, 2014). It contains abundant integral membrane proteins known as porins which support increased permeability due to which diffusion of small molecules and ions occurs across the outer membrane (Weeber et al., 2002). Additionally, specialized translocase complexes made of  $\beta$ -barrel proteins, which span the outer membrane, are embedded into the outer



membrane for the import of mitochondrial proteins. The outer membrane is commonly associated with endoplasmic reticulum for calcium signaling and lipid transfer.

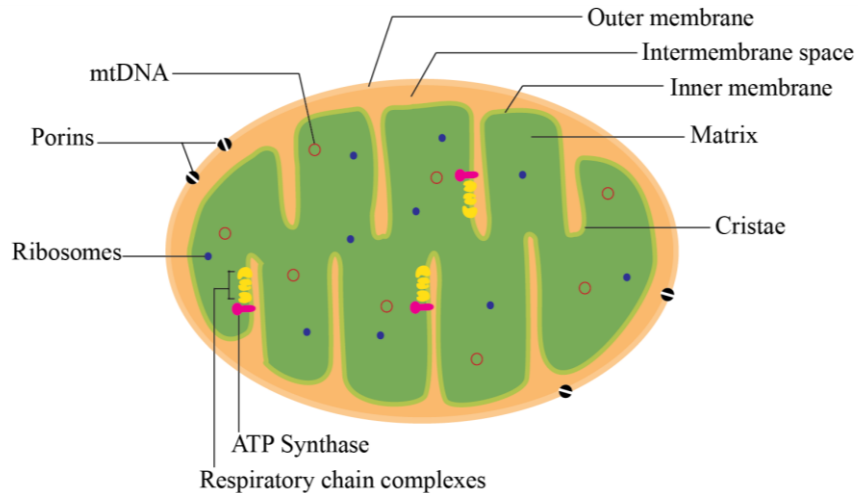


Figure 1: Illustration of Mitochondria: Different compartments of mitochondria and few components are labelled such as outer membrane (OM), inter-membrane space (IMS), inner membrane (IM), matrix, cristae. Mitochondrial few components such as porins, mitochondrial DNA (mtDNA), ribosomes, respiratory chain complexes and ATP Synthase.

Mitochondria, which lose their outer membrane are termed mitoplasts (Mejia & Hatch, 2016; Vander Heiden et al., 2000). Compared to any other compartment of mitochondria, the IMS is the thinnest section as it separates the outer membrane and inner membrane. The IMS region is porous similar to OM but maintains an oxidative environment (Bragoszewski et al., 2015). Most of the IMS proteins are found to have disulfide bridges and cysteine motifs. Special reductases reduce the disulfide bonds and reduced cysteine residues serve as a coordination site for metal ions. The IMS region has Mia40 and Erv1 as oxidoreductase and sulfhydryl oxidase respectively to insert disulfide bonds into IMS proteins. Comparatively, the inner membrane is equipped with higher amount of cardiolipin and phospholipid, which supports the integration of respiratory chain complexes and oxidative phosphorylation machinery responsible for an immense amount of ATP production. Permeability developed

across the inner membrane also favours maintenance of the electrochemical proton gradient generated by oxidative phosphorylation (Osman et al., 2011). The inner membrane covers a larger surface since it is folded into large membrane invaginations called cristae. The mitochondrial morphology is largely affected by the absence and presence of cristae. The respiratory chain supercomplexes are abundantly present in the folded cristae region, whereas the MICOS complex is present at the cristae junctions. In the inner membrane encloses the matrix, an aqueous compartment that contains many soluble enzymes, DNA, nucleotide factors, ribosomes, small organic molecules, and inorganic ions. Many processes such as citric acid or Krebs cycle take place in the matrix (Cogliati et al., 2016; Frey et al., 2002).

Mitochondria are often termed “powerhouse of cell”. The respiratory chain supercomplexes together make use of reduced substrate to remove electrons, which are transferred to oxygen. During this process, proton pumping from the mitochondrial matrix to intermembrane space takes place which produces a proton gradient across the inner membrane. The proton gradient is utilized to produce ATP by the ATP synthase (Kühlbrandt, 2015). Process of ATP production is highly valuable for cellular liability as its necessity for cellular metabolism could not be replaced. Mitochondria owns circular DNA (mtDNA), mutations of mtDNA could be collectively summarized to be factors associated with impaired function of the respiratory chain, which leads to an increment of reactive oxygen species (ROS) production. The generation of ROS is a vicious cyclic event increasing the possibility of cell dysfunction. Mitochondria possess an antioxidant system to handle the respiratory chain generated ROS, which compensates to endure any damage to the cellular or mitochondrial process (Brand et al., 2013). It is still a topic of debate about how functional decline of mitochondria leads to enhancement of ROS while ageing.

Mitochondria are involved in various functions such as biosynthesis of amino acids and lipids, iron-sulfur cluster, metabolism, signalling, and few other functions (Malina et al., 2018; Stehling & Lill, 2013). Mitochondria are not only restricted to ATP production, but also intracellular  $\text{Ca}^{2+}$  (Calcium) ions concentrations are regulated in a controlled manner. The endoplasmic reticulum is primarily known for storage of calcium, and mitochondria are one of the reservoirs for storage of intracellular calcium (Rizzuto et al., 2012). The presence of  $\text{Ca}^{2+}$  ions is found to be affecting a few

enzymes which are part of the citric acid cycle. The enzymes such as pyruvate dehydrogenase phosphatase, NAD<sup>+</sup> linked isocitrate dehydrogenase and 2-oxoglutarate dehydrogenase are involved in citric acid cycle and activated in the presence of Ca<sup>2+</sup> ions (Rutter & Denton, 1988). The calcium acquired by mitochondria helps in various ways, such as maintenance of calcium homeostasis, promoting apoptogenic factors either for cell death or mitosis. It is still under study about physiological role and relevance of Ca<sup>2+</sup> in mitochondrial metabolism (Britti et al., 2018; Duchen, 2000; Patergnani et al., 2011).

In recent times, mitochondrial protein synthesis, protein translocation, and protease mechanisms performed by membrane-embedded multi-subunit translocase channels are recognized as known hallmarks for cellular health and metabolism (Duchen, 2000; Jackson et al., 2018; Mackenzie & Payne, 2007). Mitochondrial mutation and functional impairment of such mitochondrial machinery are related to various metabolic disorders and neurodegenerative diseases. Quantitative proteomics study has identified few mitochondrial proteins (such as upregulation of TIMM17A protein) which serve as a diagnostic marker for cancer (De Paepe, 2012). In human mitochondria the TIM17 protein is encoded by two genes, TIMM17A and TIMM17B involved in the formation of translocase complex, TIM23. Similarly, biochemical studies focus on the understanding of mitochondrial involvement in apoptosis and it was shown that during apoptosis most of the mitochondrial intermembrane space proteins are released into the cytosol or nucleus (Rainbolt et al., 2013). Some of these proteins like Apoptosis-inducing factor (AIF); flavoprotein and Cytochrome c, are directly involved to activate cellular apoptosis (Sevrioukova, 2011). The balance between cellular metabolism and biogenesis of metabolic intermediates in mitochondria and various organelles within the cell serves as a marker for cell wellbeing.

Mitochondria are dynamic, encounter rapid changes even involving fusion and fission, which demands the support of proteases constantly to maintain a balance between nuclear and mitochondrial proteins. Mitochondria possess a variety of proteases which are part of the protein processing and largely involved in mitochondrial protein quality assurance. Depending upon the physiological relevance, mitochondrial proteases are categorized among which the most abundant is the

energy-dependent AAA proteases (Glynn, 2017). The proteases work efficiently and stringently while processing of protein. Mitochondrial protein homeostasis is an indicator of the cellular environment since the accumulation of misfolded protein in any compartment of mitochondria results in lower efficiency of protein import. The mistargeted or lower amount of imported mitochondrial protein could commence stress conditions, which could lead to mitochondrial destruction through mitophagy (Pickles et al., 2018; Saita et al., 2013). Together with proteases mitochondria are also well equipped with stress response factors to handle stress and cross-talk among other organelles. Many mitochondrial proteins are studied as a potential target for gene therapy. Mitochondrial deficiency and mutations are related to many severe pathophysiological disorders like autism, cardiac dysfunction, neurodegenerative diseases, and many more. Most of the mitochondrial disease models that are known to study neurodegenerative diseases and age-related diseases focus mostly on facts that if the causative factor is either related to respiratory complex or mitochondrial protein import dysfunction (Gao & Zhang, 2018; Guo et al., 2013; Johri & Beal, 2012). Few popular and most studied research topics across investigators are deficiency of mitochondrial respiratory chain complexes, destabilization of mitochondrial bioenergetics, membrane polarity, imbalance between the mitochondrial protein import and protease activity.

## **II.B Biogenesis of mitochondrial precursor proteins**

The endosymbiotic theory is widely accepted, highlighting the scientific background about the origin of mitochondria. The endosymbiotic theory elucidates that mitochondria are the decedents of ancient  $\alpha$ -proteobacteria. As per the theory, a primitive eukaryotic cell engulfed ancient  $\alpha$ -proteobacteria for the symbiotic association. The energy was utilized by the host eukaryotic cell for its cellular process in exchange for sanctuary and security to the engulfed  $\alpha$ -proteobacteria from the surrounding (Kurland & Andersson, 2000; Malina et al., 2018). During the evolution process, mitochondria became more centric to encode only essential genes on their mtDNA. Lack or destruction of any mitochondrial gene results in destabilized respiratory complexes and loss of mitochondrial DNA. The nuclear genome adopted

most of the mitochondrial genes that were transferred from mitochondrial DNA to nuclear DNA during evolution. The nuclear genome acclimated mitochondrial genes, which resemble interdependency relationship. For that reason, many mitochondrial proteins are similar or orthologs of the bacterial proteins in terms of their composition (Jaussi, 1995). The nuclear genome encodes more than 99% of mitochondrial proteins. These nuclear genes of mitochondrial origin are translated by the cytoplasmic ribosomes, and referred as mitochondrial precursor proteins. The distinct feature of precursor proteins is to carry a mitochondrial targeting signal (MTS) (Gray, 1989). Precursor proteins are distinguished as either cleavable or non-cleavable type. The cleavable type of precursor proteins maintains either single or multiple sites for cleavage.

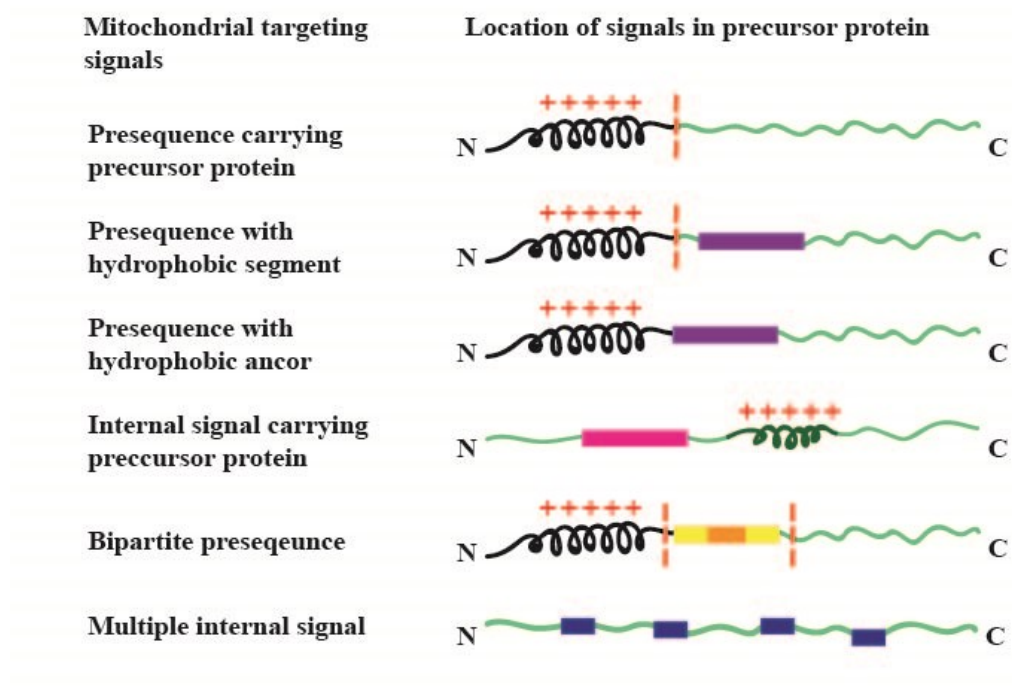


Figure 2: Mitochondrial precursor proteins: Nuclear encoded mitochondrial precursor proteins possess either cleavable (dashed vertical line) or non-cleavable signal serving as mitochondrial targeting signal. The precursor proteins with presequence (positively charged amino acids at N terminus (+)) could also possess both cleavable or non-cleavable hydrophobic segments and bipartite presequences. Few precursor proteins have either single internal signal or multiple non-cleavable signals, which are part of mature protein.

Depending upon the site-specificity, clipping of the precursor protein is performed by specific processing peptidases and mitochondrial proteases (Baker et al., 2012). The most ordinarily known cleavable type of precursor protein is the one, which carries the presequence generally towards the N-terminal end. There could be variability in the size of presequence. Usually, it is made of 10-80 amino acids. Presequence carrying precursor proteins could possess positively charged, hydrophobic, and hydroxylated amino acids. The fundamental feature of presequence is to form amphipathic  $\alpha$ -helices, which represent one positively charged surface and other as hydrophobic surface (Pfanner, 2000; Pfanner & Wiedemann, 2002). In most cases, the presequence is followed by a cleavable hydrophobic segment for some inner membrane proteins. A few outer membrane precursor proteins have presequence anchored with non-cleavable hydrophobic segment (Dudek et al., 2013). The second most common precursor proteins are the one that lacks cleavable sequence. Instead, the non-cleavable sequence is part of the mature protein and serves as internal signal for the import of the precursor protein. There are also other types of sequences such as bipartite presequence, and multiple internal non-cleavable signals which are distributed across the precursor protein and cooperate for efficient targeting (Bragoszewski et al., 2015; Lister et al., 2005; Pfanner & Geissler, 2001).

Mitochondrial precursor proteins follow multiple sets of modes and prerequisite for its import into and across mitochondrial membranes. Newly synthesized mitochondrial precursor proteins are imported into mitochondria by two different mechanisms, co-translational and post-translational import mechanism. In the co-translational mechanism, cytosolic ribosomes are bound to the mitochondrial surface to be closely associated with the translocase complexes (Bykov et al., 2020). The precursor proteins are synthesized in a close environment and transported across the mitochondrial outer membrane, while cytosolic ribosomes are still connected (Pfanner et al., 1997; Verner, 1993). Due to experimental limitations, it is suspected that the co-translational mechanism would transport only a few mitochondrial precursor proteins. The most common mechanism observed for the import of mitochondrial precursor protein is the post-translational mechanism. In this mechanism, cytosolic chaperones bind to the newly synthesized mitochondrial precursor protein by the cyclic exchange of ATP to ADP. The purpose of cytosolic chaperones is to protect the precursor protein from unwanted aggregation and improper folding in the cytosol (Neupert, 1997;

Straub et al., 2016). Cytosolic chaperons (Hsp70 and Hsp90) assist newly synthesized precursor proteins in docking at the receptor sites of the translocase of outer membrane (TOM) complex (Opaliński et al., 2018). Receptor sites are involved in early-stage recognition of precursor protein to promote import across mitochondrial membranes.

## **II.B.1 Mitochondrial precursor protein import pathways**

One of the crucial features followed by the mitochondrial precursor proteins while import across the membranes is to maintain their linear form or partially unfolded form to pass through the translocase complexes (Randall, 1990). Depending upon the type of signal carried by the precursor protein, distinct import pathways are followed as mentioned in table (1). There are only five import pathways known to date, which are highly dynamic and involve different translocase complexes in a coordinated fashion. The TOM complex is preeminent and serves as the general import pore for all the five observed import pathways till now. The small TIM proteins present in the IMS act as aid while import of precursor protein from the TOM complex to another translocase complex (Wiedemann et al., 2006). The small TIM complex is made up of Tim9, Tim10, which are the main soluble form, and along with Tim12, the small TIM chaperons form a hexameric chaperon complex. The small TIM complex is ATP independent but perform a similar role as cytosolic chaperons (Koehler et al., 1999; Petrakis et al., 2009). They bind to the multi-spanning hydrophobic precursor proteins, also called carrier proteins, to prevent unwanted aggregation and misfolding in the aqueous IMS phase. These small TIM chaperons are directly recruited for direct transfer of precursor protein either to the SAM complex or TIM22 complex (Weinhäupl et al., 2020).

The carrier pathway and  $\beta$ -barrel pathway utilize small TIM chaperons. The outer membrane precursor proteins are assembled into an oligomeric complex via  $\beta$ -barrel pathway. The TOM and SAM complex are involved in this pathway favoured by Tom22 protein of the TOM complex and Sam37 protein of the SAM complex. Precursor proteins with transmembrane  $\beta$ -barrel topology are processed (Zeth, 2010).

The role of the small TIM chaperone in this pathway is only to deliver the precursor protein from the IMS end of Tom40 to the SAM complex.

Type of precursor protein	Translocase complex involved	Type of pathway
$\beta$ -barrel precursor protein	SAM	$\beta$ -barrel pathway
Precursor protein with Cysteine motifs	MIA	Mitochondrial intermembrane space assembly
Precursor of metabolite carrier protein	TIM22	Carrier pathway
Cleavable Presequence	TIM23-PAM	Presequence pathway
Hydrophobic stop-transfer signal	TIM23	Lateral sorting pathway

Table 1: Different types of import pathways which are carried out by various translocase complexes of the mitochondria. The assembly of complexes is dependent upon the type of precursor protein. The general import pore embedded in the outer membrane, TOM complex remains common partner of other translocase complexes for all the mentioned pathway.

The SAM complex folds  $\beta$ -barrel proteins and then releases them into the lipid phase of the outer membrane (Stojanovski et al., 2007; Taylor & Pfanner, 2004). The precursor proteins, which possess multiple targeting signals, are quite hydrophobic; hence they are also assisted by the small TIM proteins. These types of precursor proteins are generally metabolite carrier proteins imported via the Carrier pathway in membrane potential depended manner. In this pathway, when the precursor protein arrives at the IMS side, Tom40 recruits the small TIM proteins, which help in recognition and import of metabolite carrier proteins to the TIM22 complex (Mokranjac et al., 2005; Rampelt et al., 2020; Wagner et al., 2008). Precursor proteins enter Tim22, the pore forming subunit of the TIM22 complex and are subsequently laterally released into the inner membrane (Murphy et al., 2001).



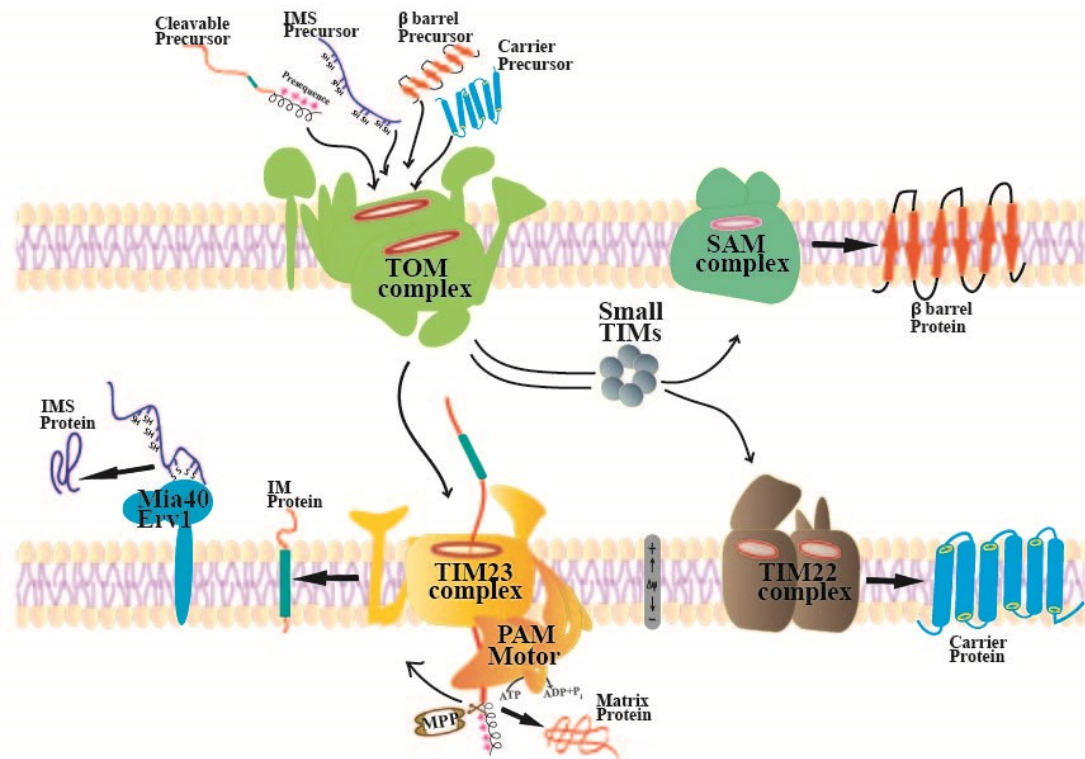


Figure 3: Mitochondrial precursor proteins contain cleavable or non-cleavable signal sequences, which are recognized by different membrane-embedded translocase complex. Different pathways are followed by the precursor protein depending upon destination and type of precursor protein. The mitochondrial translocase of the outer membrane (TOM) is involved in 5 different types of import pathway laboring as general import pore. The precursor of metabolite carrier proteins and  $\beta$ -barrel precursor proteins are assisted by mitochondrial chaperons (small TIMs). The TIM22 complex recognizes internal signals such as non-cleavable hydrophobic segments of metabolite carrier precursor proteins and inserts them into the inner membrane via the so called carrier pathway. The  $\beta$ -barrel precursor proteins follow the  $\beta$ -barrel pathway and are sorted and assembled into the outer membrane via the sorting and assembly machinery (SAM) along with the TOM complex. The precursor proteins containing specific cysteine residues when imported to the IMS side of the TOM complex are first identified and then with the help of Mia40 and Erv1 disulfide bonds are formed at the sites of cysteine residues due to which these precursor proteins are released into the intermembrane space via the mitochondrial intermembrane space assembly (MIA) pathway. The cleavable presequence carrying precursor proteins are imported into the matrix via the presequence pathway. In this pathway, presequence translocase-associated motor (PAM) binds to the TIM23 complex and pulls the precursor protein towards the matrix by cyclic hydrolysis of

ATP. The presequence is cleaved by mitochondrial processing peptidase (MPP) upon arrival towards matrix. The PAM complex dissociates from the TIM23 complex if precursor proteins with presequence are followed by hydrophobic stop-transfer signal and further TIM23 complex is assisted with Tim21 and Mgr2 to laterally release the precursor protein across inner membrane via the lateral sorting pathway. The membrane potential across the inner membrane induces electrophoretic effect to drive import conducted by the TIM23 and TIM22 complexes.

Few precursor proteins such as IMS precursor proteins or presequence carrying precursor protein do not use small TIM proteins. They instead directly establish contact with the TOM complex as prerequisite for import of precursor protein. When the precursor protein with characteristic cysteine motifs arrive at the IMS side, Tom40 is directly assisted by the mitochondrial import and assembly (MIA) machinery present in the intermembrane space (Banci et al., 2009; Koch & Schmid, 2014). The interaction between the precursor protein and MIA machinery is based upon hydrophobic interactions and transient intermolecular disulfide bonds. The imported precursor proteins towards the IMS side are oxidized by Mia40, which is re-oxidized by Erv1. Erv1 is essential for respiration and vegetative growth assisted by zinc-binding protein (Hot13). In this pathway, electrons generated while oxidation of cysteine carrying precursor protein and Mia40 are transferred to cytochrome c of the respiratory chain complex (Koch & Schmid, 2014; Ramesh et al., 2016). The TOM and TIM23 complexes are involved in 2 different import pathways for import of 2 types of precursor protein. There are at least 2 standard features while import of presequence carrying precursor protein and hydrophobic precursor protein. First, the precursor protein is in contact with Tom40 and Tom22 when it arrives towards the IMS side and recognized by Tim50. Second, Tim50 as part of the TIM23 complex displaces the precursor protein towards the TIM23 translocase pore. In the TIM23 complex, Tim17 and Tim23 are closely associated forming translocase pore (Bohnert et al., 2007; Straub et al., 2016). Further, the insertion of precursor protein into the TIM23 complex is due to membrane potential across the inner membrane, which generates the electrophoretic effect on positively charged amino acids of the precursor protein (Sato et al., 2019). Then subsequently, precursor protein is pulled towards matrix by ATP hydrolysis performed by the presequence translocase associated protein import motor, PAM complex (S. Ting et al., 2014). The PAM complex is a multi-subunit

machinery involved only in import of presequence carrying matrix targeted protein. Further, the presequence is clipped by mitochondrial processing peptidase (MPP) followed by other proteases to remove destabilizing N terminal amino residues. The folding of imported and clipped precursor proteins is performed by mitochondrial chaperons (Hsp60 and Hsp10) (van der Laan et al., 2010). The PAM complex is released from the TIM23 complex when an internal hydrophobic signal is embedded within precursor protein. The TIM23 complex along with Tim21 and Mgr2 are involved in lateral sorting of precursor protein across the inner membrane. The inner membrane peptidase (IMP) clips the sorting signal before the precursor protein is released into the IMS region (Bolender et al., 2008; Pfanner, 2000; Stojanovski et al., 2014). The participation of various translocase complexes are still studied, considering there is a lot more to learn.

## **II.B.2 The general import gate of the outer membrane, TOM complex**

The mitochondrial translocase complexes are generally multi-subunit molecular machineries located in every mitochondrial compartment. In the outer membrane, channels such as voltage-dependent anion channels (VDACs) are also present. It is the primary transporter of nucleotides, ions, and metabolites. The VDAC channel spans the outer membrane of the mitochondria similar to that of antiparallel  $\beta$ -strands (outer membrane  $\beta$ -barrels) present in gram-negative bacteria (Colombini et al., 1996; Zeth, 2010). One such multi-subunit machinery known to be required for its own biogenesis is the TOM complex. The illustration of the TOM complex is shown in figure 4, it is made up of Tom20, Tom22, Tom70, Tom40, and small TOM subunits such as Tom5, Tom6, and Tom7 (Model et al., 2002). All TOM components except Tom40 have single transmembrane segments and do not hold sequence similarity (Ahting et al., 2001). Few components that are Tom20 and Tom70 have receptor sites revealed towards cytosol. These receptor sites actively participate in recognition and docking of mitochondrial precursor proteins (Straub et al., 2016).

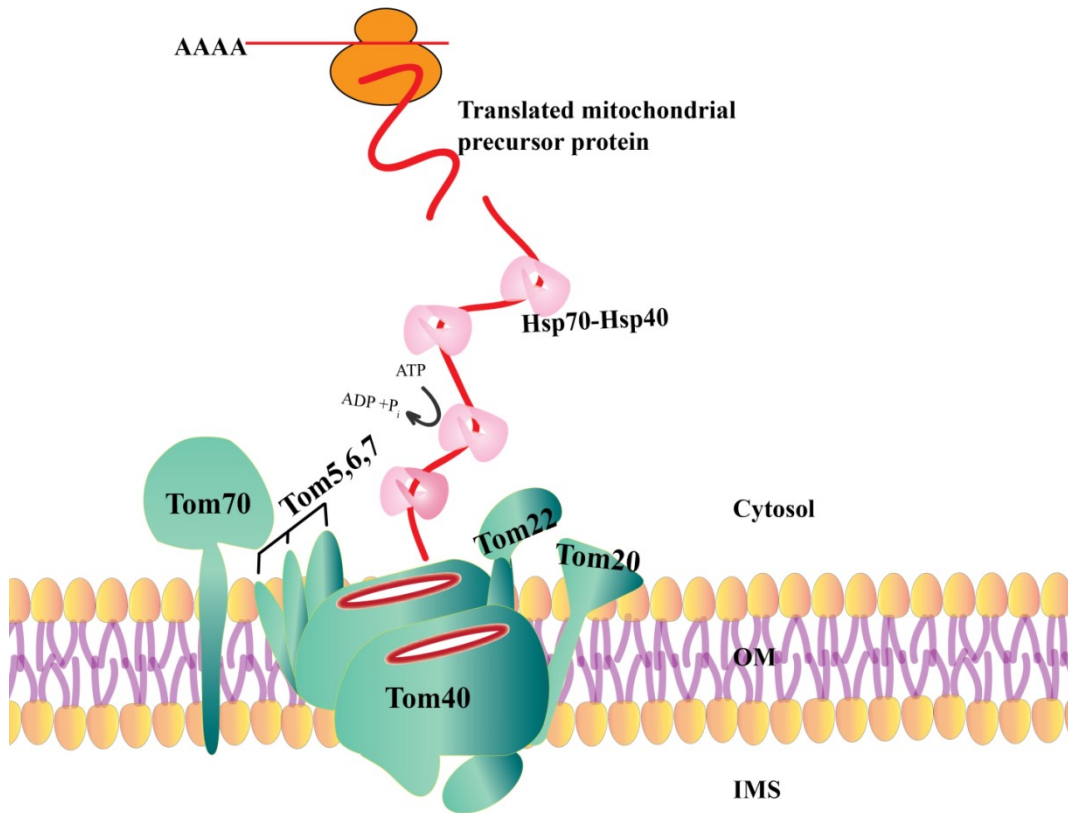


Figure 4: The newly synthesized mitochondrial precursor protein could be imported either by co-translational or post translational. The cytosolic chaperones (Hsp70 and Hsp40) binds and through hydrolysis of ATP, they import the mitochondrial precursor proteins towards the translocase of the outer membrane (TOM complex). The TOM complex contains three cytosolic faced receptor units, Tom22, Tom20 and Tom70 involved in recognition and transfer of precursor protein to the central pore. The Tom40 forms central dual protein conducting pore performing import of various types of precursor protein across the outer membrane. Few small sub units, Tom5, Tom6 and Tom7 of the TOM complex support stability of the TOM complex. OM, outer membrane; IMS intermembrane space.

Tom20 and Tom70 are peripheral TOM components known as primary receptor units of the TOM complex. Tom20 is involved in recognizing N-terminal positive charged sequences, whereas precursor proteins with internal targeting sequences are anchored at the Tom70 receptor site. Both types of acquired precursor proteins by Tom20 and Tom70 are transferred to Tom22, which acts as a central receptor (Stan, 2000). The substrate specificity of Tom20, Tom22, and Tom70 is

overlapping; hence they could easily substitute each other. Individual deletion of either Tom20 or Tom70 does not affect the viability of yeast. In yeast, double deletion of Tom20 and Tom70 cannot be achieved and to rescue such kind of growth defect of yeast, overproduction of Tom22 is required (Brix et al., 1999; Yamano et al., 2008).

On the IMS side, Tom22 interacts with another translocase complex (TIM23 complex) as a prerequisite for the transfer of precursor proteins (Pfanner & Meijer, 1997). In the absence of Tom22, dimers of Tom40 proteins are formed. Upon the association of Tom22, Tom40 is oriented in the form of dual pore channel (Tucker & Park, 2019). The Tom40 protein belongs to the superfamily of  $\beta$ -barrel protein and with 19 transmembrane sheet segments. It forms two different regions inside the pore, hydrophilic and hydrophobic, which provide specificity to the precursor protein. The hydrophobic carrier proteins interact with the hydrophobic pore of Tom40, and import of matrix proteins is carried out by the hydrophilic pore (Bausewein et al., 2017; Frey et al., 2002). The presence of small TOM subunits is speculated to promote the assembly and stability of the TOM complex. However, any specific role is unknown, as they are non-essential (Ahting et al., 1999; Rapaport, 2005).

### **II.B.3 Presequence translocase complex, TIM23 complex**

The mitochondrial inner membrane is equipped with more diverse translocase complexes compared to the outer membrane. One such translocase complex is the TIM23 complex, which is involved in 2 different import mechanisms that import presequence carrying precursor proteins and hydrophobic stop-transfer signal carrying precursor proteins. Precursor proteins with a presequence are matrix targeted, and hydrophobic signal carrying precursor proteins are laterally sorted into the inner membrane (Koehler, 2000; Wiedemann & Pfanner, 2017). Depending on the signal carried by the precursor protein, the TIM23 complex shifts dynamically between 2 different forms, TIM23<sup>CORE</sup> and TIM23<sup>SORT</sup> (Chacinska et al., 2010; Straub et al., 2016). Import of matrix targeted precursor proteins are performed by forming TIM23<sup>CORE</sup> form in association with the PAM complex. The TIM23<sup>SORT</sup> form is aided by Mgr2 and Tim21, due to which the PAM complex dissociates from the TIM23 complex

(Chacinska et al., 2005; Pfanner et al., 2019). The core components of the TIM23 complex are Tim17, Tim23, and Tim50 proteins, as shown in figure 7.

The Tim50 protein is an essential part of the TIM23 complex made up of a single transmembrane segment anchored in the inner membrane. It supports maintain a permeability barrier across the inner membrane (Mokranjac et al., 2003). Tim50 has a large exposed domain towards the IMS, divided into two parts as the presequence binding domain (PBD) and core domain. The specific role of both domains is still studied. It is observed that PBD and core domain interacts with incoming precursor proteins to support the function of Tim50 protein (Weinhäupl et al., 2018). Mostly the PBD domain acts as one of the initial contact site for the mitochondrial precursor protein. The PBD domain also interacts with the IMS exposed domain of Tom22. Hence collectively, Tim50 is one of the first TIM23 complex component to establish contact with the mitochondrial precursor protein, which arrives towards IMS (Chacinska et al., 2003; Dayan et al., 2019). The function of Tim50 is to induce a gating effect that activates the TIM23 complex only when a specific contact with an incoming precursor protein is established (Straub et al., 2016). It is evident from many experiments that were performed to observe the import function of the TIM23 complex that the Tim50 protein recognizes both the precursor proteins (either a presequence carrying precursor protein or internal signal carrying precursor protein) with similar affinity (Pareek et al., 2013). It is speculated that primary recognition of these two types of precursor proteins performed by Tim50 would be principally involved in indicating or adjusting the TIM23 complex either as TIM23<sup>CORE</sup> or TIM23<sup>SORT</sup> form. In the absence of Tim50, the mitochondrial precursor proteins remain attached to the IMS exposed domain of Tom22, and the TIM23 complex remains at a dormant state. Mutations in Tim50 results in reduced binding efficiency with precursor protein and destabilization of the TIM23 complex (Bohnert et al., 2007; Wurm & Jakobs, 2006). Tim23 and Tim17 proteins are essential, integral membrane proteins, with Tim23 being the principal translocase pore-forming subunit, and Tim17 is necessary for stabilization of the translocation channel (S. Y. Ting et al., 2014). Experimental strategies that focus on learning about the assembly and formation of the TIM23 complex suggest that the Tim23 precursor protein is imported via the TIM22 complex and assembles in the inner membrane whereas the import and assembly mechanism by which Tim17 forms a stabilizing unit of TIM23 complex remains unclear.

It is known that together, Tim23 and Tim17 are involved in two different pathways for import of precursor proteins since mutations in either of them affect import of precursor proteins across the inner membrane and towards matrix. The Tim23 and Tim17 proteins are made 4 transmembrane segments (TM1, TM2, TM3 and T;4) due to shared homology connected by loops exposed either towards matrix or IMS as shown in figure 6 transmembrane segments span across the inner membrane, forming TIM23 complex. Various mutants generated by single or double amino acid substitution are used to study the individual roles of Tim23 and Tim17. The majority of mutations bearing double amino acid substitution results in no viable yeast cells. It is found that TM1 and TM2 of the Tim23 protein are involved in early substrate capture in the complex. TM2 recruits Tim17 to serve as a stability factor for forming the complex (Bauer et al., 1998; Demishtein-zohary et al., 2015). The structure of TIM23 complex is not yet known. However, several independent studies have helped in predicting the most relevant structure of the TIM23 complex best to fit its orientation and interactions with other constituents.

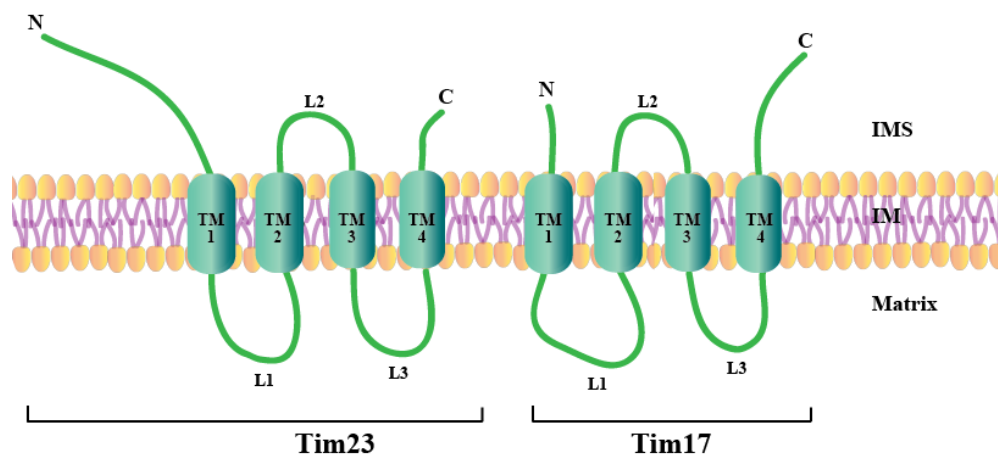


Figure 5: Model illustrating transmembrane (TM) helices of Tim17 and Tim23, essential components of the TIM23 complex. The four homologous TM segments of Tim17 and Tim23 are embedded into the inner membrane (IM) with connecting loops, L1 and L3, exposed towards the matrix and L2 towards intermembrane space (IMS). The TM segments of Tim23 forms the central protein import conducting pore of the TIM23 complex, whereas destabilized complex is observed if mutations are made in TM segments of Tim17. The N and C terminal domain of Tim23 and Tim17 are of variable length.

It is observed that the TIM23 complex has a heterotetrameric form by dissecting and studying the role of each TM segment and connecting loops of the Tim23 and Tim17 protein (Potting et al., 2018; Wrobel et al., 2016). It is known that the N-terminus of Tim23, which is exposed towards the IMS, interacts with the PBD domain of Tim50 to function cooperatively for the recognition and transfer of mitochondrial precursor proteins into the main translocase conducting pore of the TIM23 complex (Pfanner & Geissler, 2001). Mutants of TM1 and TM2 of Tim23 showed various defects affecting precursor proteins import, assembly of the TIM23 complex, and membrane polarity. These defects were rescued by the over-expression of the Tim17 gene (Wrobel et al., 2016; Yano et al., 2014). The mutations in TM1 and TM2 of Tim17 result in a destabilized interaction with Tim23, and a mutation in TM3 shows less binding efficiency with the PAM complex (Chacinska et al., 2005).

### **II.3.4 Alliance of the TIM23 complex**

The TIM23 and PAM complex associate together to perform the presequence pathway. The membrane potential drives the import of the precursor protein across the inner membrane and entering of TIM23 complex by the positively charged amino acids at the preproteins N-terminus (Neupert & Herrmann, 2007). Further, the PAM complex provides a significant motive force that drives the precursor protein import towards the matrix. The PAM complex is a multi-subunit machinery assembled to perform a Brownian ratchet mechanism powered by hydrolysis of ATP as an energy source. So it is often termed as PAM motor (Kulawiak et al., 2013; Schmidt et al., 2010). The PAM complex is made of mtHsp70, Tim44, Pam18, Pam16, Pam17, and Mge1, as shown in figure 7. The mitochondrial heat shock protein (mtHsp70) is a chaperone forming the PAM complex's core component. It is known to be involved in the process of import and folding of the precursor proteins. It physically interacts with the TIM23 complex and tightly binds to the unfolded precursor protein with its peptide domain (Craig, 2018; Moro et al., 2002). It interacts with the precursor proteins by trapping and pulling towards a matrix driven by ATP binding and hydrolysis. Mostly photoactivatable cross-linking experiments are performed to know about interactions



between TIM23 complex and PAM complex (Jensen & Johnson, 1999; Y. Li et al., 2004). It is found that that the matrix exposed loop (Loop1) between TM1 and TM2 of the Tim23 protein interacts with the Tim44 protein. Such interactions strengthen the motor system for other PAM components binding (Schendzielorz et al., 2017; Schiller et al., 2008). Tim44 is an essential peripheral inner membrane protein of the PAM complex found to be evolutionary conserved. Various experiments that used mutants of Tim44 and truncated forms of Tim44 showed that the N-terminus of Tim44 is involved in the interaction with mtHsp70, Pam16, and the TIM23 complex (Wiedemann & Pfanner, 2017).

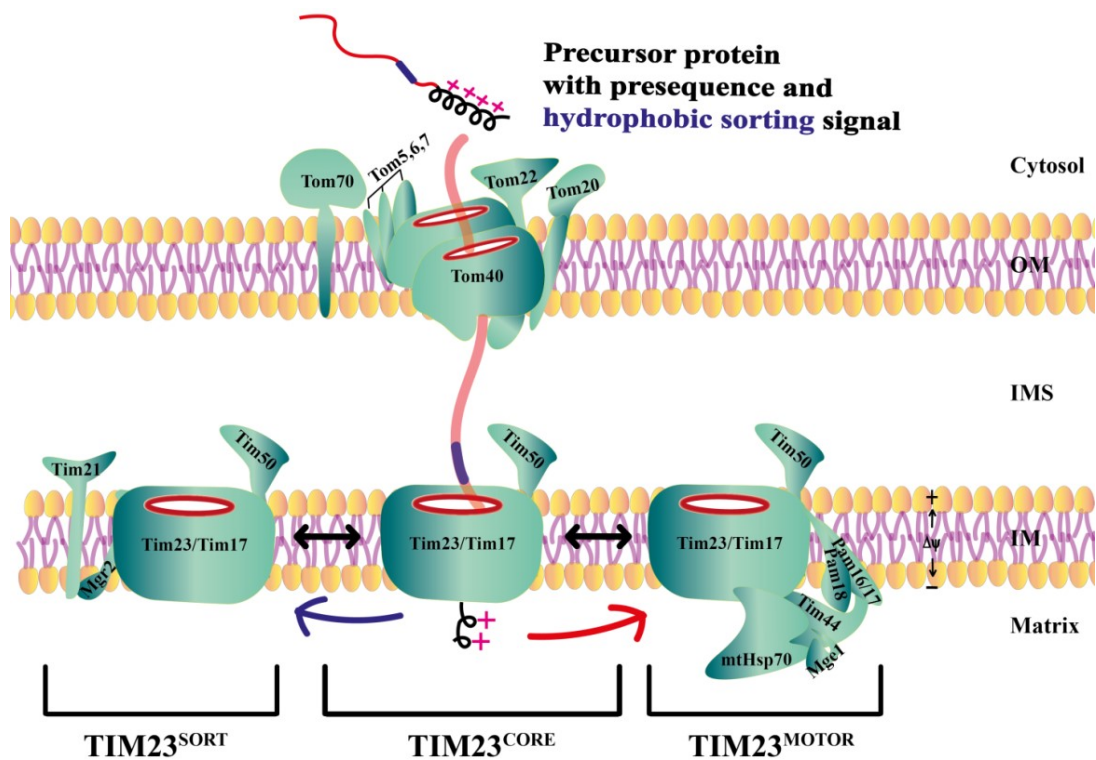


Figure 6: Overview of distinct forms of the TIM23 complex. Precursor proteins with a cleavable presequence followed by an internal hydrophobic segment are recognized by the cytosolic exposed Tom20 and Tom22 receptors of the TOM complex and transferred to Tom40, central import conducting pore across the outer membrane. The TIM23<sup>CORE</sup> and TOM complex interaction is a prerequisite for transferring precursor proteins, whereas TIM23<sup>CORE</sup> maintains a dynamic interaction with the presequence translocase-Associated motor (PAM). The TIM23<sup>CORE</sup> machinery has Tim50 as receptor unit, Tim23 as central import conducting pore, and Tim17 as a regulatory unit. The binding of the PAM complex forms the TIM23<sup>MOTOR</sup> form, and dissociation of the PAM complex is complemented with the assistance of Tim21 and

Mgr2 to form TIM23<sup>SORT</sup> form. TOM, translocase of the outer membrane; OM, outer membrane; IMS, intermembrane space; IM, inner membrane;  $\Delta\psi$ , membrane potential.

Tim44 ensures that all subunits of the PAM complex function in a coordinated manner for pulling the precursor protein except for Pam17. The Pam17 protein is known to interact with Tim17. It is not an essential component of the PAM complex, but its absence results in an import defect for matrix targeted precursor proteins. It also serves as a stability factor for the Pam18 and Pam16 proteins (Miyata et al., 2017; M. van der Laan et al., 2005). Pam18 and Pam16 are two membrane-bound chaperons with J-protein domain and act as stimulatory and regulatory components of the PAM complex. Pam18 is the stimulatory protein that stimulates the ATPase activity of mtHsp70, whereas Pam16 is a regulatory protein that controls the activity of Pam18 (Frazier et al., 2004; Rampelt et al., 2020). The PAM complex is equipped with Mge1, a nucleotide exchange factor to perform hydrolysis of ATP to ADP while mtHSP70 pulls the presequence carrying precursor protein towards the matrix (Allu et al., 2015). Once Mge1 releases ADP from the mtHsp70, a new round of reaction cycle takes place. This cyclic event continues until the mitochondrial precursor protein is fully pulled into the matrix.

The internal (hydrophobic) signal embedded in the presequence carrying precursor protein induces a dynamic shift of the TIM23<sup>CORE</sup> form to the TIM23<sup>SORT</sup> form with the equally combined effect of binding and release of the PAM complex with the TIM23 complex (Chacinska et al., 2010; Straub et al., 2016). The TIM23<sup>SORT</sup> form of the TIM23 complex is generated by 2 accessory proteins, which are Mgr2 and Tim21, as shown in figure 1. Mgr2 is a non-essential, small hydrophobic protein, commonly known as lateral gatekeeper. Our group discovered it in 2014 and found that it is required to couple Tim21 with the TIM23 complex (Gebert et al., 2012). The Mgr2 protein shows a higher interaction rate towards the positively charged cluster of amino acids. The cluster of amino acids that proceed the hydrophobic amino acids, due to which the precursor protein is halted (stopped) for a while inside the TIM23 complex and then slowly released (transferred) into the inner membrane as the stop-transfer mechanism. In the case of a defective or compromised hydrophobic signal, the precursor protein is by default imported into the matrix, which shows that the

presence of Mgr2 employs a quality control function. In the absence of Mgr2, the precursor protein is released at a higher rate into the inner membrane (Ieva et al., 2014; Mirzalieva et al., 2019; Schendzielorz et al., 2018; Steffen & Koehler, 2014). The second accessory protein of the TIM23<sup>SORT</sup> form is Tim21. There are two characteristics of Tim21. First, it binds to the IMS domain of the Tom22 protein generating the TOM-TIM23 supercomplex. The formation of the TOM-TIM23 supercomplex is not to initiate any import pathway (Kulawiak et al., 2013; Wiedemann et al., 2007). It is a kind of interaction between TOM and TIM23 complex for the displacement of the precursor protein into the translocation pore of Tim23, which shows a gradual decrease of accumulation precursor protein over the TIM23 complex; hence it acts as an antagonist of Tim50. The antagonist feature of Tim21 promotes dissociation of the PAM complex (Kang et al., 2016; Murcha et al., 2012). Second, the Tim21 protein supports the membrane potential across the inner membrane by associating the TIM23 complex closer to the proton-pumping respiratory chain complexes to promote lateral sorting of precursor protein across the inner membrane (Banerjee et al., 2015; Gustafsson et al., 2016; Jornayvaz, 2014). The respiratory chain complexes generate membrane potential essential for ATP production and import of precursor protein across inner membrane by the mitochondrial ATP synthase.

### III. AIM

Import defects of matrix targeted precursor proteins and laterally sorted precursor protein were first observed by Prof. Agnieszka Chacinska and her group while studying the generation of 2 different forms of the TIM23 complex. Their observation supported that Tim17 is crucial for recruiting the PAM complex and sorting of precursor protein with hydrophobic signals across the inner membrane. It is already known that overexpression of Tim17 rescues inner membrane depolarization and import defects of the TIM23 complex; nevertheless, the principal role of Tim17 is unclear. Recently our lab has shown that the Mgr2 protein is involved in lateral sorting of precursor protein into the membrane. The interaction of Tim17 and Mgr2 is also highlighted, which suggests Tim17 might be an active participant in the recognition of precursor proteins and the import process.

I wanted to understand the engagement of Tim17 during the import of different precursor proteins. In this study, I have used temperature-sensitive (*ts*) mutants of Tim17, *ts97B*, and *ts98B* to understand the import of different precursor proteins. The precursor proteins, which possess hydrophobic stop-transfer signals, and matrix targeted precursor proteins are employed to understand the import behavior. The different form (intermediate and mature) of the precursor protein generated while *in vitro* import of radiolabeled cytochrome *b<sub>2</sub>* constructs were used to study the import response. In contrast, the binding efficiency of the PAM complex to the precursor protein is also studied. Previously our group has observed that Mgr2 functions as a lateral gatekeeper, and its overexpression delays lateral sorting of hydrophobic precursor protein across the inner membrane. I wanted to observe if the deletion of Mgr2 in *tim17ts* mutants affects Tim17 performance. I have used this approach to know how Tim17 and Mgr2 cooperate to release the precursor protein into the inner membrane. In the second part of this study, I wanted to observe if point mutation (G267C) of *cst6*, one of the transcriptional factors of the Tim23 protein, could induce alterations in the expression of different translocase complex proteins. The overexpression of the Tim23 gene aims to understand the gain of function as an increased import of matrix targeted precursor protein and few translocase complex proteins of TOM and PAM complex while allotropic expression of Atp9.

## IV. Material and Methods

### IV. A Yeast strains and media

The Wild Type strain (WT), *Saccharomyces cerevisiae* YPH499 (*genotype: MATa ura3-52 lys2-801\_amber ade2-101\_ochre trp1-Δ63 his3-Δ200 leu2-Δ1*) was used. In the WT, a vector plasmid pFL39 (CEN\_TRP1) expressing a non-mutated Tim17 gene was introduced to complement the chromosomal deletion of Tim17::ADE2. Similarly, the *tim17ts* mutants carry plasmid with mutation introduced by random mutagenesis for targeted Tim17 gene to complement the chromosomal deletion of Tim17::ADE2. The Tim17WT, *ts97B* and *ts98B* were generated by Dr. Bernard Guiard (Centre de Génétique Moléculaire, Center National de la Recherche Scientifique, Gif-Sur-Yvette, France). The media used to grow the Tim17WT, *ts97B* and *ts98B* is 1% bacto yeast extract, 2% bacto peptone, 3% glycerol (YPG). The pRS426 vector plasmid with pPGK promoter was used for overexpression of MGR2 (MGR2<sup>↑</sup>), and growth was supported by 0.66% bacto yeast nitrogen base, 2% peptone, 0.2% glucose, 3% glycerol and 0.192% Ura drop out mix (-URA media). Deletion of Mgr2 ( $\Delta mgr2$ , MGR2::URA) in *ts98B* mutant was performed by homologous recombination using URA cassette. The Tim17WT $\Delta mgr2$ , *ts98B* $\Delta mgr2$  were grown in YPG media. The strains of *cst6* mutants were provided from Prof. Jean paul di Rago lab, the nuclear genome of *cst6-1* carries point mutation (G276C) identified by Whole-genome transcription profiling and same mutation in *cst6-2* was introduced by CRISPR/Cas9 technique. The *cst6* mutants were grown in YPG medium. The yeast strains were freshly streaked from glycerol stocks for spot assay and isolation of mitochondria. Addition of 2% Agar was used along with YPG and -URA media to incubate the yeast strains on solid media.

## IV.B Spot assay

The yeast strains were freshly streaked from glycerol stocks for spot assay on YPG and –URA media with 2% Agar. A single colony was used to inoculate culture and incubated overnight in a shaker incubator (Thermo Scientific MAXQ600). The Tim17WT, *ts97B* and *ts98B* were incubated at 24°C, whereas WT and *cst6* mutants were incubated at 30°C. The optical density at 600 nm (OD<sub>600</sub>) was measured and the culture diluted to an OD<sub>600</sub> of =0.5. After 5 hours of incubation, OD<sub>600</sub> was measured again and normalized to 0.1 OD<sub>600</sub>. Serial dilution up to 10<sup>5</sup> fold was performed for each strain and 0.5 µl of each dilution was spotted onto agar plates. The plates were incubated for 4 days at different temperatures.

## IV.C Mitochondria isolation

The isolation of mitochondria used for the experiments in this study was performed by differential centrifugation method. Yeast strains were freshly streaked on plates and a single colony used for inoculation of 50 ml primary culture for isolating mitochondria. Overnight primary cultures of yeast strains were incubated (*tim17ts* mutants at 24°C, and *cst6* mutants at 30°C) in a shaker incubator (Thermo Scientific MAXQ600) at 200 rpm and further used to inoculate 2 L volume of media for mitochondrial isolation. A large amount of media was incubated in the Innova<sup>®</sup>44 Incubator shaker series at 130 rpm. For isolation of mitochondria, a final OD<sub>600</sub> of 1.5 to 1.7 was considered. The final culture was centrifuged at 4000 rpm at 18°C in a Sorvall BIOS16 centrifuge for 10 minutes, and then harvested cells were washed with 250 ml of distilled water, re-centrifuged at 4000 rpm for weighing the pellet. Buffers used for isolation of mitochondria are added according to per gram of yeast cells. The pellet was resuspended in (2 ml/g yeast) DTT buffer (100 mM Tris/H<sub>2</sub>SO<sub>4</sub>, pH 9.4; 10 mM dithiothreitol, DTT) and incubated for 20 minutes in a Thermo Scientific MAXQ600 shaker incubator. Cells were centrifuged at 4000 rpm at 18°C in a Sorvall BIOS16 centrifuge for 10 minutes, and the supernatant was discarded. The pellet was washed with 200 ml of 1.2 M sorbitol and re-centrifuged at 4000 rpm at 18°C. The supernatant

was discarded. The washed pellet was used to generate spheroplasts. First, pellet is resuspended in zymolase buffer (7 ml/g yeast) without zymolase enzyme (20 mM KPi, pH 7.4; 1.2 M sorbitol), and then zymolase enzyme (4 mg/g yeast) was added. After which incubation for 40 minutes is performed (*tim17ts* mutants are incubated at 24°C and *cst6* mutants are incubated at 30°C) in Thermo Scientific MAXQ600 shaker incubator at 90 rpm. Generation of spheroplasts was observed by lysing 20 µl of the cell suspension in 1 ml distilled water, decrease in OD<sub>600</sub> was observed displaying spheroplasts burst. After incubation, spheroplasts were centrifuged at 4000 rpm for 10 minutes at 18°C, and the supernatant was discarded. The spheroplasts were placed on ice, and subsequent steps are performed at 4°C. The pellets were roughly suspended in homogenization buffer ([7 ml/g yeast], 0.6 M sorbitol; 10 mM Tris/HCl pH 7.4; 1 mM EDTA; 0.1% bovine serum albumin, BSA; 1 mM freshly added phenylmethylsulfonyl fluoride, PMSF). Spheroplasts were manually broken in adounce homogeniser (potter, 60 ml volume) with Teflon pestle. Minimum 30 ml of generated spheroplasts was added into the potter and 15x strokes were applied. Damaged cells were collected in F21-8 x 50y centrifuge tubes and centrifuged for 5 minutes at 3000 rpm in a F21-8x50 centrifuge Rotor in a Sorvall superspeed Centrifuge. The supernatant was transferred into new centrifuge tubes and re-centrifuged at 4000 rpm for 10 minutes. Again, supernatant was placed into new centrifuge tubes and centrifuged for 15 minutes at 12000 rpm to pellet mitochondria. Isolated mitochondria are resuspended in 5 ml SEM buffer (250 mM sucrose; 10 mM MOPS pH 7.2; 1 mM EDTA pH 8) with 25 µl freshly prepared 0.2 M PMSF and centrifuged again at 12000 rpm for 15 minutes. Pelleted mitochondria were suspended in 200 µl of SEM buffer by carefully pipetting up and down and further estimation of protein concentration was performed. The protein standard, IgG (1.4 mg/ml) and 1x Rotiquant (Roti<sup>®</sup>Quant 5x conc.) were used to perform the Bradford assay. Different range (10 to 50 µg) of IgG protein to final 50 µl volume and triplicates of different quantities of isolated mitochondria was used to measure the absorbance either in the Teccan plate reader or photometer. The concentration of isolated mitochondria (per µl) was determined by interpolation (value of absorbance versus concentration). The protein concentration was adjusted to (10 mg/ml) and 60 µl aliquots were flash frozen in liquid nitrogen and then stored at -80°C.

#### IV.D. Steady-state level

The stored mitochondria (10 mg/ ml) are used to prepare 3 different concentrations such as 10  $\mu\text{g}$ , 20  $\mu\text{g}$ , and 30  $\mu\text{g}$  to which 1x Laemmli buffer (2% sodium dodecyl sulfate, SDS; 10% glycerol; 60 mM Tris/HCl pH 6.8; 0.1 mg/ml bromophenol blue; 2 mM PMSF; 0.2 M DTT and for *tim17ts* mutants  $\beta$ -mercaptoethanol) was added and denatured for 5 minutes at higher temperature (35°C used for *tim17ts* mutants and 95°C used for *cst6* mutants). Prepared samples were loaded in 10% Tris Tricine gel which is prepared from 49.5% acrylamide (48% [w/v] Acrylamide; 1.5% [w/v] Bis-acrylamide), 1.5x gel buffer (3 M Tris/HCl pH 8.45; 0.3% SDS) and run for 3.5 hours at 55 mA using cathode buffer (1 M Tris; 1 M Tricine; 1% SDS, pH 8.25) and anode buffer (2 M Tris/HCl, pH 8.9). After electrophoresis, gels were transferred onto a polyvinylidene fluoride (PVDF) membranes. Activation of PVDF membrane in 100% Methanol are required before transfer. A semi dry blot system was used to transfer proteins from gel to PVDF membrane using running buffer (20 mM Tris; 150 mM glycine; 0.02% SDS; 20% ethanol). The sample was transferred at 250 mA for 2.5 hours. Further, staining and detaining of PVDF membrane in Coomassie (0.2% Coomassie Brilliant Blue R-250, 50% methanol and 10% Acetic acid, 40% dH<sub>2</sub>O and in detaining solution 0.2% Coomassie Brilliant Blue R-250 is not added) was performed to ensure the transfer of samples. Incubation of PVDF membrane for 30 minutes in skim milk (5% skim milk in TBS, [20 mM Tris; 125 mM NaCl]) and then overnight incubation in primary antibody at 4°C and finally in secondary antibody (anti Rabbit-HRP) for 1.5 hours at room temperature was performed. Each step of incubation of PVDF was followed by 3x washing for 5 minutes in TBST (0.1% Tween additionally added into TBS), and afterward, membranes were incubated with enhanced chemiluminescence (ECL) Western blotting detection solutions Amersham™ ECL™ Prime Western Blotting Detection (Reagent Solution A [luminol solution] and solution B [peroxide solution]). The Amersham Imager 600 blot and gel imager was used to capture images.



## IV.E Solubilization of membrane protein complexes

To observe the membrane complexes in their native form, 50  $\mu\text{g}$  of isolated mitochondria was solubilized by resuspending (15x) using pipette in solubilization buffer (20 mM Tris/HCl, pH 7.4; 0.1 mM EDTA, pH 8; 50 mM NaCl; 10% glycerol; freshly prepared 1 mM PMSF) with 1% digitonin. Solubilized samples were incubated for 15 minutes on ice and centrifuged at 14000 rpm at 4°C for 5 minutes. The supernatant is collected in new 1.5 ml centrifuge tubes and loading buffer (5% [w/v] Coomassie brilliant blue G-250; 100 mM Bis-Tris/HCl pH 7.0; 500 mM 6-aminocaproic acid) was added to the final concentration of 1x. Before loading the solubilized samples, a short spin of about 1 or 5 minutes was performed. Samples were loaded onto Blue Native PAGE (BN-PAGE) prepared from 49.5% acrylamide (48% [w/v] Acrylamide, 3% [w/v] Bis-acrylamide) and 3x gel buffer (200 mM Amino n-capronic acid; 150 mM Bis-Tris/HCl pH 7.0). In this study, the gradient gel of 6-13% BN-PAGE was used to observe the TOM complexes components and 6-16.5% BN PAGE was used to observe the TIM23 complexes components. The electrophoresis was performed in the Hoefer SE600 cooled vertical electrophoresis system at 4°C using running buffer (cathode buffer, 50 mM Tricine pH7.0; 15 mM Bis-Tris [with and without 0.02% Coomassie G] and anode buffer, 50 mM Bis-Tris/HCl pH 7.0) at running conditions 120 V, 15 mA for overnight. Further, transfer of samples onto the PVDF membrane, decoration with antibodies was performed as mentioned for the steady state level.

## IV.F Preparation of Lysate

The cytochrome  $b_2$  DHFR plasmids (to final concentration 2-4 ng/ $\mu\text{l}$ ) of different constructs for 1 reaction was added in 100  $\mu\text{l}$  of rabbit reticulolysate (TNT<sup>®</sup> SP6 Quick Master Mix, Promega) with 10  $\mu\text{l}$  of [<sup>35</sup>S] methionine (Methionine, L-[<sup>35</sup>S]-, 1mCi (37MBq), PerkinElmer) and incubated for 90 minutes at 30°C. The *in vitro* translation process was stopped by adding 8  $\mu\text{l}$  ice cold 0.2 M methionine and 18  $\mu\text{l}$  of 1.5 M sucrose. The prepared lysates were first shock frozen in liquid nitrogen and then stored at -80°C. Further, these lysates carrying precursor proteins were used for import experiments.

## IV.G *In vitro* import experiments

Isolated mitochondria (63  $\mu\text{g}$ ) were suspended into 50  $\mu\text{l}$  of import buffer (10 mM MOPS/KOH, pH 7.2; 250 mM sucrose; 80 mM KCl; 5 mM  $\text{MgCl}_2$ ; 2 mM  $\text{KH}_2\text{PO}_4$ , 5 mM methionine, and 3% BSA). The addition of 2 mM Adenosine triphosphate (ATP) and 2 mM Nicotinamide adenine dinucleotide (NADH) in import buffer was performed to energize isolated mitochondria. For every 50  $\mu\text{l}$  of final import reaction 4  $\mu\text{l}$  of lysate carrying precursor protein was used to initiate import process at 25°C. In order to dissipate the membrane potential ( $\Delta\psi$ ), AVO mix (8 mM antimycin, 1 mM valinomycin, and 20 mM oligomycin) was used before the addition of the precursor protein and without AVO mix is treated as control. Samples were removed at indicated time points. To irreversibly fold the DHFR moiety, 5 mM methotrexate (MTX) and for reversible folding 2 mM dihydrofolate (DHF) and 2 mM nicotinamide adenine dinucleotide phosphate, reduced form (NADPH) along with 5 mM creatine phosphate (CP) and 0.1 mg/ml creatine kinase (CK) was added into the import buffer. Import reactions were terminated by adding of 1  $\mu\text{l}$  AVO mix and incubated for 2 minutes on ice. Where indicated (+PK) samples were treated for 15 minutes by adding 50 mg/ml proteinase K (PK) and freshly prepared 0.2 mM PMSF was added to terminate the PK digestion. The samples were centrifuged at 15000 rpm for 10 minutes at 4°C. Further, samples were twice washed with SEM buffer (250 mM sucrose; 10 mM MOPS pH 7.2; 1 mM EDTA pH 8) followed by centrifugation at 15000 rpm for 10 minutes at 4°C. Samples were resuspended in 1x laemmli buffer and denatured at 95°C before loading on 10% Tris Tricine gel and run for 3.5 hours at 50 mA. Gels were stained in staining solution (50% (v/v) ethanol in water with 10% (v/v) acetic acid and 0.2% Coomassie dye) and destained in (50% (v/v) methanol in water with 10% (v/v) acetic acid). Gels were dried using a vacuum drier for 1.5 hours at 75°C. The protein marker on the dried gel was labelled with radioactive ink and incubated in a phosphor imager cassette. Radiolabeled imported proteins were detected by autoradiography using Phosphor screen. The phosphor screen was placed down on the Typhoon Scanner machine's glass platen, and the grid area is selected with pixel size 100 is selected for scanning. After scanning, Phosphor Screen Image Eraser was used to clean the phosphor screen. The image was further quantified using Fiji or imageJ.

## List of primary antibodies

### List of Antibodies used for BN-PAGE

Antibody	Ref. Number	Dilution
Tom40	168-12	1:500
Cox4	578-5	1:2000
Tom70	657-4	1:500
Tim21	3894-7	1:500
Tim23	133-14	1:500

### List of Antibodies used for Tris-Tricine Gel

Antibody	Ref. Number	Dilution
Tim23	3878-4	1:500
Tim50	Affinity purified	
Tim17	1845-3	1:800
Mgr2	3121-7	1:1000
Tim21	3883-1	1:500
Tim44	1836-7	1:500
Pam18	751-4	1:250
Pam17	274-5	1:400
Tim10	217-8	1:500
Atp20	1516-4	1:500
Cox4	578-5	1:2000
Tom22	104-IV	1:500
Tom40	168-12	1:500
Tom70	657-4	1:500
Cor1	1538-4	1:500

## Composition of Gel Electrophoresis (Single gel composition)

Composition of BN-PAGE (gradient)	6%	13%	16.5%
Acrylamide 49.5%	1.07 ml	2.35 ml	3.05 ml
3x Gel buffer	3 ml	3 ml	3 ml
Glycerol	-	1.8 ml	1.8 ml
dH <sub>2</sub> O	4.88 ml	1.81 ml	1.11 ml

10% APS	38 $\mu$ l	30 $\mu$ l	30 $\mu$ l
TEMED	3.8 $\mu$ l	3 $\mu$ l	3 $\mu$ l

Composition of 10% Tris-Tricine gel

Acrylamide 49.5%	3ml
3x Gel buffer	5ml
dH <sub>2</sub> O	7ml
10% APS	100
TEMED	10 $\mu$ l

**List of chemicals**

**Company name**

[ <sup>35</sup> S] methionine	PerkinElmer
6-aminocaproic acid	Sigma-Aldrich
Acrylamide/Bis-acrylamide	Carl Roth GmbH
Adenosine triphosphate (ATP)	Roche
Agar	Becton Dickinson
Antimycin	Sigma-Aldrich
Bacto peptone	Becton Dickinson
Bacto yeast extract	Becton Dickinson
Bacto yeast nitrogen base	Becton Dickinson
Bis-Tris	Carl Roth GmbH
Bovine serum albumin, BSA	Sigma-Aldrich
Coomassie brilliant blue R-250	Carl Roth GmbH
Creatine kinase (CK)	Roche
Creatine phosphate (CP)	Roche
Digitonin	Matrix Bioscience
Oligomycin	Sigma-Aldrich
Peptone	Becton Dickinson
Proteinase K	Roche
Roti <sup>®</sup> Quant	Carl Roth GmbH
Sodium dodecyl sulfate [SDS]	Carl Roth GmbH
Sucrose	MP Biomedicals
TNT <sup>®</sup> SP6 Quick Master Mix	Promega GmbH

Tricine	Carl Roth GmbH
Tris	Carl Roth GmbH
Ura drop out mix	MP Biomedicals
Valionomycin	Sigma-Aldrich
Zymolase	Nacalai tesque
Secondary Antibody (Anti Rabbit)	Merck Millipore

## V. Result

### V.A Characterization of temperature sensitive mutants of Tim17

Tim17 and Tim23 have similarities related to transmembrane topology to form the translocase conducting pore, and Tim50 induces gating effect when precursor protein needs to be imported across the inner membrane. In humans, Tim17 is encoded by two genes as Tim17a and Tim17b, whereas in yeast, only one gene is responsible for encoding Tim17 (Iacovino et al., 2009; Matta et al., 2017). *Saccharomyces cerevisiae* provides various possibilities for genetic manipulations of the mitochondrial genome and nuclear genome, making it a desirable candidate to study functional aspect of essential genes. In *Saccharomyces cerevisiae*, it is possible to create temperature-sensitive (*ts*) mutants of the targeted gene regulated by temperature as controlling factor (Ben-Aroya et al., 2010; Z. Li et al., 2011). In this study, Tim17 temperature-sensitive mutants (*ts97B* and *ts98B*) are used. These temperature-sensitive (*ts*) mutants possess the ability to regulate the targeted essential gene in its normal behavior, similar like wild type (Tim17WT) at the permissive (22°C to 24°C) temperature. At an elevated temperature like 37°C, *ts* mutants turn off the regulation or shut down the expression of the Tim17 gene and act like mutants. Due to the restrictive regulation of essential targeted genes at different temperatures, it is possible to manipulate the regulation of the Tim17. The conditional Tim17 temperature-sensitive (*tim17ts*) mutants were generated using a random mutagenesis approach by Dr. Bernard Guirad (Centre de Génétique Moléculaire, Center National de la Recherche Scientifique, Gif-Sur-Yvette, France). In this study, Tim17WT (wild type) has no mutation, and the *tim17ts* mutants have single substitution of amino acids in different regions. The *ts97B* has only one mutation in the TM2 region, and *ts98B* has three different mutations at TM1, TM3, and C terminal, as mentioned in table (2).

<i>tim17ts</i> mutant name	Amino acid substitution
<i>ts97B</i>	G63S (TM2)
<i>ts98B</i>	W32R (TM1), N90K (TM3), and S152P (C terminal)

Table 2: Information about mutation of the *tim17ts* mutants.

The characterization study of *tim17ts* mutants was performed by spot assay to observe growth response on different media such as YPD (fermentable media due to presence of glucose) and YPG (non-fermentable media due to addition of glycerol) at different temperatures. In YPG media, ethanol is added to understand if *tim17ts* mutants could be viable under stress conditions. The spot assay is performed as one of the preliminary observation to understand if mutations cause any growth defect. The overnight primary cultures of Tim17WT, *ts97B*, and *ts98B* were incubated at the permissive temperature (24°C) in YPG media. The overnight cultures are diluted to OD<sub>600</sub> of 0.5 and allowed to grow for 5 hours at 24°C. After 5 hours, the observed OD<sub>600</sub> was again normalized to 0.1 OD<sub>600</sub>. The normalized samples were serially diluted up to fivefold and used for spot assay. It is observed that at permissive temperature function of Tim17 in both the *tim17ts* mutants is intact as they were able to grow on both fermentable and non-fermentable media, as shown in figure 7(a). Nevertheless, it was observed that at non-permissive temperature (37°C), both *tim17ts* mutants failed to grow on non-fermentable media and stress condition. The failure in growth of *ts97B* and *ts98B* mutants at 37°C is due to limited regulation of Tim17, an essential gene of the TIM23 complex. From the spot assay, I have observed that the *tim17ts* mutants are functionally active at permissive temperature, and growth is severely affected at higher temperatures leading to cell death.

Further, I wanted to know if the mutations of *ts97B* and *ts98B* affect protein stability of subunits of the TIM23 complex and its partner proteins. For this purpose, the steady-state level of different mitochondrial proteins was performed using isolated mitochondria from Tim17WT, *ts97B*, and *ts98B* yeast cells. Different concentrations (5 µg, 10 µg, and 15 µg ) of Tim17WT, *ts97B*, and *ts98B* mitochondria were loaded on Tris Tricine electrophoresis gel and transferred onto the PVDF membranes. These

membranes were decorated with antibodies against few mitochondrial proteins of the TOM complex (Tom70, Tom22) and core proteins of the TIM23 complex (Tim23, Tim17, Tim50) TIM23<sup>SORT</sup> form (Tim21, Mgr2) and TIM23<sup>CORE</sup> form (Tim44, Pam17). Few proteins from the respiratory chain complex (Cox4, Atp20) were used as control. It was observed that the translocase proteins of the TOM complex, TIM23<sup>SORT</sup> form, and TIM23<sup>CORE</sup> form of isolated mitochondria Tim17WT, *ts97B*, and *ts98B* have comparable uniform state of protein levels, as shown in figure 7 (b). The isolated mitochondria of *ts98B* have an insignificantly lower amount of Tim23 and Tim50 protein. The antibody could not detect the Tim17 protein in *ts98B* due to mutations close to the epitope.

Isolated mitochondria of Tim17WT and *tim17ts* mutants were solubilized into mild detergent (1% of digitonin), run on BN-PAGE, and further transferred onto the PVDF membranes. It is known that the size of the TIM23<sup>CORE</sup> form is approximately 230 kDa and the TIM23<sup>SORT</sup> form is approximately 130 kDa in size. Depending upon the size variation of the TIM23 complex, two different forms that are TIM23<sup>CORE</sup> and TIM23<sup>SORT</sup> are observed. In order to observe both the forms of the TIM23 complex, transferred samples onto the PVDF membrane are decorated with the antibody against Tim23, whereas only TIM23<sup>SORT</sup> is observed using the antibody against Tim21. The PVDF membranes are treated with antibody against Tim23, as shown in figure 7(c), detects only in Tim17WT, and the TIM23<sup>CORE</sup> form remains undetectable in *ts97B* and *ts98B* mutants. The reason behind absence of TIM23<sup>CORE</sup> form in *tim17ts* mutants could be that mutations in the TM segments of Tim17, which could possibly result into collapsing the structural stability when isolated mitochondria are solubilized in detergent. The obscure orientation of the TIM23 complex in isolated mitochondria would dissociate a few components. As the components fall apart, the TIM23<sup>CORE</sup> form could not be detected in BN-PAGE. As shown in figure 7(c), the PVDF membrane decorated with the antibody against Tim21 detects TIM23<sup>SORT</sup> form in the Tim17WT, *ts97B*, and *ts98B*. Additionally to know if the mutations of *tim17ts* mutants have any effect on respiratory chain complexes, the antibody against Cytochrome C oxidase subunit 4 (Cox4) of the respiratory chain complex was used. Mutations of Tim17 do not affect the respiratory chain complexes as solubilized mitochondria of Tim17WT, *ts97B*, and *ts98B* shows the presence of dimers of its subunits III and IV, which are major regulation sites for oxidative phosphorylation.



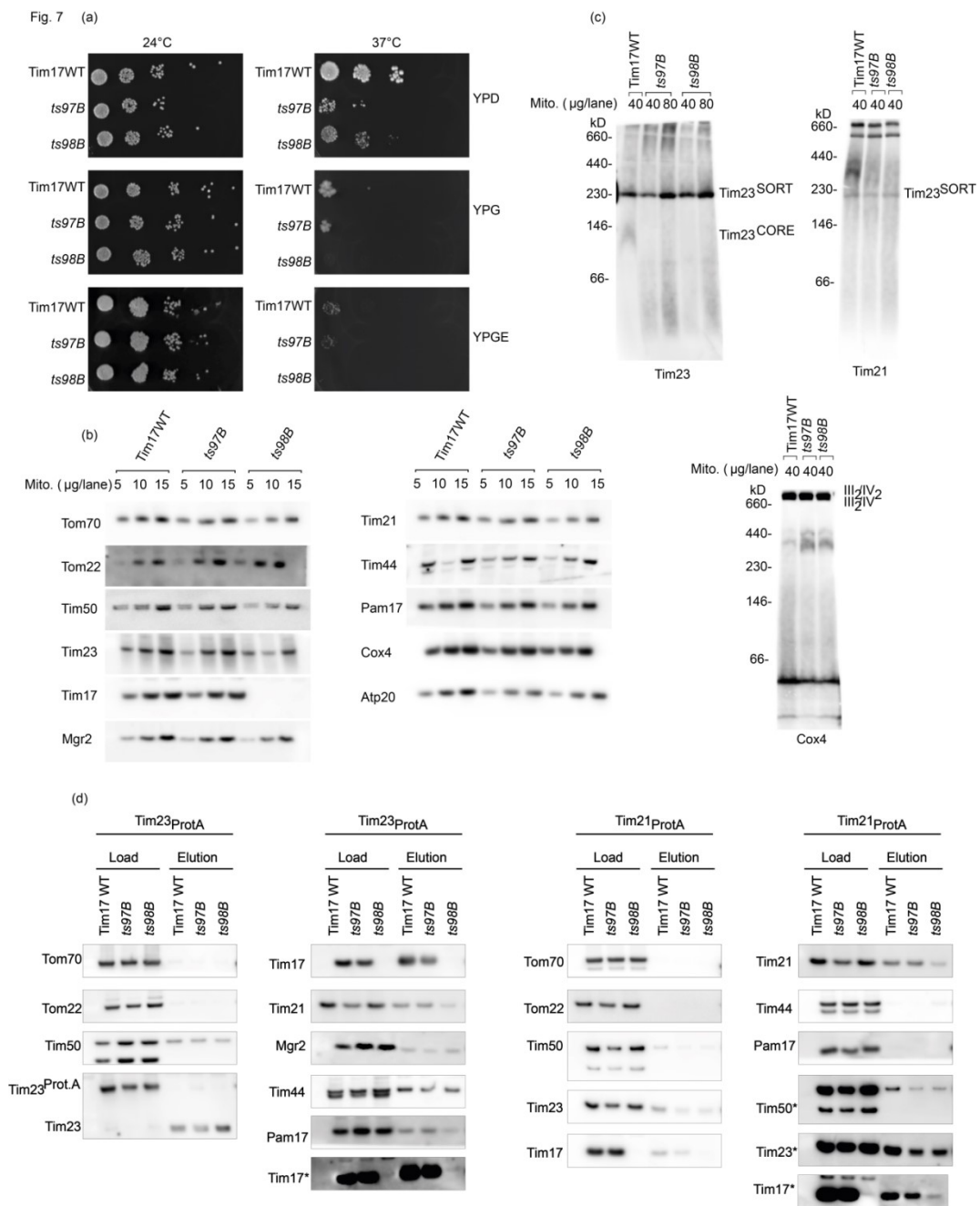


Figure 7: Characterization of temperature sensitive mutants of Tim17. (a) The aliquots corresponding to  $9 \times 10^4$  cells and two tenfold dilutions of Tim17WT, *ts97B* and *ts98B* were spotted onto YPD, YPG and YPGE plates which were incubated for four days at 24°C and 37°C. (b) Different concentration (10, 20 and 30  $\mu\text{g}$ ) of isolated mitochondria of Tim17WT,

*ts97B* and *ts98B* used for the steady-state level of different mitochondrial proteins shown by western blot of Tris Tricine electrophoresis gel using the indicated antibodies. (c) Isolated mitochondria of Tim17WT, *ts97B* and *ts98B* were re-suspended and solubilized into 1% digitonin containing solubilization buffer to observe the TIM23 complexes and respiratory chain supercomplexes shown by western blot of BN-PAGE using the indicated antibodies. (d) Mitochondria isolated from Tim17WT, *ts97B* and *ts98B* expressing Tim23 and Tim21 ProteinA tag, were solubilized with digitonin and incubated with IgG-Sepharose beads to perform IgG affinity pulldown of TIM23 complexes. Samples were analyzed by Tris Tricine electrophoresis gel and followed by western blot and decorated with indicated antibodies. Load contains 20% of the material present in Elution. The asterisk sign (\*) means longer exposure duration of PVDF membrane using indicated antibody.

Further proteinA-tag Tim23 and proteinA-tag Tim21 isolated mitochondria of Tim17WT, *ts97B*, and *ts98B* was used to perform affinity pull-down. The proteinA-tag Tim23 was used to copurify the TIM23 and PAM subunits, whereas TIM23<sup>SORT</sup> and respiratory chain complexes subunits are copurified using proteinA-tag Tim21. The proteinA-tag Tim23 and proteinA-tag Tim21 isolated mitochondria of *tim17ts* mutants were lysed with digitonin. Mitochondrial extracts were subjected to IgG sepharose affinity chromatography and eluted after treatment with TEV protease enzyme. The load (total amount of protein; digitonin lysed fraction) and elution (affinity bound protein eluted via TEV protease cleavage) are analyzed by electrophoresis gel followed by immunoblotting. As shown in figure 7(d), the PVDF membranes were decorated with antibodies against few mitochondrial proteins of the TOM complex (Tom70, Tom22) and core proteins of the TIM23 complex (Tim23, Tim17, Tim50) TIM23<sup>SORT</sup> form (Tim21, Mgr2) and TIM23<sup>CORE</sup> form (Tim44, Pam17). It was observed that less amount of Tim17 was copurified in proteinA-tagTim23*ts98B* and proteinA-tagTim21*ts98B*. The proteinA-tagTim23*ts98B* copurified less amount of Pam17. It is known that Pam17 interacts only with Tim17; hence upon lysis of isolated mitochondria, ineffective binding due to proteinA-tag would result in a low amount of copurification. Similarly, proteinA-tag Tim21 *ts97B* and proteinA-tag Tim21*ts98B* have less Tim50, which could be due to readily disintegration from the TIM23 complex.

## V.B Differential import response of *tim17ts* mutant

To study the precursor protein import behavior carried out by of the *tim17ts* mutants, I used different constructs of cytochrome  $b_2$ , a native protein of the IMS region. The nuclear genome encodes cytochrome  $b_2$  (L(+)-lactate cytochrome c oxidoreductase) (Ndi et al., 2018). It is one of the subunits of the respiratory chain complex III. The precursor form of cytochrome  $b_2$  is synthesized in the cytosol and via post-translational mechanism presented to cytosolic receptor sites of the TOM complex (Cruciat et al., 2000). The bipartite presequence of cytochrome  $b_2$  precursor protein and unique cleavage sites are the most important feature. Besides, cytochrome  $b_2$  possess a heme-binding domain and flavin domain. The heme-binding domain (HBD) essentially needs ATP while its import across the matrix (Click et al., 1993). It is known that the HBD domain could independently form a mature state when laterally sorted across the inner membrane despite the flavin domain. Researchers have employed bipartite presequence of cytochrome  $b_2$  precursor protein and cleavage sites along with a short stretch of the HBD to understand the import and processing of mitochondrial precursor protein (Esaki et al., 1999). It is well known that the TOM and TIM23 complexes perform the import of cytochrome  $b_2$  precursor protein. The membrane potential is an important factor required during insertion and import across the inner membrane (Krayl et al., 2007). The import process of cytochrome  $b_2$  is a two-step process. First, it is imported towards the matrix with the help of the PAM complex. The second stop, is laterally sorted across the inner membrane to form a mature state (Gasser et al., 1982). Whereas the precursor protein of cytochrome  $b_2$  is cleaved twice before processed into the mature form.

In order to understand this, the precursor protein of cytochrome  $b_2$  can be divided into two sections, such as presequence (residues 1-31) and hydrophobic segment (residues 32-80) (Geissler et al., 2000). The presequence is a matrix targeting signal composed of positively charged amino acids at the N terminal end of cytochrome  $b_2$  precursor protein. The presequence actively engages TOM and TIM23 complex and is further pulled towards matrix by inward force via ATP hydrolysis employed by the PAM complex. The presequence when exposed towards matrix, mitochondrial protease peptidase (MPP) recognizes shot sequence motif to cleave presequence from rest of the precursor protein. Few amino acids that resemble

unstable after MPP cleavage are trimmed by octapeptidyl amino-peptidase (oct1) (Gomes et al., 2017).

After this cleavage, the precursor protein of cytochrome  $b_2$  is exported to the IMS due to the internal hydrophobic segment responsible for lateral sorting of precursor protein into the inner membrane. The hydrophobic segment is cleaved by the inner membrane peptidase (IMP) before releasing into IMS (Gakh et al., 2002). The cleavage of cytochrome  $b_2$  precursor protein in a sequential manner is helpful to understand the biogenesis by pulse-chase import experiments as discussed later.

To study the precursor protein import behavior of the *tim17ts* mutants, I have used different constructs of the cytochrome  $b_2$  (radioactive labelled [ $^{35}\text{S}$ ] Methionine precursor protein, b2 used for *in vitro* import experiments). The constructs have different lengths as they differ in the size of the HBD region, as illustrated in figure 8. In order to perform *in vitro* import experiments, the C terminal is fused with DHFR moiety. The dihydrofolate reductase (DHFR), a protein of cytosolic origin that could not be imported into the isolated mitochondria. The DHFR moiety can be useful while performing experiments due to various other reasons. First, the antibody against cytochrome  $b_2$  could hardly recognize the immune bolts results, whereas antibody against DHFR exhibit higher recognition useful for immune blotting when import experiments performed using purified or radiolabelled precursor protein. Second, the natural ligands such as dihydrofolate reductase and NADPH are used to reversibly fold the DHFR moiety and then removed by washing with import buffer lacking ligands. Few covalent ligands such as methotrexate (MTX) are also used to fold DHFR moiety irreversibly. The b2 constructs such as b<sub>2</sub>(220)-DHFR and b<sub>2</sub>(167)-DHFR possess internal hydrophobic signal due to which they are laterally sorted across the inner membrane. Deletion of 19 amino acids, which compromises internal hydrophobic segment when removed, the precursor protein is redirected towards the matrix while import. The b<sub>2</sub>(167)<sub>Δ</sub>-DHFR, lacking hydrophobic signal, is used for matrix targeted import. Different plasmids carrying the construct of cytochrome  $b_2$  with SP6 promoter is used to prepare radiolabelled lysate in a cell-free transcription and translation system containing rabbit reticulocyte with [ $^{35}\text{S}$ ] Methionine. The lysate contains precursor protein, which is used to perform various *in vitro* import experiments.

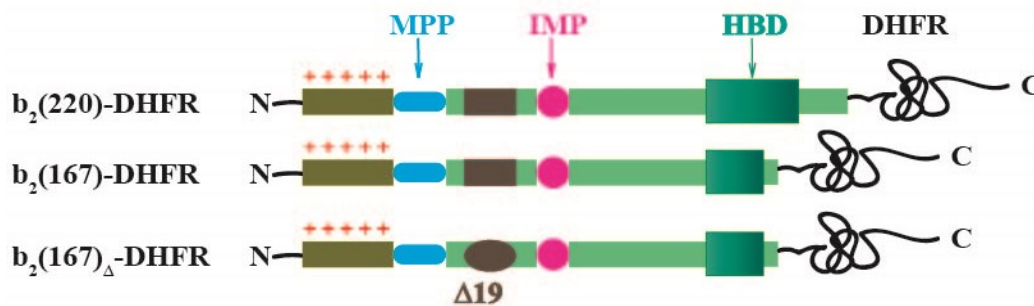


Figure 8: Schematics of cytochrome  $b_2$  construct used for preparing lysate. The cytochrome  $b_2$  constructs possess two cleavage site, MPP (mitochondrial protease peptidase) and IMP (inner membrane protease). The positively charged presequence at N terminal end serves as mitochondrial targeting signal and C terminal is fused with cytosolic protein dihydrofolate reductase (DHFR). The internal non-cleavable hydrophobic segment of cytochrome  $b_2$  is deleted ( $\Delta 19$ ) in  $b_2(167)_\Delta$ -DHFR construct, whereas unaltered in  $b_2(220)$ -DHFR and  $b_2(167)$ -DHFR. The size of cytochrome  $b_2$  is different depending upon the variable length of the heme-binding domain (HBD).

The *in vitro* import of radiolabeled lysate carrying precursor protein enables understanding of the precursor proteins import pathway, processing, and cleavage pattern within isolated mitochondria. The pattern of import is observed by the generation of different fragments such as mature (m) and intermediate (i) forms of precursor (p) protein. The different imported and processed precursor protein fragments can be visualized by using gel electrophoresis and autoradiography techniques. In order to perform *in vitro* import experiments, the isolated mitochondria of Tim17WT, *ts97B*, and *ts98B* are energized by re-suspended in import buffer, including ATP and NADH. The import process is started at incubation temperature (25°C) where radiolabeled lysate containing precursor protein is added to the energized mitochondria. Samples are removed at different time points to observe the import rate. One of the import reactions is treated with AVO mix (8mM antimycin, 1mM valinomycin, and 20mM oligomycin) to dissipate the membrane potential ( $\Delta\psi$ ). Import of precursor protein is restricted by the addition of AVO mix and treated as control.

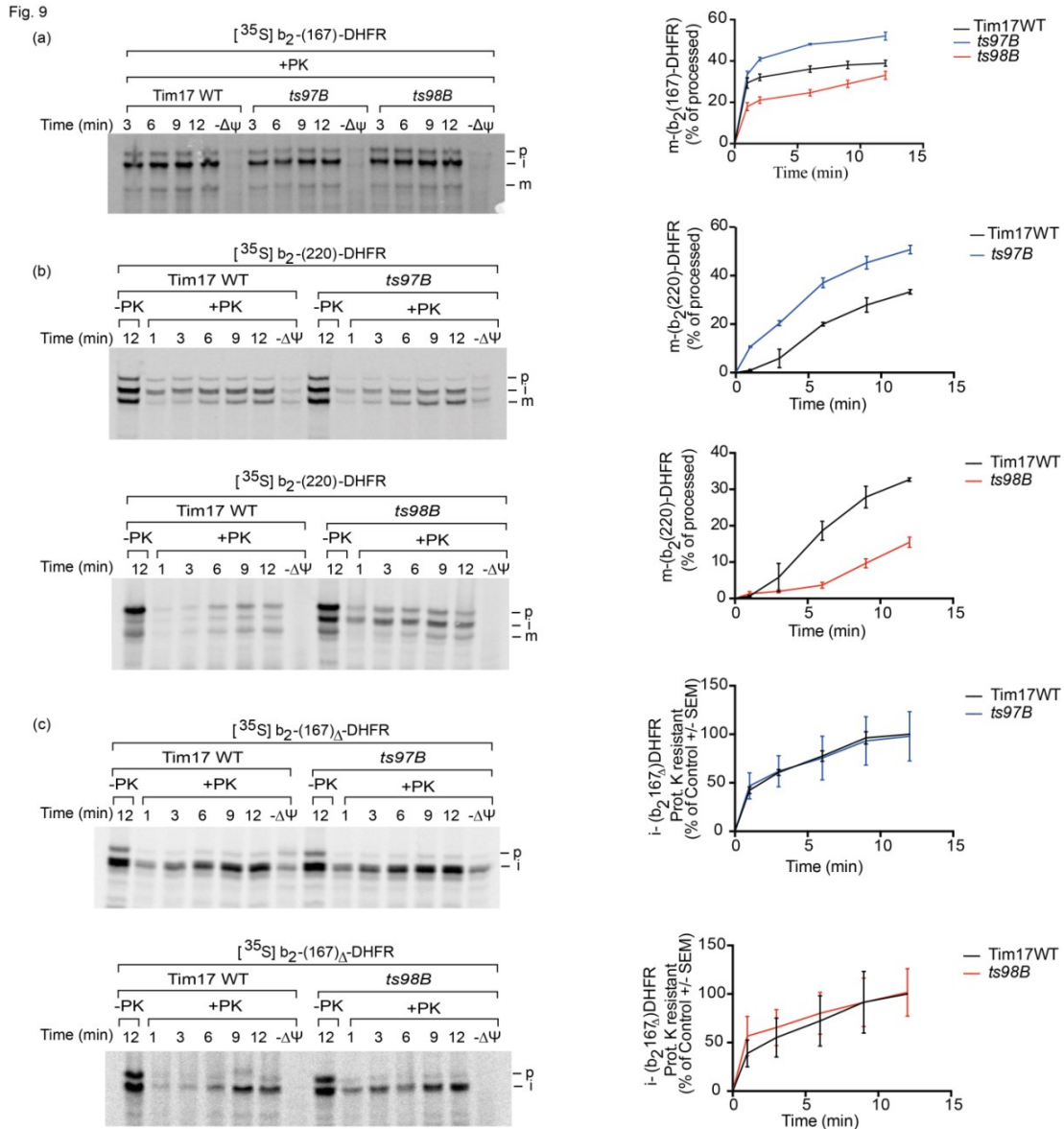


Figure 9: *In vitro* import of lysate carrying precursor protein (a)  $[^{35}\text{S}]b_2-(167)\text{-DHFR}$ , (b)  $[^{35}\text{S}]b_2-(220)\text{-DHFR}$  and (c)  $[^{35}\text{S}]b_2-(167)\Delta\text{-DHFR}$  into the Tim17WT, *ts97B* and *ts98B* isolated mitochondria. Import is performed by adding isolated mitochondria to the lysate at 25°C at different time intervals (min) and terminated by adding AVO mix. Import of precursor protein is restricted by the addition of AVO mix and treated as control. Import reaction further treated with proteinase K (+PK) and SEM (-PK). The proteinase K resistant mature (m), intermediate (i) and precursor (p) forms were analyzed using digital autoradiography. The proteinase K protected values of m and i forms are quantified using Fiji and used for plotting graph in prism graph pad. The sum of m and i forms are considered as the total amount of precursor protein imported to secure state. The value of m form is divided by the sum (i+m) to calculate the

percentage of processed b<sub>2</sub>-(167)-DHFR and b<sub>2</sub>-(220)-DHFR whereas for analysis of b<sub>2</sub>-(167)<sub>Δ</sub>-DHFR import amount of i-form in the proteinase resistant (+PK) samples are quantified and longest time point of Tim17 WT is set to 100% as control. The individual value of i forms divided by the control is calculated. Data are represented as mean ± SEM (n = 3, A), (n=3, B), and (n=3, C). (-Δψ), membrane potential.

Further, the addition of proteinase K (PK) is performed to digest the accumulated precursor (p) protein formed during import. The precursor proteins (<sup>35</sup>S]b<sub>2</sub>-(220)-DHFR and [<sup>35</sup>S]b<sub>2</sub>-(167)-DHFR), which are laterally sorted across inner membrane precursor proteins are cleaved twice. First, presequence is cleaved by the Mitochondrial processing peptidase (MPP) and the second cleavage is at the amino terminus of precursor protein performed by the Inner membrane protease (IMP) to remove destabilizing amino acid residues. The mature form is formed when imported precursor protein after processed by the mitochondrial intermediate peptidase (IMP) and laterally sorted across the inner membrane. The [<sup>35</sup>S]b<sub>2</sub>-(220)-DHFR and [<sup>35</sup>S]b<sub>2</sub>-(167)-DHFR shows two forms of imported precursor protein that is intermediate (i) and mature (m) form; used for quantification to understand the import kinetics. It is observed from the figure 9 (a), and 9 (b), [<sup>35</sup>S]b<sub>2</sub>-(220)-DHFR and [<sup>35</sup>S]b<sub>2</sub>-(167)-DHFR has the gradual increase of mature form in *ts97B* compared to Tim17WT. Similarly, a higher amount of intermediate form is observed in *ts98B* compared to Tim17WT. To understand the import kinetics performed by *tim17ts* mutants, both the forms (intermediate and mature; [i+m]) are considered as the sum. Hence, sum refers to the total amount of protease protected precursor protein processed by the Tim17WT, *ts97B*, and *ts98B*. The graph is plotted using individual values of mature form, divided by the total amount of precursor protein imported at individual time points. On the other hand, [<sup>35</sup>S]b<sub>2</sub>-(167)<sub>Δ</sub>-DHFR has only an intermediate form as the b2 construct lacks sufficient sequence to form mature state. The longest time point of Tim17WT is considered as 100% import rate to understand the import rate of matrix targeted precursor protein. Each values of the intermediate form observed in *ts97B* and *ts98B* at different time point are used to calculate the amount of imported precursor protein compared to control. The Tim17WT, *ts97B*, and *ts98B* show similar import rates for matrix- targeted precursor protein, as shown in figure 9 (c). It is observed that both the *tim17ts* mutants differentially import only lateral sorting of precursor proteins that

possess hydrophobic signal, so it would be interesting to know the biogenesis of the lateral sorting of precursor proteins.

### **V.C Conditional release of the laterally sorted precursor protein in *tim17ts* mutants**

The pulse-chase experiment was performed to understand the biogenesis of hydrophobic signal carrying precursor protein in 2 steps. Biogenesis refers to the import and processing of precursor protein by exchanging intermediate form into a mature form. First, precursor protein is reversibly folded so that all the active import sites of isolated mitochondria are saturated by actively engaging the TOM-TIM23 complex. Second, in the absence of reduced substrates; the precursor protein is assumed to be released simultaneously from an actively engaged translocase complex to attain a mature state. In this experiment, [<sup>35</sup>S]b<sub>2</sub>-(220)-DHFR is used. The dihydrofolate (DHF) and nicotinamide adenine dinucleotide phosphate reduced form (NADPH) DHFR substrates are used to fold the DHFR moiety reversibly. The isolated mitochondria of Tim17WT, *ts97B*, and *ts98B* and precursor protein with folded DHFR are incubated together to engage the active import sites. This incubation could be referred to as pulse step since reversibly folded [<sup>35</sup>S]b<sub>2</sub>-(220)-DHFR gets accumulated over the TOM complex import sites of and actively engages the TIM23 complex. Upon washing off the substrates, import reactions are re-suspended into new import buffer lacking DHFR substrates. The absence of DHFR substrates allows the precursor protein to be imported at the same level as the chase. Samples are removed from the import reaction at different time points further treated with external proteinase K. Observation procured from this experiment is based on the accumulation of intermediate form and mature form. The accumulated intermediate form represents that the precursor protein might be stuck or still engaged with the TIM23 complex. The mature form of [<sup>35</sup>S]b<sub>2</sub>(220)-DHFR supports protease protected lateral release of precursor protein across the inner membrane, whereas conversion of intermediate to mature form which is dependent upon the cleavage outlines its biogenesis. The MPP cleaves presequence, and IMP cleaves the amino terminal only when precursor protein is accessible; hence the conversion of intermediate to mature form is directly dependent upon the protease accessibility. It is observed that conversion of intermediate to mature form is performed higher by *ts97B* compared to Tim17WT,



whereas in *ts98B*, conversion of intermediate to mature form is less. In *ts98B*, the increment of intermediate form concerning time is observed in figure 10 (a). The individual value of proteinase K protected mature form is divided by the total (i+m) amount of precursor protein imported at different time points. The values are used for plotting graph, representing the percentage of processes protein by the *tim17ts* mutants. It is observed that *ts97B* has a rapid formation of mature form, proposing that the lateral sorting of precursor protein across the inner membrane in *ts97B* is higher compared to Tim17WT and *ts98B*. A similar observation was made by our group while working on Mgr2 protein.

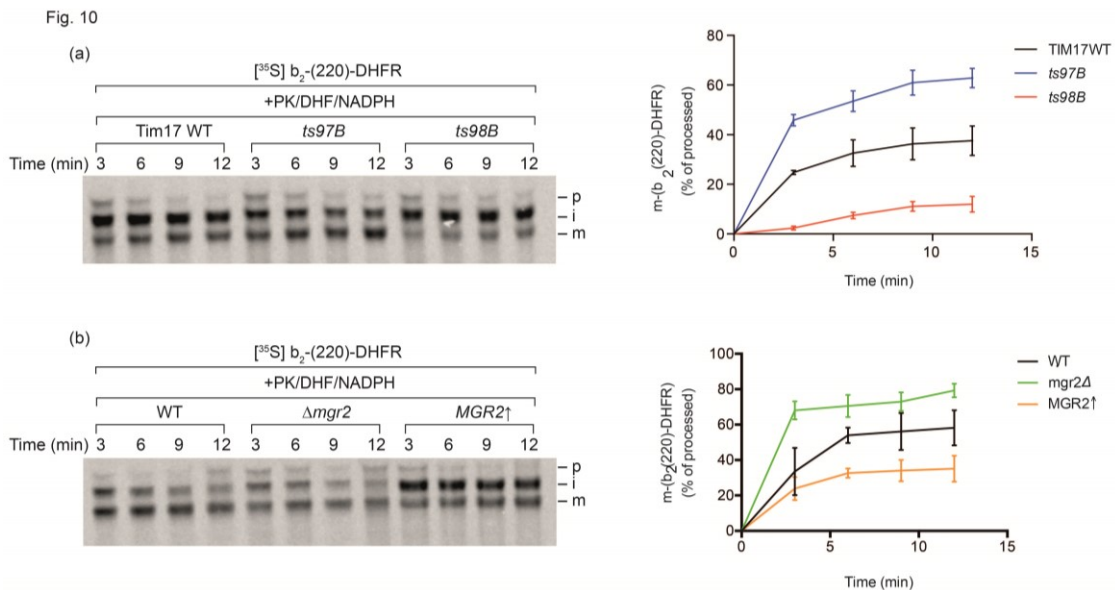


Figure 10: *In vitro* import of radiolabeled  $b_2$ -(220)-DHFR, inner membrane sorted precursor protein is performed into the Tim17WT, *ts97B* and *ts98B* isolated mitochondria at 25°C. The DHFR moiety of the precursor protein is irreversibly folded by addition of DHF and NADPH. First incubation of 10 minutes is performed for the accumulation of precursor protein into the translocon complexes to achieve active transport engagement (pulse). Further washing of mitochondria is performed and re-suspended into import buffer without DHFR substrate at 25°C. Samples are removed at indicated time points for sorting of precursor protein across the inner membrane (chase). Import reaction further treated with proteinase K. The proteinase K-resistant mature (m), intermediate (i) and precursor (p) forms were analyzed using digital

autoradiography. The proteinase K protected values of m and i forms are quantified using Fiji and used for plotting graph in prism graph pad. The sum (i+m) of two different forms are considered as the total amount of precursor protein imported to secure state. The value of m form is divided by the sum to calculate the percentage of processed b<sub>2</sub>-(220)-DHFR. Data are represented as mean ± SEM (n = 3).

I have performed the same experiment using isolated mitochondria from yeast cells Tim17WT, absence of the Mgr2 ( $\Delta mgr2$ ), and overexpression of Mgr2 (MGR2 $\uparrow$ ). It is known that Mgr2, a small hydrophobic protein, is actively involved with the lateral sorting of the mitochondrial precursor protein. The deletion of Mgr2 and overexpression has an opposite effect on the import of hydrophobic signal carrying precursor protein. In case if Mgr2 is overexpressed, the precursor proteins pause and, at a slower rate, laterally released across the inner membrane. In contrast, the absence of Mgr2 accelerates the same process. It shows that *ts97B* and  $\Delta mgr2$  have similar import responses for laterally sorted precursor protein, as the formation of intermediate to mature form is higher in  $\Delta mgr2$ . In the presence of overexpressed MGR2, the accumulation of intermediate form is similar to *ts98B*. The intermediate form accumulation could be due to the binding of the PAM complex with the precursor protein still exposed to the matrix. Further, I wanted to know the influence of the import-driving activity of the PAM complex.

## **V.D Mgr2 rescues the translocation defect of *ts97B* mutant**

The import of positively charged presequence carrying precursor protein is driven by membrane potential ( $\Delta\psi$ ) and cyclic ATP hydrolysis carried by the PAM complex. Membrane potential drives the import of precursor protein across the inner membrane through the TIM23 complex by electrophoretic force. The PAM complex binds to the matrix exposed precursor protein. Further, ATP hydrolysis is carried by the PAM complex to pull the precursor protein from the TOM-TIM23 complex. Experimentally this import process could be divided into two consecutive steps, first engage the TOM and TIM23 complexes actively by folded precursor protein and then disrupt the membrane potential to evaluate import solely based on ATP hydrolysis. The [<sup>35</sup>S]b<sub>2</sub>-(220)-DHFR precursor protein has presequence followed by the hydrophobic sorting signal for lateral sorting across the inner membrane is used. The addition of methotrexate (MTX) is to irreversibly fold the C terminal DHFR moiety of [<sup>35</sup>S]b<sub>2</sub>-(220)-DHFR precursor protein. The advantage of adding MTX is that the precursor proteins DHFR moiety could not be linearized or unfolded even if the MTX is washed away, which imposes constant demand of the PAM complex to pull the precursor protein strongly against the TOM complex. The isolated mitochondria of Tim17WT, *ts97B* and *ts98B* are incubated with irreversibly folded DHFR moiety of [<sup>35</sup>S]b<sub>2</sub>-(220)-DHFR precursor protein. During this incubation, precursor protein (unfolded N terminal part) actively engages the TOM and TIM23 complex in the presence of membrane potential across the inner membrane. In contrast, the DHFR moiety (tightly/irreversibly folded) is pulled against the TOM and TIM23 complex by the PAM complex. In the second step, valinomycin is added to dissipate the membrane potential. Samples are removed at different time points to assess binding efficiency of the PAM complex in absence of membrane potential. One of the import reaction is treated as control with unimpaired membrane potential. Further, samples with dissipated membrane potential are treated with proteinase K to digest the accumulated residual precursor protein. In the figure 11 (a) and (b), intermediates forms are observed in only Tim17WT and *ts98B*, which shows that the PAM complex efficiently binds to [<sup>35</sup>S]b<sub>2</sub>-(220)-DHFR preventing it from

backsliding through the TOM and TIM23 complexes. In *ts97B*, the precursor protein is accessible to externally added protease K due to the PAM complexes weak binding.

Fig. 11

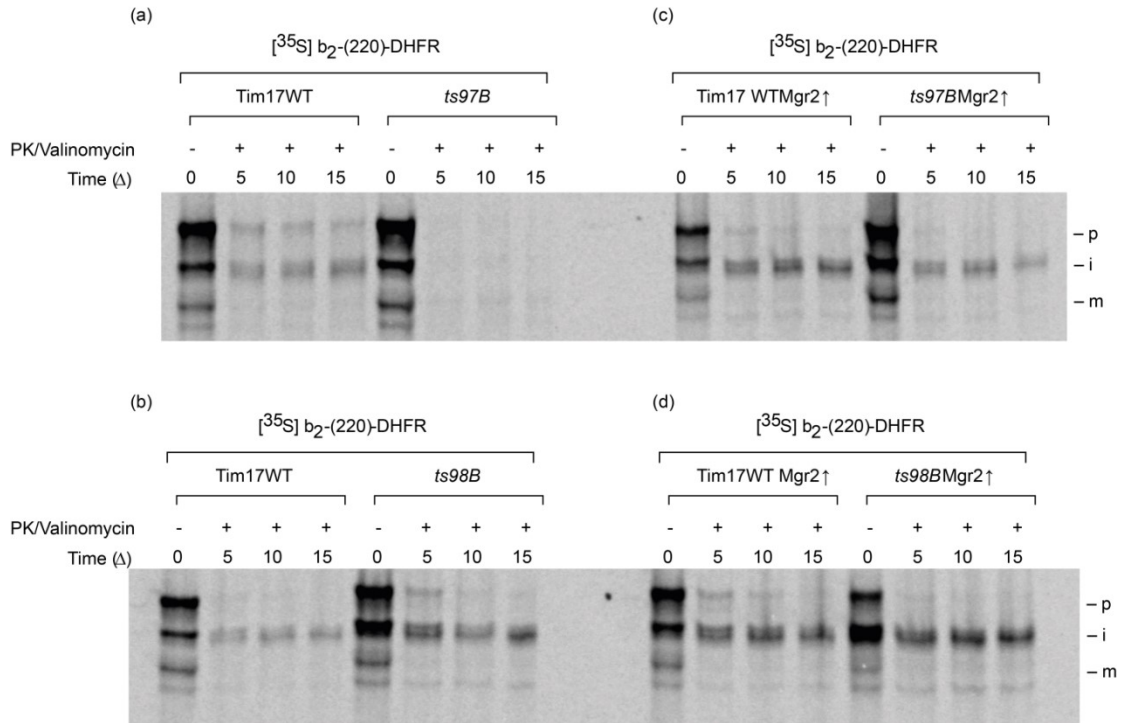


Figure 11: *In vitro* import of radiolabeled b<sub>2</sub>-(220)-DHFR precursor protein is used to perform import at 25°C into Tim17WT, *ts97B* and *ts98B* and overexpression of Mgr2 (Mgr2↑) isolated mitochondria, incubated for 15 mins. Valinomycin is added to dissipate the membrane potential and placed again at 25°C. Samples are removed at different time interval (Δt). Import reaction further treated with proteinase K (+PK) and SEM (-PK). The proteinase K-resistant mature (m), intermediate (i) and precursor (p) forms were analyzed using digital autoradiography.

Further, I wanted to know if Mgr2 protein could rescue the impaired import activity of *ts97B* in the absence of membrane potential. It is known that Mgr2 interacts with positively charged amino acids present before the hydrophobic region and restricts import of hydrophobic precursor protein with a compromised sorting signal. I have used pFL39 plasmid carrying pPGK promoter for overexpression of Mgr2 gene. Isolated mitochondria of Tim17WT, *ts97B*, and *ts98B* in the presence of excess MGR2 protein are used for same experiment. It is observed from the figure 11 (c); (d), that proteinase K protected intermediate form in *ts97B* is observed due to MGR2 overexpression. The excess of MGR2 slightly increases intermediate form in *ts98B* and Tim17WT as well. Hence, the PAM complex weak binding performance to bind with presequence of precursor protein is rescued by MGR2 overexpression

I wanted to know if overexpression of MGR2 affects the protein stability of the TIM23 complexes. Different concentrations (10 µg, 20 µg and 30 µg) of Tim17WT, *ts97B* and *ts98B* isolated mitochondria with and without MGR2 overexpression were loaded on SDS electrophoresis gel and transferred onto PVDF membranes. These membranes were decorated with antibodies against few mitochondrial proteins of the TIM23 complex proteins (Tim23, Tim17) TIM23<sup>SORT</sup> form (Tim21, Mgr2) and TIM23<sup>CORE</sup> form (Tim44, Pam18) and Tim10 protein (subunit of small TIM complex). It was observed that the TIM23 complex, TIM23<sup>SORT</sup> form, and TIM23<sup>CORE</sup> form proteins have similar protein levels in Tim17WT and *tim17ts* mutants, which indicates that the rescue of PAM complex defect is primary based on the excess amount of MGR2. It would be interesting to know about import performance of *tim17ts* mutants in absence of Mgr2.

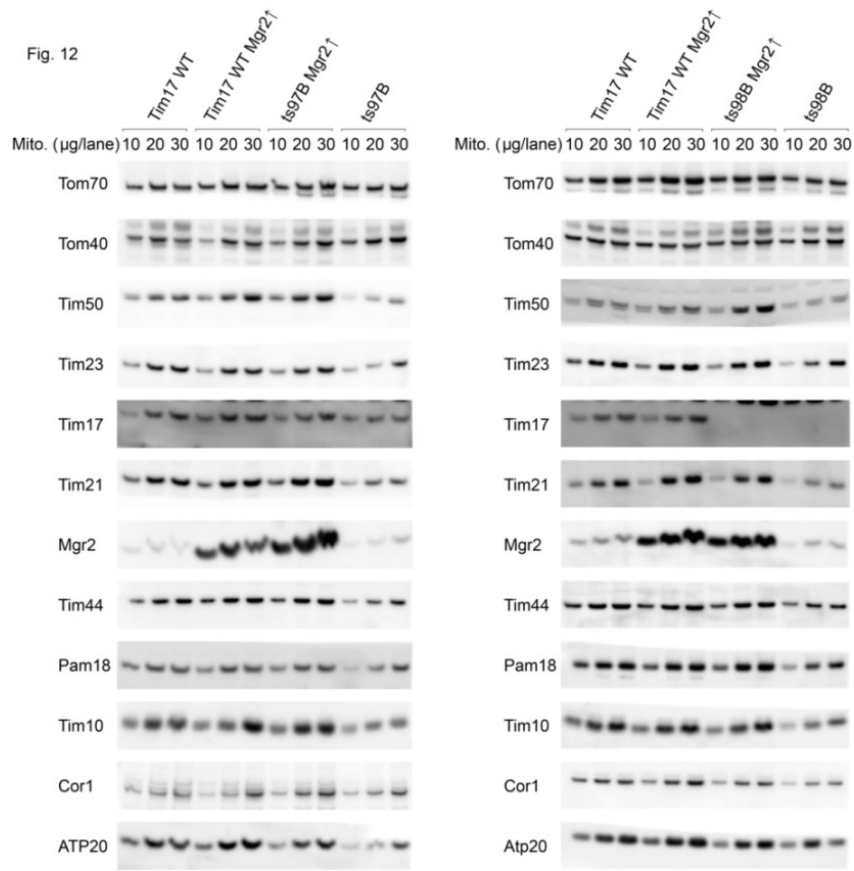


Figure 12: Different concentrations (10, 20 and 30 µg) of isolated mitochondria of Tim17WT, *ts97B* and *ts98B* and with overexpression of Mgr2 (Mgr2↑) are used for steady-state level of different mitochondrial proteins shown by western blot of SDS-PAGE using indicated antibodies.

## V.E Absence of Mgr2 retards the lateral release of precursor protein

The previous observation about Mgr2 as stabilizing factor for *ts97B* rescued compromised import of precursor protein when the membrane potential is disrupted, whereas *ts98B* is comparatively more stable. I wanted to understand the role of Mgr2 in *tim17ts* mutants. I have tried the homologous recombination method for deletion of Mgr2 in *tim17ts* mutants where uracil cassette replaces Mgr2 gene. The deletion of Mgr2 in *ts97B* resulted in no viable colony. Isolated mitochondria of Tim17WT,

Tim17WT $\Delta mgr2$ , *ts98B* $\Delta mgr2$  and *ts98B* at different concentrations (10  $\mu$ g, 20  $\mu$ g and 30  $\mu$ g) was used to observe proteins steady-state level of the TIM23 complex. Samples were run on gel electrophoresis and transferred onto the PVDF membrane. Transferred samples were decorated with the antibodies against TIM23 complex (Tim23, Tim17), TIM23<sup>SORT</sup> form (Tim21 and Mgr2), and TIM23<sup>CORE</sup> form (Tim44 and Pam18) along with respiratory complex protein (Cox4) and small TIM complex (Tim10). As observed in figure 13, the absence of Mgr2 does not affect the TIM23 complex and TIM23<sup>CORE</sup> form protein stability. Only Tim21 and Cox4 protein show reduced protein levels in *ts98B* $\Delta mgr2$ .

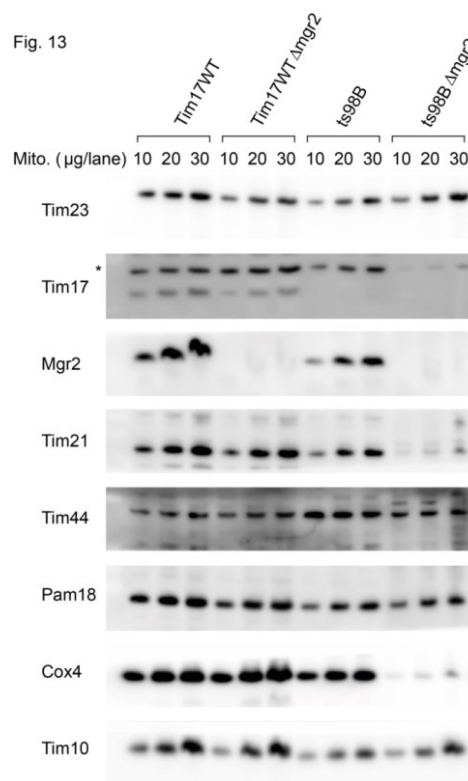


Figure 13: Different concentration (10, 20 and 30  $\mu$ g) of isolated mitochondria of Tim17WT, *ts97B* and *ts98B* and with absence of Mgr2 ( $\Delta mgr2$ ) are used for steady-state level of different mitochondrial proteins shown by western blot of gel electrophoresis using indicated antibodies.

It is already mentioned that Mgr2 recruits Tim21, which is required to position proton pumping respiratory chain complexes closer to the Tim23 complex. The Cox4 subunit is site for the regulation of oxidative phosphorylation of the respiratory chain complex.

In addition, Tim21 and Cox4 protein levels are detected in low amounts only in *ts98BΔmgr2* but Tim17WTΔ*mgr2* isolated mitochondria do not show similar observation; hence Mgr2 deletion could not be the only reason. On the other hand, less protein stability of Tim21 and Cox4 protein in *ts98BΔmgr2* could be due to deleted Mgr2 and Tim17 TM segment mutations combined effect.

I have performed import experiments with precursor proteins [<sup>35</sup>S]b<sub>2</sub>-(167)<sub>Δ</sub>-DHFR and [<sup>35</sup>S]b<sub>2</sub>-(167)-DHFR to know if the absence of Mgr2 would have impact on the import of precursor protein performed by *ts98B*. The experiment setup and quantification of the result are performed similarly to the previously explained differential import response of *tim17ts* mutants (figure: 9).

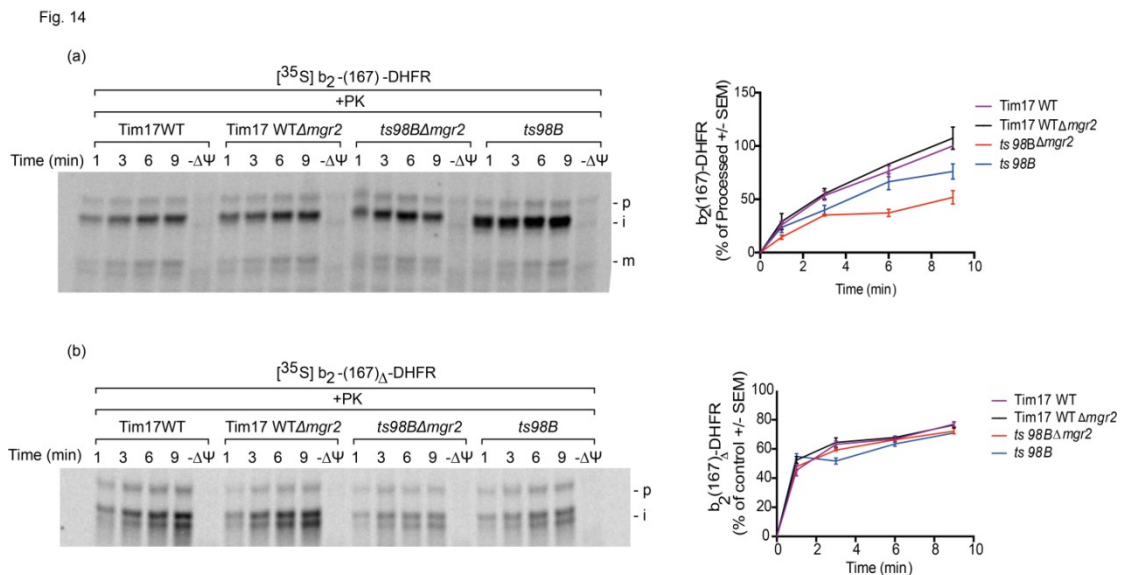


Figure 14: *In vitro* import of lysate carrying precursor protein (a) [<sup>35</sup>S]b<sub>2</sub>-(167)-DHFR and (b) [<sup>35</sup>S]b<sub>2</sub>-(167)<sub>Δ</sub>-DHFR into the isolated mitochondria. Import is performed by adding isolated mitochondria to the lysate at 25°C at different time intervals (minutes) and terminated by adding AVO mix. The addition of AVO mix dissipates membrane potential (-Δψ). Import reaction further treated with proteinase K (+PK). The proteinase K resistant mature (m), intermediate (i) and precursor (p) forms were analyzed using digital autoradiography. The proteinase K protected values of m and i forms are quantified using Fiji and used for plotting graph in prism graph pad. The sum of (i+m) forms are considered as the total amount of precursor protein imported to secure state. The value of m form is divided by the sum to



calculate the percentage of processed b<sub>2</sub>-(167)-DHFR whereas for analysis of b<sub>2</sub>-(167)<sub>Δ</sub>-DHFR import amount of i-form in the proteinase resistant (+PK) samples are quantified and longest time point of Tim17 WT is set to 100% as control. The individual value of i forms divided by the control is calculated. Data are represented as mean ± SEM (n = 3, A); and (n = 3, B).

The isolated mitochondria of Tim17WT, Tim17WT $\Delta$ *mgr2*, *ts98B* $\Delta$ *mgr2* and *ts98B* are energized with ATP and NADH. Import reaction starts with the addition of precursor protein at 25°C. Samples are collected at different time points to observe import rates followed by external proteinase K addition to digest accumulated precursor protein. One of the import reaction treated with AVO mix acts as a control. As shown in figure 14 (a) and (b), the *ts98B* $\Delta$ *mgr2* and *ts98B* show difference in import of hydrophobic signal carrying precursor protein ([<sup>35</sup>S]b<sub>2</sub>-(167)-DHFR), which are laterally sorted across the inner membrane; whereas no significant import defect for the import of [<sup>35</sup>S]b<sub>2</sub>-(167)<sub>Δ</sub>-DHFR, matrix targeted mitochondrial precursor protein. It is already observed in figure 14 (b), *ts98B* has less import of [<sup>35</sup>S]b<sub>2</sub>-(167)-DHFR precursor protein compared to Tim17WT. Deletion of Mgr2 in *ts98B* shows impact as slower release of the precursor protein. The accumulation of intermediate form and conversion to mature form is less in *ts98B* $\Delta$ *mgr2* than *ts98B*. Further, I wanted to know if the  $\Delta$ *mgr2* has any effect on the pulling efficiency of the PAM complex. The PAM complex assessment of binding efficiency of the presequence carrying precursor protein with the internal hydrophobic signal in *ts98* $\Delta$ *mgr2*, a similar experiment, as previously mentioned before (Figure 9), is performed. The DHFR moiety of the [<sup>35</sup>S]b<sub>2</sub>-(220)-DHFR is irreversibly folded by addition of MTX and incubated with isolated mitochondria of Tim17WT, Tim17WT $\Delta$ *mgr2*, *ts98B* $\Delta$ *mgr2* to engage the TOM and TIM23 complex. Further, membrane potential was dissipated by adding valinomycin, and at different time points import reaction was removed. The experimental setup was performed to understand if the precursor protein could be still pulled by the PAM complex solely based on ATP hydrolysis when Mgr2 is deleted in tim17tsmutant; *ts98B* $\Delta$ *mgr2*. As shown in figure 15, intermediate bands of precursor protein are not observed in Tim17WT $\Delta$ *mgr2*, *ts98B* $\Delta$ *mgr2*, similar to *ts97B* (Figure 9 [a]). It indicates that the absence of Mgr2 imposes weak binding efficiency of the PAM complex since it is already known that Mgr2 interacts with the enroute precursor protein while it is inside the TIM23 complex. The *ts98B* can be considered as a phenotype of Mgr2 overexpression and *ts97B* as a phenotype of  $\Delta$ *mgr2*.

Fig. 15

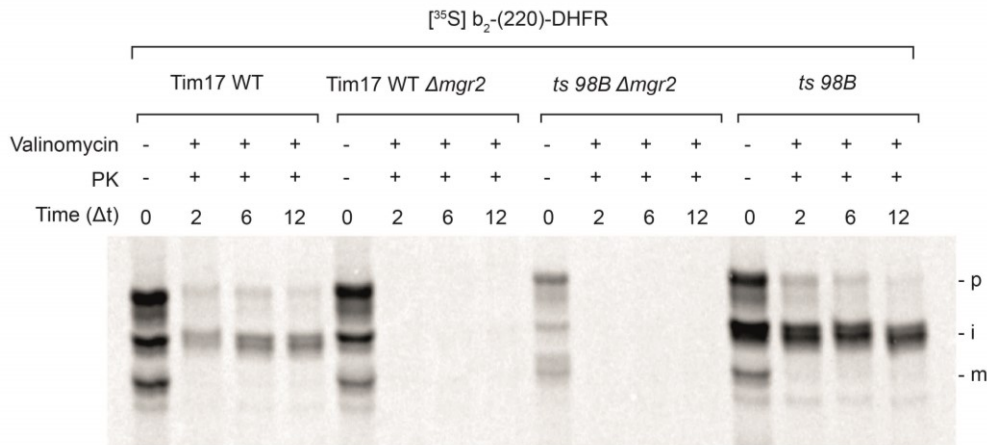


Figure 15: *In vitro* import of radiolabeled b<sub>2</sub>-(220)-DHFR precursor protein is used to perform import at 25°C into isolated mitochondria Tim17WT, *ts98B* and absence of Mgr2 followed by incubation for 15 mins. Valinomycin is added to dissipate the membrane potential and placed again at 25°C. Samples are removed at different time interval ( $\Delta t$ ). Import reaction further treated with proteinase K (+PK) and SEM (-PK). The proteinase K-resistant mature (m), intermediate (i) and precursor (p) forms were analyzed using digital autoradiography.

Further, I performed a spot assay to know about the growth response of Tim17WT, Tim17WT $\Delta mgr2$ , and *tim17ts* mutants with overexpression of Mgr2 and absence of Mgr2 as shown in Figure 16 (a) and (b). The media used for spot assay is minimal dropout media without uracil (-URA) since plasmid has a uracil marker with pPGK promoter to overexpress Mgr2 gene. The glucose and glycerol are added into the media as fermentable and non-fermentable carbon sources. In the presence of an excess of MGR2, the Tim17WT and *tim17ts* mutants could form viable colonies at permissive and elevated temperatures; suggesting that the higher expression of MGR2 rescues the growth defect of *tim17ts* mutants at elevated temperatures. The deletion of Mgr2 significantly affects the growth behavior of *ts98B* at both permissive and elevated temperatures. In comparison, the growth response of Tim17WT $\Delta mgr2$ ,

and *ts98B* are able to form viable colony at permissive (24°C), and *ts98BΔmgr2* can form viable colony but not as alike as *ts98B*. It is observed that the overexpression of Mgr2 and absence of Mgr2 shows the different effects on the growth phenotype of *tim17ts* mutants.

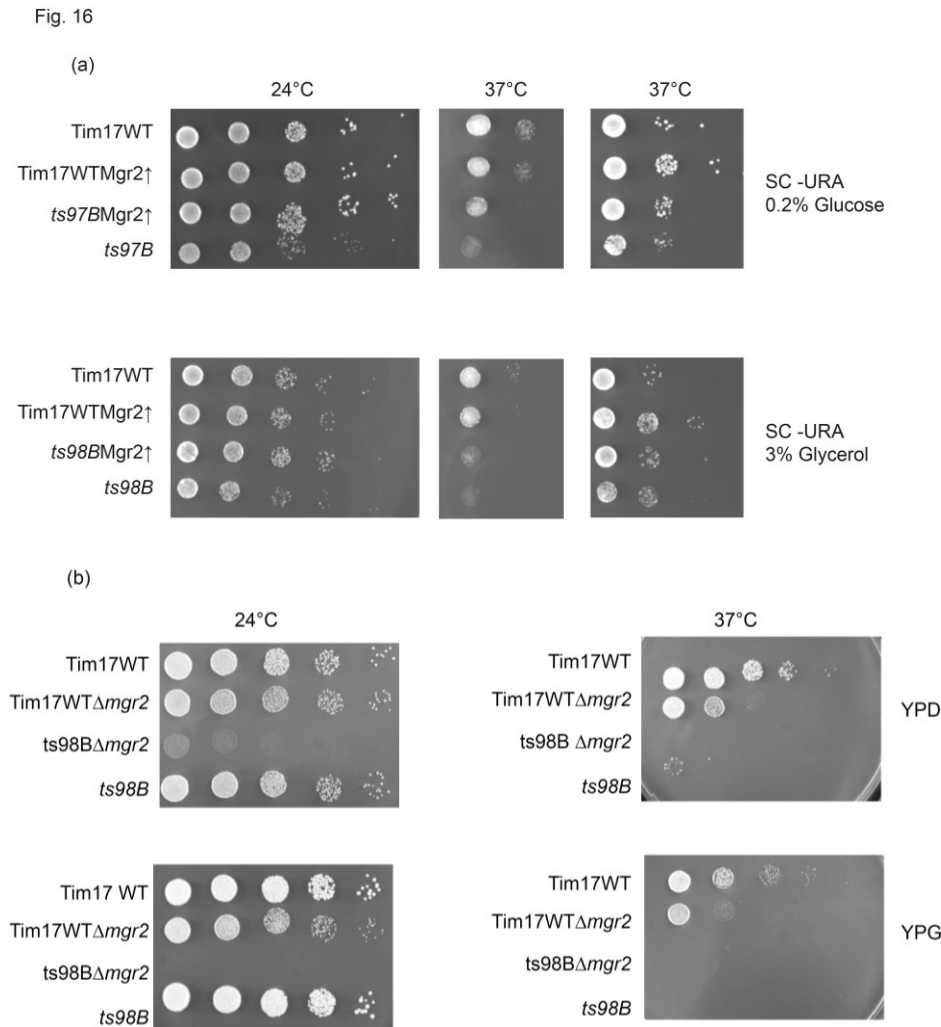


Figure 16: Overnight culture of *tim17ts* mutants and WT with over expression of Mgr2 (*Mgr2*↑) and absence of Mgr2 (*Δmgr2*) were subsequently diluted to  $OD_{600} = 0.5$  in -Ura drop out media, and YPG medium respectively and incubated for 5 hours at 24°C. Cultures were further diluted to  $OD_{600} = 0.1$  and then fivefold serially diluted samples were used for spot assay. Tim17WT, *ts97B* and *ts98B* with *Mgr2*↑ and *Δmgr2* were used for spot assay at the indicated temperatures on medium containing SC-URA (drop down media without uracil), YPD (Glucose), YPG (Glycerol), and optical density 600 nm ( $OD_{600}$ ).

## V.F Expression of Tim23 alters import precursor protein

The mitochondrial DNA (mtDNA) encodes significantly higher hydrophobic genes than the nuclear genome that forms respiratory chain complexes and oxidative phosphorylation machinery (OXPHOS). The mitochondrial OXPHOS machinery produces most ATP for cellular processes in the eukaryotic cell compared to any other organelle. Compromised OXPHOS function results in various mitochondrial-related diseases. Hence relocating the gene of OXPHOS from mtDNA to the nuclear genome for its allotropic gene expression could be a potential gene therapy approach. The group of Prof. Jean paul di Rago was interested in studying the allotropic expression of ATP9, which encodes subunit 9/c of ATP synthase. The ATP9 gene has two transmembrane segments, which are highly hydrophobic. Few changes were made for the allotropic expression of the hydrophobic ATP9 gene since the native proteins hydrophobicity could result in aggregation and become inactive during transport from cytosol to mitochondria. In the fungus, *Neurospora crassa* encodes for ATP9 in the nuclear and mitochondrial genome. Upon phylogenetic analysis, the first TM segment of the ATP9 gene from *N. crassa* was fused with the connecting loop to the second TM segment of the ATP9 gene of *S. cerevisiae* to reduce the overall hydrophobicity for cytosolic transfer of protein into mitochondria. This construction of the ATP9 gene was termed a hybrid construct. Transformation of the hybrid construct into yeast parental strain produced only one colony after a long incubation period. Whole-genome transcription profiling using a high-resolution tiling microarray was performed to identify target genes responsible for yeast cell survival. It was found that single amino acid substitution (G276C) where amino acid Glycine (G) at position 276 of *cst6* gene is substituted by Cysteine (C) of the nuclear gene of *cst6* was responsible for the survival of the yeast cell. The *cst6* belongs to the family of basic leucine zipper (bZIP). It is known as paralogue of one of the transcription factors of the Tim23 gene, which indicates that yeast cells survival could be due to the difference in expression or activity of the TIM23 complex. In collaboration with Prof. Jean paul di Rago, I was interested to know if *cst6(G276C)* affects the stability and function of Tim23 protein, which forms the TIM23 complex. I was provided with three yeast strains as mentioned in table 3, The first strain as KGY8/2 (referred to as Wild Type) is used as isogenic control and two other strains such as KGY6/2 (referred as *cst6-1*) has a point mutation

[*cst6-G276C*] of the nuclear genome, and KGY5 (referred to as *cst6-2*) has the same mutation introduced in the nuclear genome by CRISPR/Cas9 technique.

Strain name	Referred as (in this study)
KGY8/2 (Fond MR6)	Wild type (WT)
KGY 6/2 (Fond SUPO + CRISPR <i>cst6-G276C</i> )	<i>cst6-1</i>
KGY 5 (Fond SUPi + <i>cst6-G276C</i> )	<i>cst6-2</i>

Table 3: The name used in this study for the *cst6* mutant strains which were provided by Prof. Jean paul di Rago.

I performed a spot assay to observe the growth behavior of the *cst6* mutants at different temperatures. The yeast culture of WT, *cst6-1*, and *cst6-2* were incubated at 30°C overnight. The overnight culture was diluted to the OD<sub>600</sub> = 0.1 and incubated further to grow for 5 hours. After incubation, OD<sub>600</sub> was normalized to 0.05 and serially diluted up to fivefold for spot assay. The media used for spot assay has fermentable (glucose) and non-fermentable carbon source (glycerol). The growth of *cst6* mutants on both media shows no difference in growth phenotype at different temperatures (30°C and 37°C), as shown in Figure 17 (a). The slow growth of *cst6* mutants and WT at 37°C on non-fermentable media is a normal growth phenotype of yeast culture at higher temperatures. It is observed that *cst6(G276C)* amino acid substitution in yeast strains' nuclear genome does not affect the growth phenotype. Further, relative protein expression of isolated mitochondria was performed to know if the *cst6* mutation affects the protein stability of the translocase complexes such as the TOM and TIM23 complex. The steady-state level of proteins using three different concentrations of WT, *cst6-1*, and *cst6-2* isolated mitochondria was loaded on Tris Tricine electrophoresis gel and transferred onto the PVDF membrane. Membranes were decorated with antibodies against few mitochondrial proteins of the TOM complex (Tom70 and Tom22), the TIM23 complex (Tim23, Tim50, Tim17, Tim21, and Tim44) and few proteins of the respiratory chain complexes (Cox4 and Atp20).

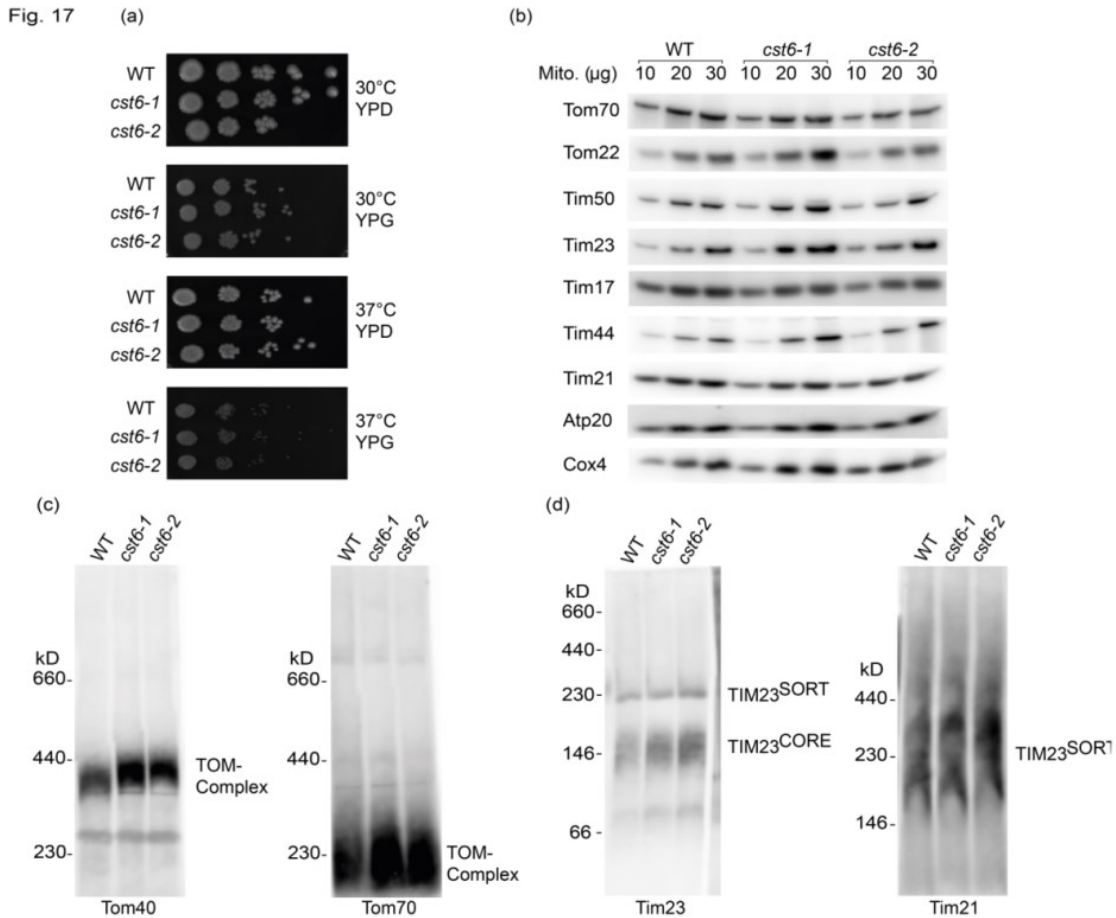


Figure 17: Overnight culture of WT, *cst6-1* and *cst6-2* were subsequently diluted to optical density 600 nm ( $OD_{600}$ ) = 0.5 in YPG medium and grown for 5 hours, Cultures were diluted to  $OD_{600}$  = 0.1 and then fivefold serially diluted samples were used for spot assay. WT, *cst6-1* and *cst6-2* were incubated for 4 days at indicated temperatures on medium containing fermentable (YPD) and non-fermentable (YPG) carbon source. (B) Steady state level of subunits of the TOM complex (Tom70 and Tom22), the TIM23 complex (Tim50, Tim23, Tim17, Tim44, and Tim21) proteins and respiratory complex proteins (Atp20 and Cox4) steady state level is performed by loading different concentration (10, 20 and 30 µg) of isolated mitochondria on electrophoresis gel followed by immuno blotting and decorated with indicated antibodies. (c) Isolated mitochondria were solubilized in digitonin to observe (c) the TOM complex and (d) the TIM23 complex, by BN PAGE electrophoresis and western blotting. The TOM and TIM complexes are decorated with mentioned antibodies.

Figure 15 (b), *cst6-1* and *cst6-2* show reduced protein levels of Tim17, Tim21, and Tom70 proteins, whereas the increased level of Tim50, Tim23, and Tim44 protein levels compared to wild type. The protein level of Atp20 and Cox4 remains similar in both the *cst6* mutants as wild type. The BN-PAGE was performed to observe membrane complex proteins in their native form. The isolated mitochondria of WT, *cst6-1*, and *cst6-2* were solubilized in 1% of digitonin and run on BN-PAGE. The PVDF membranes were decorated with antibodies against Tom40 and Tom70 protein to observe the TOM complex. The Tom40 and Tom70 antibodies detected the TOM complex of approximately 430 kDa and 230 kDa. The *cst6-1* mutant shows more formation of the TOM complex as compared to *cst6-2* and WT. The TIM23 complex has two different forms, such as TIM23<sup>SORT</sup> (formed with the Tim21 and Mgr2 subunits) and TIM23<sup>CORE</sup> (formed with the PAM complex). The Tim23 antibody is used to label both the forms, whereas the Tim21 antibody could detect only TIM23<sup>SORT</sup> complex. The TIM23<sup>CORE</sup> form is of approximately 230kDa, and the TIM23<sup>SORT</sup> form is of approximately 130 kDa. It was observed that formation of the TIM23<sup>CORE</sup> form is comparatively higher in the *cst6-2* mutant, as shown in figure 17 (d). The steady-state level and solubilized membrane complexes show that the proteins of the TIM23 complex are increased in *cst6-1* and *cst6-2* mutants. Further, *in vitro* import experiments were performed to understand how increased expression of Tim23 protein influence the import of precursor protein.

The TIM23 complex imports precursor proteins of two different types such as presequence carrying matrix targeted precursor proteins and internal signal carrying precursor proteins, which are laterally sorted across the inner membrane. In order to understand how mutation (G276C) of *cst6* affects the import activity of the TIM23 complex, both types of precursor proteins should be used to perform import experiments. To study the matrix import performed by *cst6* mutants, the b2 precursor proteins, [<sup>35</sup>S]b<sub>2</sub>-(167)<sub>Δ</sub>-DHFR and [<sup>35</sup>S]b<sub>2</sub>-(F1β)-DHFR is used whereas [<sup>35</sup>S]b<sub>2</sub>-(167)-DHFR and [<sup>35</sup>S]b<sub>2</sub>-(220)-DHFR are used to study lateral release into the inner membrane. The import buffer with ATP and NADH was used to energize isolated mitochondria of the WT and *cst6-1* and *cst6-2* mutants. The import reaction was started by the addition of lysate carrying precursor proteins and incubated at 25°C. The samples were removed at different time points and treated with proteinase K to

Fig. 18

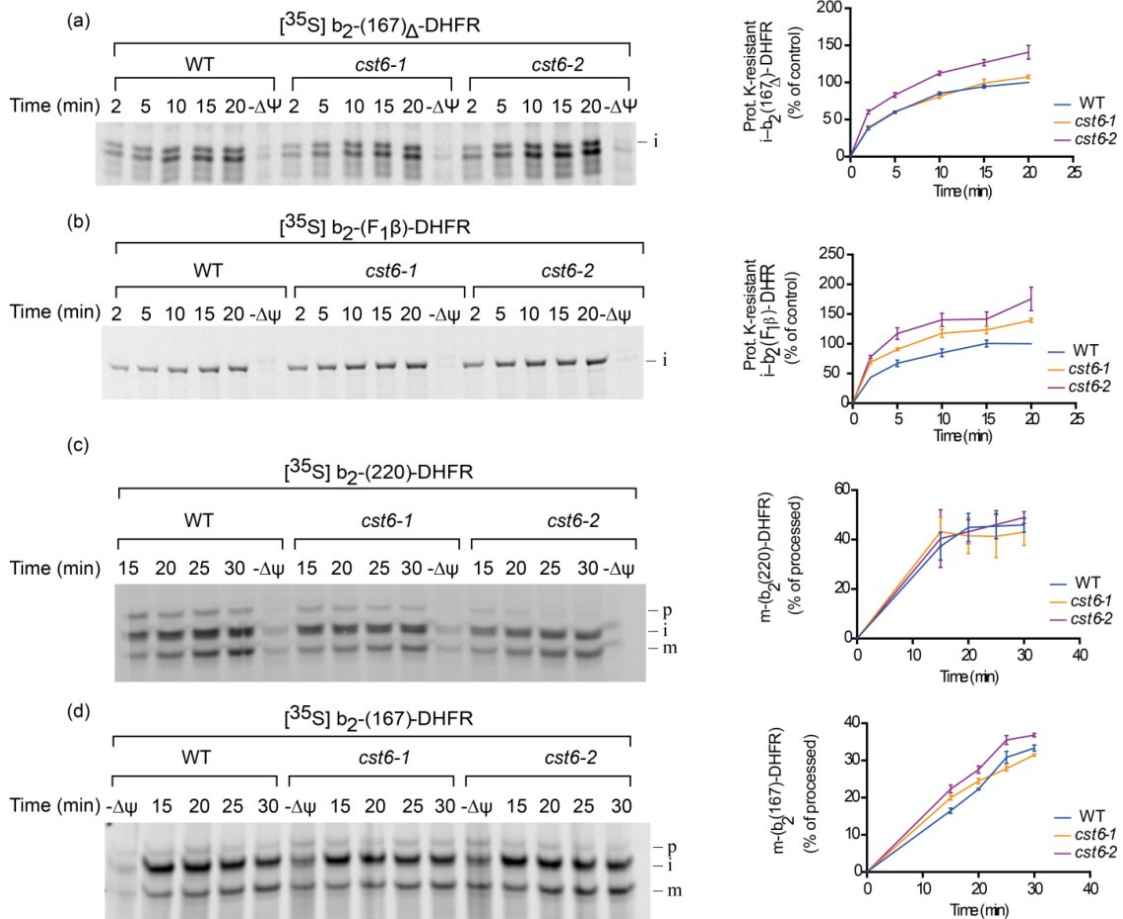


Figure18: *In vitro* matrix import is analyzed using (a)  $[^{35}\text{S}] \text{b}_2\text{-(167)}\Delta\text{-DHFR}$  (b)  $[^{35}\text{S}] \text{b}_2\text{-(f1}\beta\text{)-DHFR}$  and (c)  $[^{35}\text{S}] \text{b}_2\text{-(220)-DHFR}$  and (d)  $[^{35}\text{S}] \text{b}_2\text{-(167)-DHFR}$  lysate carrying precursor proteins are used to analyze lateral import into the inner membrane. The isolated mitochondria of WT, *cst6-1* and *cst6-2* is used to perform import experiment by adding lysate at 25°C. At different time intervals (minutes) samples were removed and reaction was terminated by adding AVO mix. Membrane potential ( $\Delta\psi$ ) of the import reaction is dissipated by addition of AVO mix. Import reaction is treated by adding external proteinase K (+PK). The proteinase K-resistant intermediate (i) forms ( $[^{35}\text{S}] \text{b}_2\text{-(167)}\Delta\text{-DHFR}$  and  $[^{35}\text{S}] \text{b}_2\text{-(f1}\beta\text{)-DHFR}$ ) were analyzed using digital autoradiography. The amount of i-form in the proteinase resistant (+PK) samples is quantified. Longest time point of WT was set to 100% for percent of control. Data are represented as mean  $\pm$  SEM (n = 3). The proteinase K-resistant mature (m) and intermediate (i) forms ( $[^{35}\text{S}] \text{b}_2\text{-(220)-DHFR}$  and  $[^{35}\text{S}] \text{b}_2\text{-(167)-DHFR}$ ) were analyzed using digital



autoradiography. The amount of proteinase K protected m-form was divided by the sum (i+m) for the percent of processed. Data are represented as mean  $\pm$  SEM (n = 3)

digest the accumulated precursor protein. One of the import reactions was impaired by the addition of AVO mix to dissipate the membrane potential serves as control. From the import experiments, as shown in figure 18 (a), it was observed that the *cst6-2* mutants imports  $b_2(167)_\Delta$ -DHFR, matrix targeted precursor protein at a much faster rate than the WT and *cst6-2*. In import reaction with  $b_2(F1\beta)$ -DHFR, the import of *cst6-1* and *cst6-2* show significantly higher import kinetics than the WT. The slower import of  $b_2(167)_\Delta$ -DHFR compared to  $b_2(F1\beta)$ -DHFR precursor protein in *cst6-2* could be due to either reason. Firstly, precursor protein of the  $\beta$ -subunit of the F1F0-ATP synthase is a native protein of inner membrane and requires different level of membrane potential compared to the cytochrome  $b_2$  precursor protein. The absence of heme domain in the  $b_2$ -F1 $\beta$ -DHFR favors efficient binding of the PAM complex to pull the precursor protein inward towards the matrix at lesser expense of ATP. Comparatively, while import of  $b_2$ -F1 $\beta$ -DHFR, the PAM could initiate a new round of ATP hydrolysis cycle to import the precursor protein early than the  $b_2(167)_\Delta$ -DHFR. Second, the deletion of 19 amino acid carrying hydrophobic sequence is performed to redirect the  $b_2(167)_\Delta$ -DHFR precursor protein towards matrix and in contrast, no modification or deletion of amino acid is required to direct the  $b_2$ -F1 $\beta$ -DHFR precursor protein. The difference in import rate of matrix targeted precursor protein by *cst6-1* and *cst6-2* was much prominent for  $b_2$ -F1 $\beta$ -DHFR compared to  $b_2(167)_\Delta$ -DHFR. Whereas the laterally sorting precursor protein, as shown in figure 18 (c) and (d). It is observed that the *cst6-1* and *cst6-2* shows a similar level of intermediate form and mature form of the precursor protein  $b_2(220)$ -DHFR compared to WT. The import rate of *cst6-1* and *cst6-2* is slightly different for the precursor protein  $b_2(167)$ -DHFR. Although keeping in account that both the precursor protein has a difference in length only due to a few amino acid sequences, it includes the heme-binding domain. To pull the heme-binding domain against the TOM and TIM23 complex, the PAM complex requires more energy and duration. It is suggested that an increase in import rate or difference between import rates of *cst6-1* and *cst6-2* could be possible observed only if long interval of time points were employed. Also, similar import experiments can be performed by using purified cytochrome  $b_2$  because radiolabelled precursor protein tends to have dynamic import rate.

## VI. Discussion

The general import pore composed of twin pore, TOM complex is known to be formed majorly by Tom40,  $\beta$ -barrel structure with other constituents such as Tom20, Tom21 and Tom70 as part of multisubunit machinery. Similarly, it was suggested by few groups about TIM23 complex (composed of alpha helices) possess twin pore together formed by Tim23 and Tim17 in the inner membrane for import of precursor protein across the inner membrane and into the matrix (Lister et al., 2005; Pareek et al., 2013). Such theories are still under debate since structure of the TIM23 complex is unclear. In comparison, patch-clamp studies have shown that Tim17p does not perform any channel activity or form translocase pore in the absence of Tim23p (Martinez-Caballero et al., 2007). Transmembrane segments of the Tim23 and Tim17 facing either towards matrix or IMS were incorporated with mutation and studied individually to understand the architecture of the TIM23 complex. The shared homology of TM segments of Tim23 and Tim17 supports the formation of the TIM23 complex, where voltage-gated import channel is formed by Tim23 and stabilized by Tim17 (Lister et al., 2005).

Biogenesis of the TIM23 complex and import regulation by Tim23 is intensively studied, which shows that mutations in Tim23 results in reduced import activity and destabilized complex (Potting et al., 2018). Due to the relative homology of TM segments, overexpression of Tim17 rescues the import and substrate recognition defect of Tim23 to an extent. The TM1 and TM2 of Tim17 are physically involved in maintaining the stoichiometry of the TIM23 complex (Günsel & Mokranjac, 2019). The formation of two dynamically inter-changeable states of the TIM23 complex, TIM23<sup>CORE</sup> and TIM23<sup>SORT</sup> are formed while importing precursor protein with presequence and hydrophobic internal signal. While studying the formation of these two states, Prof. Agnieszka Chacinska group has reported *tim17* mutants, *tim17-4* and *tim17-5*, to behave similarly like PAM complex mutant and delayed response regarding lateral sorting process of the hydrophobic precursor protein (Chacinska et al., 2010; Chacinska et al., 2005).

In this study, *tim17ts* mutants; *ts97B* and *ts98B* show steady protein level of TIM23 complex components regardless of mutation found in TM2 of *ts97B*; TM1 and TM3 of *ts98B*. The integrity of the translocase complex depends on the amount of each constituent involved in forming the assembly. Few components of the PAM complex, such as Pam17, are less eluted while performing pulldown using ProteinA-tag Tim23 isolated mitochondria of *ts98B*, which could be due to the mutations in TM1 and TM3 region of Tim17. It is known that matrix facing TM segments of Tim17 interact with the PAM complex components, such as Tim44 and Pam17 (Pareek et al., 2013; van der Laan et al., 2005). The reduced amount of PAM components observed in *ts98B* could be due to weaker binding influenced by mutations; however, functional and interactive patterns of Tim17 and PAM complex are still under study.

Experiments used to understand import kinetics of *tim17ts* mutants shows that the matrix targeted presequence carrying precursor protein is imported efficiently with no significant difference. Import rate of *ts97B* and *ts98B* shows an opposing response only during the import of laterally sorted precursor protein across the inner membrane. As compared to Tim17WT, *ts97B* shows high, and *ts98B* shows low import kinetics. The differential import rate shows that restrictive regulation of Tim17 in *ts97B* and *ts98B* does not affect the import of matrix targeted precursor protein. In order to understand the differential sorting behavior of *tim17ts* mutants, the pulse-chase experiment was performed since the biogenesis of precursor protein allows us to understand the difference between processing level of precursor protein. In the pulse-chase experiment, accumulated intermediate form resembles engaged TOM-TIM23 complex (pulse) and release of precursor protein forms mature state upon cleavage (chase). The C terminal DHFR moiety of the hydrophobic signal carrying precursor protein; b<sub>2</sub>-220-DHFR, is reversibly folded to engage the TOM-TIM23 complex, represents the active engagement of the import sites. It forms integration of TOM-TIM23 complexes before the lateral release of precursor protein across the inner membrane as a non-rate limiting step. The precursor protein is released from the engaged TOM-TIM23 complex only in the absence of DHFR substrates, which allows interpreting the result based upon precursor proteins cleavage. The cleavage of precursor is possible only when precursor protein is accessible after succeeding release from the TIM23 complex. Upon the cleavage of the precursor protein, converting intermediate to mature state of precursor protein represents efficiency and

activity of Tim17 for importing laterally sorted precursor protein. It is observed that significantly higher sorting of precursor protein is performed by *ts97B* and retarded in *ts98B*. Our group has reported that hydrophobic precursor protein is rapidly released in the absence of Mgr2 and retarded if Mgr2 is overexpressed (Ieva et al., 2014). It could be summarized that *ts97B* is a phenocopy of  $\Delta mgr2$  mutant and *ts98B* is a phenocopy of MGR2 overexpression. Also the biogenesis of hydrophobic precursor protein displayed by *ts97B* and *ts98B* in the pulse chase experiment is similar to the mutants of Mgr2. The Mgr2, a small hydrophobic protein, is actively involved with the lateral sorting of precursor protein across the inner membrane (Gebert et al., 2012). The deletion of Mgr2 and overexpression has an opposing effect on the import of hydrophobic protein. The mechanism of Mgr2 reveals that precursor proteins halt inside the TIM23 complex and are laterally released at a slower rate (stop-transfer mechanism) across the inner membrane (Steffen & Koehler, 2014). In contrast, Mgr2 deletion accelerates the lateral release of precursor protein. A novel subunit ROMO1 of the TIM23 complex in a human was identified to be an orthologue of Mgr2. Like Mgr2, ROMO1 is also required to establish the connection of Tim23 with respiratory chain complexes via Tim21 (Matta et al., 2020; Richter et al., 2019). Hence, the activity of Mgr2 remains to be conserved as an active participant for recognition and import of precursor protein.

In order to understand how Tim17 decodes lateral sorting of hydrophobic precursor protein, membrane potential was dissipated to observe the binding efficiency of the PAM complex. In the absence of membrane potential, the import process could be evaluated solely based on ATP hydrolysis. The PAM complex performs ATP hydrolysis to pull the precursor protein towards matrix, and upon cleavage of presequence, the hydrophobic signal implies lateral insertion. The PAM complexes weak binding suggests that the precursor protein is not sufficiently pulled against the TOM-TIM23 complex to attain a certain state against protease. It is observed that in *ts97B*, the PAM complex holds weak binding of precursor protein. The precursor protein in *ts97B* backslides through the TOM complex and accessible to externally added proteinase K. The overexpression of Mgr2 from an external plasmid shows the defect of *ts97B* could be rescued. Suggesting that Tim17 performs the lateral release of the precursor protein as an opening towards the inner membrane and Mgr2 provides stability for the same. The group of Prof. Peter Rehling have used

Tim17-PAM18 fusion construct, which results in the displacement of Mgr2 from the TIM23 complex. The displacement of Mgr2 is due to the overlapping of binding sites at the lateral gate, regulated by the PAM18 (Schendzielorz et al., 2018). We speculate that the fusion construct supports constant contact with the PAM complex and would not support the release of precursor protein across the inner membrane; hence, use of *tim17ts* mutants to understand the biogenesis of precursor protein with the sorting signal is more consistent. This study suggests that Tim17 is a regulatory unit and preferably interacts and recognizes the inner membrane precursor proteins. The Tim17 would be actively involved in the lateral sorting of precursor protein across the inner membrane. Further, it is observed that deletion of Mgr2 in *ts98B* mutant does not affect the import of matrix targeted precursor proteins and protein stability of components of the TIM23 complex is unaltered. In contrast, only import of hydrophobic precursor protein becomes more retarded. Interestingly, the PAM complexes pulling efficiency in the absence of Mgr2 to pull the precursor protein against TOM-TIM23 complex observed in *ts98B* is same as *ts97B*. The growth defect of *tim17ts* mutants is rescued by the excess of Mgr2, which strengthens the observation that Tim17 and Mgr2 together are involved in laterally sorting the precursor protein where Tim17 actively recognizes the precursor protein and Mgr2 delays the release as a gatekeeper.

The transfer of mitochondrial gene ATP9 to the nuclear genome to understand the genes allotopic expression could be beneficial for several reasons (Martos et al., 2012). One of them is to reduce the burden of mtDNA mutation over mitochondrial metabolism, and therapeutic approach towards mtDNA linked to disease, especially related to dysfunction of respiratory chain complexes. The yeast cell employed for the allotopic expression encountered amino acid substitution for survival resulting in *cst6* mutant. The *cst6* is known to be one of the transcriptional factors of Tim23 protein and belongs to the bZIP family similar like ATFS-1. In case of any stress condition encountered by cell, ATFS-1 acts as transcription factor to activate mitochondrial unfolded protein response (UPRmt), including mitochondrial matrix protease (Wu et al., 2018). To understand effects of transcriptional attenuation of Tim23 due to *cst6* mutation, we had collaboration with Prof. Jean Paul di Rago to understand the effect of *cst6* mutation on the regulation of the TIM23 complex.

One of the studies performed to understand transcriptional attenuation of Tim17A in *C. elegans*, explains how mitochondrial matrix misfolded proteins lead to activation of UPR<sub>mt</sub>, which in turn leads to adaptive measures such as transcriptional program promoting mitochondrial recovery (negative feedback loop) (Jovaisaite & Auwerx, 2015; Rainbolt et al., 2013). The Tim23 protein actively participates in the import of precursor protein by maintaining its organized collaborative interaction with the TOM complex, PAM complex, and other accessory proteins. A difference in the relative steady-state level of TIM23 complex proteins is observed. The *cst6* mutants show reduced levels of Tim17, Tim21, and Tom70 proteins, whereas the increased level of Tim50, Tim23, and Tim44 compared to wild type. The *cst6* is one of the translational factors of the Tim23 gene; the difference in protein steady state of TIM23 complex proteins could respond to altered import rate. The increased import of matrix targeted precursor protein is observed in the *cst6* mutants, which could be due to the increased expression of Tim50, Tim23, Tim44, and Tom22 proteins (Oliveira & Hood, 2018). It is observed that the higher and lower stability level of few set of proteins observed in *cst6-1* and *cst6-2*, could be the reason for the increased import of matrix targeted precursor protein since mitochondrial matrix is more equipped with protease machinery to process the precursor protein.

The transcriptional attenuation of Tim23 in *cst6* mutants could not be fully explained by increased import of matrix targeted precursor protein since there could be various upstream or downstream process undertaken by *cst6* mutants. It was shown by Dr. Schmidt group that PKA dependent phosphorylation of Tom70 regulates the activity of the TOM complex. The cAMP-dependent protein kinase A (PKA), phosphorylation activity is regulated differentially in the presence and absence of fermentable carbon source (glucose) (Schmidt et al., 2011). The cooperation and function of cytosolic chaperons and TOM complex have already been shown by many research groups, which conclude that via ATP hydrolysis, Hsp70 together with Hsp40 docks the metabolite carrier precursor protein at the recognition site of Tom 70. Further, these precursor proteins are transferred to Tom40, major twin pore-forming import transduction opening for import across the outer membrane. In the presence of glucose, PKA phosphorylates Tom40 residue Ser174 (one among the wide variety of targets) (Rao et al., 2012). The modification hampers interaction of Hsp70 and Tom40 and results in the decreased import of carrier protein to the inner membrane.

Collectively, it shows that the decreased import of carrier protein is not related to the Tom70 decreased activity (Opalińska & Meisinger, 2014). In contrast, phosphorylation modulates the protein import in response to either cellular, mitochondrial or environmental hindrance. This description supports that the increased expression of the Tim23 and higher import activity could be not only be limited to the transcriptional level but it could be also related to metabolic and developmental stage.

Our study supports that the Tim23 is preferably involved in importing matrix targeted precursor protein as shown by import response of different precursor proteins in *cst6-1* and *cst6-2* mutants due to transcriptional attenuation of Tim23. The *tim17ts* mutants show that the Tim17 is actively involved for lateral sorting of hydrophobic precursor protein across the membrane and Mgr2 is a regulatory unit that participates in lateral sorting along with Tim17 which forms an opening towards the inner membrane. As a further perspective, factors responsible for the interaction of precursor protein with Mgr2 and PAM complex could be related to the interdependence strategy practiced by Tim17 and Tim23 for import either across the inner membrane or towards the matrix.

## VII. References

1. Ahting, U., Thieffry, M., Engelhardt, H., Hegerl, R., Neupert, W., & Nussberger, S. (2001). Tom40, the pore-forming component of the protein-conducting TOM channel in the outer membrane of mitochondria. *Journal of Cell Biology*, 153(6), 1151–1160. <https://doi.org/10.1083/jcb.153.6.1151>
2. Ahting, U., Thun, C., Hegerl, R., Typke, D., Nargang, F. E., Neupert, W., & Nussberger, S. (1999). The Tom Core Complex. *Journal of Cell Biology*, 147(5), 959–968. <https://doi.org/10.1083/jcb.147.5.959>
3. Allu, P. K., Marada, A., Boggula, Y., Karri, S., Krishnamoorthy, T., & Sepuri, N. B. V. (2015). Methionine sulfoxide reductase 2 reversibly regulates Mge1, a cochaperone of mitochondrial Hsp70, during oxidative stress. *Molecular Biology of the Cell*, 26(3), 406–419. <https://doi.org/10.1091/mbc.E14-09-1371>
4. Anderson, A. J., Jackson, T. D., Stroud, D. A., & Stojanovski, D. (2019). Mitochondria—hubs for regulating cellular biochemistry: Emerging concepts and networks. *Open Biology*, 9(8). <https://doi.org/10.1098/rsob.190126>
5. Baker, M. J., Mooga, V. P., Guiard, B., Langer, T., Ryan, M. T., & Stojanovski, D. (2012). Impaired folding of the mitochondrial small TIM chaperones induces clearance by the i-AAA protease. *Journal of Molecular Biology*, 424(5), 227–239. <https://doi.org/10.1016/j.jmb.2012.09.019>
6. Banci, L., Bertini, I., Cefaro, C., Ciofi-Baffoni, S., Gallo, A., Martinelli, M., Sideris, D. P., Katrakili, N., & Tokatlidis, K. (2009). MIA40 is an oxidoreductase that catalyzes oxidative protein folding in mitochondria. *Nature Structural and Molecular Biology*, 16(2), 198–206. <https://doi.org/10.1038/nsmb.1553>
7. Banerjee, R., Gladkova, C., Mapa, K., Witte, G., & Mokranjac, D. (2015). Protein translocation channel of mitochondrial inner membrane and matrix-exposed import motor communicate via two-domain coupling protein. *ELife*, 4, 1–17. <https://doi.org/10.7554/eLife.11897>
8. Bauer, M. F., Sirrenberg, C., Neupert, W., & Brunner, M. (1998). Biogenesis of Tim23 and Tim17, integral components of the TIM machinery for matrix-targeted preproteins. *EMBO Journal* 17(6), 1569–1576. <https://doi.org/10.1093/emboj/17.6.1569>
9. Bausewein, T., Mills, D. J., Langer, J. D., Nitschke, B., Nussberger, S., & Kühlbrandt, W. (2017). Cryo-EM Structure of the TOM Core Complex from *Neurospora crassa*. *Cell*, 170(4), 693–700.e7. <https://doi.org/10.1016/j.cell.2017.07.012>
10. Ben-Aroya, S., Pan, X., Boeke, J. D., & Hieter, P. (2010). Making temperature-sensitive mutants. In *Methods in Enzymology* (2nd ed., Vol. 470, Issue C). Elsevier Inc. [https://doi.org/10.1016/S0076-6879\(10\)70008-2](https://doi.org/10.1016/S0076-6879(10)70008-2)
11. Bohnert, M., Pfanner, N., & van der Laan, M. (2007). A dynamic machinery for import of mitochondrial precursor proteins. *FEBS Letters*, 581(15), 2802–2810. <https://doi.org/10.1016/j.febslet.2007.03.004>
12. Bolender, N., Sickmann, A., Wagner, R., Meisinger, C., & Pfanner, N. (2008). Multiple pathways for sorting mitochondrial precursor proteins. *EMBO Reports*, 9(1), 42–49. <https://doi.org/10.1038/sj.embor.7401126>
13. Bragoszewski, P., Wasilewski, M., Sakowska, P., Gornicka, A., Böttinger, L., Qiu, J., Wiedemann, N., Chacinska, A. (2015). Retro-translocation of mitochondrial intermembrane space proteins. *Proceedings of the National Academy of Sciences of the United States of America*, 112 (25) 7713–7718, <https://doi.org/10.1073/pnas.1504615112>
14. Brand, M. D., Orr, A. L., Perevoshchikova, I. V., & Quinlan, C. L. (2013). The role of mitochondrial function and cellular bioenergetics in ageing and disease. *British Journal of Dermatology*, 169(SUPPL.2), 1–8. <https://doi.org/10.1111/bjd.12208>



15. Britti, E., Delaspre, F., Tamarit, J., & Ros, J. (2018). Mitochondrial calcium signalling and neurodegenerative diseases. *Neuronal Signal*, 2 (4), 1–11. <https://doi.org/10.1042/NS20180061>
16. Brix, J., Rüdiger, S., Bukau, B., Schneider-Mergener, J., & Pfanner, N. (1999). Distribution of binding sequences for the mitochondrial import receptors Tom20, Tom22, and Tom70 in a presequence-carrying preprotein and a non-cleavable preprotein. *Journal of Biological Chemistry*, 274(23), 16522–16530. <https://doi.org/10.1074/jbc.274.23.16522>
17. Bykov, Y. S., Rapaport, D., Herrmann, J. M., & Schuldiner, M. (2020). Cytosolic Events in the Biogenesis of Mitochondrial Proteins. *Trends in Biochemical Sciences*, 45(8), 1–18. <https://doi.org/10.1016/j.tibs.2020.04.001>
18. Chacinska, A., van der Laan, M., Mehnert, C. S., Guiard, B., Mick, D. U., Hutu, D. P., Truscott, K. N., Wiedemann, N., Meisinger, C., Pfanner, N., & Rehling, P. (2010). Distinct forms of mitochondrial TOM-TIM supercomplexes define signal-dependent states of preprotein sorting. *Molecular and Cellular Biology*, 30(1), 307–318. <https://doi.org/10.1128/mcb.00749-09>
19. Chacinska, A., Lind, M., Frazier, A. E., Dudek, J., Meisinger, C., Geissler, A., Sickmann, A., Meyer, H. E., Truscott, K. N., Guiard, B., Pfanner, N., & Rehling, P. (2005). Mitochondrial presequence translocase: Switching between TOM tethering and motor recruitment involves Tim21 and Tim17. *Cell*, 120(6), 817–829. <https://doi.org/10.1016/j.cell.2005.01.011>
20. Chacinska, A., Rehling, P., Guiard, B., Frazier, A. E., Schulze-Specking, A., Pfanner, N., Voos, W., & Meisinger, C. (2003). Mitochondrial translocation contact sites: Separation of dynamic and stabilizing elements in formation of a TOM-TIM-preprotein supercomplex. *EMBO Journal*, 22(20), 5370–5381. <https://doi.org/10.1093/emboj/cdg532>
21. Glick, B. S., Wachter, C., Reid, G. a, & Schatz, C. (1993). Import of cytochrome. *Protein Science*, 2, 1901–1917. <https://doi/pdf/10.1002/pro.5560021112>
22. Cogliati, S., Enriquez, J. A., & Scorrano, L. (2016). Mitochondrial Cristae : Where Beauty Meets Functionality. *Trends in Biochemical Sciences*, 41(3), 261–273. <https://doi.org/10.1016/j.tibs.2016.01.001>
23. Colombini, M., Blachly-Dyson, E., & Forte, M. (1996). VDAC, a channel in the outer mitochondrial membrane. *Ion Channels*, 4, 169–202. [https://doi.org/10.1007/978-1-4899-1775-1\\_5](https://doi.org/10.1007/978-1-4899-1775-1_5)
24. Craig, E. A. (2018). Hsp70 at the membrane: Driving protein translocation. *BMC Biology*, 16(1), 1–11. <https://doi.org/10.1186/s12915-017-0474-3>
25. Cruciat, C. M., Brunner, S., Baumann, F., Neupert, W., & Stuart, R. A. (2000). The cytochrome bc1 and cytochrome c oxidase complexes associate to form a single supracomplex in yeast mitochondria. *Journal of Biological Chemistry*, 275(24), 18093–18098. <https://doi.org/10.1074/jbc.M001901200>
26. Dayan, D., Bandel, M., Günzel, U., Nussbaum, I., Prag, G., Mokranjac, D., Neupert, W., & Azem, A. (2019). A mutagenesis analysis of Tim50, the major receptor of the TIM23 complex, identifies regions that affect its interaction with Tim23. *Scientific Reports*, 9(1), 1–10. <https://doi.org/10.1038/s41598-018-38353-1>
27. De Paepe, B. (2012). Mitochondrial Markers for Cancer: Relevance to Diagnosis, Therapy, and Prognosis and General Understanding of Malignant Disease Mechanisms. *ISRN Pathology*, 2012, 1–15. <https://doi.org/10.5402/2012/217162>
28. Demishtein-Zohary, K., Günzel, U., Marom, M., Banerjee, R., Neupert, W., Azem, A., & Mokranjac, D. (2017). Role of Tim17 in coupling the import motor to the translocation channel of the mitochondrial presequence translocase. *ELife*, 6, 1–11. <https://doi.org/10.7554/eLife.22696>
29. Demishtein-zohary, K., Marom, M., Neupert, W., & Mokranjac, D. (2015). GxxxG motifs hold the TIM23 complex together. *FEBS Journal*, 282, 2178–2186. <https://doi.org/10.1111/febs.13266>

30. Duchen, M. R. (2000). Topical Review Mitochondria and calcium : from cell signalling to cell death. *Journal of Physiology*, 529(1), 57–68. <https://doi.org/10.1111/j.1469-7793.2000.00057.x>
31. Dudek, J., Rehling, P., & van der Laan, M. (2013). Mitochondrial protein import: Common principles and physiological networks. *Biochimica et Biophysica Acta - Molecular Cell Research*, 1833(2), 274–285. <https://doi.org/10.1016/j.bbamcr.2012.05.028>
32. Ernster, L., & Schatz, G. (1981). Mitochondria : A Historical Review. *Journal of Cell Biology*, 91(12), 227-255. <https://doi.org/10.1083/jcb.91.3.227s>
33. Esaki, M., Kanamori, T., Nishikawa, S. I., & Endo, T. (1999). Two distinct mechanisms drive protein translocation across the mitochondrial outer membrane in the late step of the cytochrome b<sub>2</sub> import pathway. *Proceedings of the National Academy of Sciences of the United States of America*, 96(21), 11770–11775. <https://doi.org/10.1073/pnas.96.21.11770>
34. Frazier, A. E., Dudek, J., Guiard, B., Voos, W., Li, Y., Lind, M., Meisinger, C., Geissler, A., Sickmann, A., Meyer, H. E., Bilanchone, V., Cumsy, M. G., Truscott, K. N., Pfanner, N., & Rehling, P. (2004). Pam16 has an essential role in the mitochondrial protein import motor. *Nature Structural and Molecular Biology*, 11(3), 226–233. <https://doi.org/10.1038/nsmb735>
35. Frey, T. G., Renken, C. W., & Perkins, G. A. (2002). Insight into mitochondrial structure and function from electron tomography. *Biochimica et Biophysica Acta - Bioenergetics*, 1555(1–3), 196–203. [https://doi.org/10.1016/S0005-2728\(02\)00278-5](https://doi.org/10.1016/S0005-2728(02)00278-5)
36. Gakh, O., Cavadini, P., & Isaya, G. (2002). Mitochondrial processing peptidases. *Biochimica et Biophysica Acta - Molecular Cell Research*, 1592(1), 63–77. [https://doi.org/10.1016/S0167-4889\(02\)00265-3](https://doi.org/10.1016/S0167-4889(02)00265-3)
37. Gao, F., & Zhang, J. (2018). Mitochondrial quality control and neurodegenerative diseases. *Neuronal Signaling*, 2(4), 1–8. <https://doi.org/10.1042/ns20180062>
38. Gasser, S. M., Ohashi, A., Daum, G., Böhni, P. C., Gibson, J., Reid, G. A., Yonetani, T., & Schatz, G. (1982). Imported mitochondrial proteins cytochrome b<sub>2</sub> and cytochrome c<sub>1</sub> are processed in two steps. *Proceedings of the National Academy of Sciences of the United States of America*, 79(2), 267–271. <https://doi.org/10.1073/pnas.79.2.267>
39. Gebert, M., Schrempp, S. G., Mehnert, C. S., Heißwolf, A. K., Oeljeklaus, S., Ieva, R., Bohnert, M., von der Malsburg, K., Wiese, S., Kleinschroth, T., Hunte, C., Meyer, H. E., Haferkamp, I., Guiard, B., Warscheid, B., Pfanner, N., & van der Laan, M. (2012). Mgr2 promotes coupling of the mitochondrial presequence translocase to partner complexes. *Journal of Cell Biology*, 197(5), 595–604. <https://doi.org/10.1083/jcb.201110047>
40. Geissler, A., Krimmer, T., Bomer, U., Guiard, B., Rassow, J., & Pfanner, N. (2000). Membrane potential-driven protein import into mitochondria: The sorting sequence of cytochrome b<sub>2</sub> modulates the  $\Delta\psi$ -dependence of translocation of the matrix-targeting sequence. *Molecular Biology of the Cell*, 11(11), 3977–3991. <https://doi.org/10.1091/mbc.11.11.3977>
41. Glynn, S. E. (2017). Multifunctional mitochondrial AAA proteases. *Frontiers in Molecular Biosciences*, 4, 1-34. <https://doi.org/10.3389/fmolb.2017.00034>
42. Gomes, F., Palma, F. R., Barros, M. H., Tsuchida, E. T., Turano, H. G., Alegria, T. G. P., Demasi, M., & Netto, L. E. S. (2017). Proteolytic cleavage by the inner membrane peptidase (IMP) complex or Oct1 peptidase controls the localization of the yeast peroxiredoxin Prx1 to distinct mitochondrial compartments. *Journal of Biological Chemistry*, 292(41), 17011–17024. <https://doi.org/10.1074/jbc.M117.788588>
43. Gray, M. W. (1989). Origin and evolution of mitochondrial DNA. *Annual Review of Cell Biology*, 5, 25–50. <https://doi.org/10.1146/annurev.cb.05.110189.000325>
44. Günzel, U., & Mokranjac, D. (2019). A journey along the TIM23 complex , the major protein translocase of the mitochondrial inner membrane. *Biologia Serbica*, 41(2), 27–35. <https://doi.org/10.5281/zenodo.3532063>

45. Guo, C. Y., Sun, L., Chen, X. P., & Zhang, D. S. (2013). Oxidative stress, mitochondrial damage and neurodegenerative diseases. *Neural Regeneration Research*, 8(21), 2003–2014. <https://doi.org/10.3969/j.issn.1673-5374.2013.21.009>
46. Gustafsson, C. M., Falkenberg, M., & Larsson, N.-G. (2016). Maintenance and Expression of Mammalian Mitochondrial DNA. *Annual Review of Biochemistry*, 85(1), 133–160. <https://doi.org/10.1146/annurev-biochem-060815-014402>
47. Iacovino, M., Granycome, C., Sembongi, H., Bokori-Brown, M., Butow, R. A., Holt, I. J., & Bateman, J. M. (2009). The conserved translocase Tim17 prevents mitochondrial DNA loss. *Human Molecular Genetics*, 18(1), 65–74. <https://doi.org/10.1093/hmg/ddn313>
48. Ieva, R., Schrempp, S. G., Opaliński, Ł., Wollweber, F., Höß, P., Heißwolf, A. K., Gebert, M., Zhang, Y., Guiard, B., Rospert, S., Becker, T., Chacinska, A., Pfanner, N., & VanderLaan, M. (2014). Mgr2 functions as lateral gatekeeper for preprotein sorting in the mitochondrial inner membrane. *Molecular Cell*, 56(5), 641–652. <https://doi.org/10.1016/j.molcel.2014.10.010>
49. Jackson, T. D., Palmer, C. S., & Stojanovski, D. (2018). Mitochondrial diseases caused by dysfunctional mitochondrial protein import. *Biochemical Society Transactions*, 46(5), 1225–1238. <https://doi.org/10.1042/BST20180239>
50. Jaussi, R. (1995). Homologous Nuclear-Encoded Mitochondrial and Cytosolic Isoproteins: A Review of Structure, Biosynthesis and Genes. *European Journal of Biochemistry*, 228(3), 551–561. <https://doi.org/10.1111/j.1432-1033.1995.tb20294.x>
51. Jensen, R. E., & Johnson, A. E. (1999). Protein translocation: Is Hsp70 pulling my chain? *Current Biology*, 9(20), 779–782. [https://doi.org/10.1016/S0960-9822\(00\)80012-3](https://doi.org/10.1016/S0960-9822(00)80012-3)
52. Johri, A., & Beal, M. F. (2012). Mitochondrial dysfunction in neurodegenerative diseases. *Journal of Pharmacology and Experimental Therapeutics*, 342(3), 619–630. <https://doi.org/10.1124/jpet.112.192138>
53. Jornayvaz, F. R., and Shulman, G. I. (2014). Regulation of mitochondrial biogenesis. *Essays Biochem*, 47, 69–84. <https://doi.org/10.1042/bse0470069>.
54. Jovaisaite, V., & Auwerx, J. (2015). The mitochondrial unfolded protein response-synchronizing genomes. *Current Opinion in Cell Biology*, 33, 74–81. <https://doi.org/10.1016/j.ceb.2014.12.003>
55. Kang, Y., Baker, M. J., Liem, M., Louber, J., McKenzie, M., Atukorala, I., Ang, C. S., Keerthikumar, S., Mathivanan, S., & Stojanovski, D. (2016). Tim29 is a novel subunit of the human TIM22 translocase and is involved in complex assembly and stability. *ELife*, 5(08), 1–23. <https://doi.org/10.7554/eLife.17463>
56. Koch, J. R., & Schmid, F. X. (2014). Mia40 targets cysteines in a hydrophobic environment to direct oxidative protein folding in the mitochondria. *Nature Communications*, 3041(5). <https://doi.org/10.1038/ncomms4041>
57. Koehler, C. M. (2000). Protein translocation pathways of the mitochondrion. *FEBS Letters*, 476(1–2), 27–31. [https://doi.org/10.1016/S0014-5793\(00\)01664-1](https://doi.org/10.1016/S0014-5793(00)01664-1)
58. Koehler, C. M., Merchant, S., & Schatz, G. (1999). How membrane proteins travel across the mitochondrial intermembrane space. *Trends in Biochemical Sciences*, 24(11), 428–432. [https://doi.org/10.1016/S0968-0004\(99\)01462-0](https://doi.org/10.1016/S0968-0004(99)01462-0)
59. Krayl, M., Lim, J. H., Martin, F., Guiard, B., & Voos, W. (2007). A Cooperative Action of the ATP-Dependent Import Motor Complex and the Inner Membrane Potential Drives Mitochondrial Preprotein Import. *Molecular and Cellular Biology*, 27(2), 411–425. <https://doi.org/10.1128/mcb.01391-06>
60. Kühlbrandt, W. (2015). Structure and function of mitochondrial membrane protein complexes. *BMC Biology*, 13(1), 1–11. <https://doi.org/10.1186/s12915-015-0201-x>

61. Kulawiak, B., Höpker, J., Gebert, M., Guiard, B., Wiedemann, N., & Gebert, N. (2013). The mitochondrial protein import machinery has multiple connections to the respiratory chain. *Biochimica et Biophysica Acta - Bioenergetics*, 1827(5), 612–626. <https://doi.org/10.1016/j.bbabi.2012.12.004>
62. Kurland, C. G., & Andersson, S. G. E. (2000). Origin and Evolution of the Mitochondrial Proteome. *Microbiology and Molecular Biology Reviews*, 64(4), 786–820. <https://doi.org/10.1128/mmbr.64.4.786-820.2000>
63. Lane, N. (2011). Energetics and genetics across the prokaryote-eukaryote divide. *Biology Direct*, 6(1), 1–35. <https://doi.org/10.1186/1745-6150-6-35>
64. Li, Y., Dudek, J., Guiard, B., Pfanner, N., Rehling, P., & Voos, W. (2004). The presequence translocase-associated protein import motor of mitochondria: Pam16 functions in an antagonistic manner to Pam18. *Journal of Biological Chemistry*, 279(36), 38047–38054. <https://doi.org/10.1074/jbc.M404319200>
65. Li, Z., Vizeacoumar, F. J., Bahr, S., Li, J., Warringer, J., Vizeacoumar, F. S., Min, R., Vandersluis, B., Bellay, J., Devit, M., Fleming, J. A., Stephens, A., Haase, J., Lin, Z. Y., Baryshnikova, A., Lu, H., Yan, Z., Jin, K., Barker, S., Boone, C. (2011). Systematic exploration of essential yeast gene function with temperature-sensitive mutants. *Nature Biotechnology*, 29(4), 361–367. <https://doi.org/10.1038/nbt.1832>
66. Lister, R., Hulett, J. M., Lithgow, T., & Whelan, J. (2005). Protein import into mitochondria: Origins and functions today. *Molecular Membrane Biology*, 22(1–2), 87–100. <https://doi.org/10.1080/09687860500041247>
67. Mackenzie, J. A., & Payne, R. M. (2007). Mitochondrial protein import and human health and disease. *Biochimica et Biophysica Acta - Molecular Basis of Disease*, 5, 509–523. <https://doi.org/10.1016/j.bbadis.2006.12.002>
68. Malhotra, K., Sathappa, M., Landin, J. S., Johnson, A. E., & Alder, N. N. (2013). Structural changes in the mitochondrial Tim23 channel are coupled to the proton-motive force. *Nature Structural and Molecular Biology*, 20(8), 965–972. <https://doi.org/10.1038/nsmb.2613>
69. Malina, C., Larsson, C., & Nielsen, J. (2018). Yeast mitochondria: An overview of mitochondrial biology and the potential of mitochondrial systems biology. *FEMS Yeast Research*, 18(5), 1–17. <https://doi.org/10.1093/femsyr/foy040>
70. Martinez-Caballero, S., Grigoriev, S. M., Herrmann, J. M., Campo, M. L., & Kinnally, K. W. (2007). Tim17p regulates the twin pore structure and voltage gating of the mitochondrial protein import complex TIM23. *Journal of Biological Chemistry*, 282(6), 3584–3593. <https://doi.org/10.1074/jbc.M607551200>
71. Martos, A., Tetaud, E., Aiyar, R. S., Sellem, C. H., Sagot, I., Gagneur, J., & De, M. (2012). Experimental Relocation of the Mitochondrial ATP9 Gene to the Nucleus Reveals Forces Underlying Mitochondrial Genome Evolution. *PLoS Genetics*, 8(8). <https://doi.org/10.1371/journal.pgen.1002876>
72. Matta, S. K., Kumar, A., & D'Silva, P. (2020). Mgr2 regulates mitochondrial preprotein import by associating with channel-forming Tim23 subunit. *Molecular Biology of the Cell*, 31(11), 1112–1123. <https://doi.org/10.1091/mbc.E19-12-0677>
73. Matta, S. K., Pareek, G., Bankapalli, K., Oblesha, A., & D'Silva, P. (2017). Role of Tim17 Transmembrane Regions in Regulating the Architecture of Presequence Translocase and Mitochondrial DNA Stability. *Molecular and Cellular Biology*, 37(6). <https://doi.org/10.1128/mcb.00491-16>
74. Mejia, E. M., & Hatch, G. M. (2016). Mitochondrial phospholipids: role in mitochondrial function. *Journal of Bioenergetics and Biomembranes*, 48(2), 99–112. <https://doi.org/10.1007/s10863-015-9601-4>
75. Mirzalieva, O., Jeon, S., Damri, K., Hartke, R., Drwesh, L., Demishtein-zohary, K., Azem, A.,

- Dunn, C. D., & Peixoto, P. M. (2019). Deletion of Mgr2p Affects the Gating Behavior of the TIM23 Complex. *Frontiers in Physiology*, 9(1), 1–5. <https://doi.org/10.3389/fphys.2018.01960>
76. Miyata, N., Tang, Z., Conti, M. A., Johnson, M. E., Douglas, C. J., Hasson, S. A., Damoiseaux, R., Chang, C. E. A., & Koehler, C. M. (2017). Adaptation of a genetic screen reveals an inhibitor for mitochondrial protein import component Tim44. *Journal of Biological Chemistry*, 292(13), 5429–5442. <https://doi.org/10.1074/jbc.M116.770131>
77. Model, K., Prinz, T., Ruiz, T., Radermacher, M., Krimmer, T., Kühlbrandt, W., Pfanner, N., & Meisinger, C. (2002). Protein translocase of the outer mitochondrial membrane: Role of import receptors in the structural organization of the TOM complex. *Journal of Molecular Biology*, 316(3), 657–666. <https://doi.org/10.1006/jmbi.2001.5365>
78. Mokranjac, D., Paschen, S. A., Kozany, C., Prokisch, H., Hoppins, S. C., Nargang, F. E., Neupert, W., & Hell, K. (2003). Tim50, a novel component of the TIM23 preprotein translocase of mitochondria. *EMBO Journal*, 22(4), 816–825. <https://doi.org/10.1093/emboj/cdg090>
79. Mokranjac, D., Popov-Čeleketić, D., Hell, K., & Neupert, W. (2005). Role of Tim21 in mitochondrial translocation contact sites. *Journal of Biological Chemistry*, 280(25), 23437–23440. <https://doi.org/10.1074/jbc.C500135200>
80. Moro, F., Okamoto, K., Donzeau, M., Neupert, W., & Brunner, M. (2002). Mitochondrial protein import: Molecular basis of the ATP-dependent interaction of MtHsp70 with Tim44. *Journal of Biological Chemistry*, 277(9), 6874–6880. <https://doi.org/10.1074/jbc.M107935200>
81. Murcha, M. W., Wang, Y., & Whelan, J. (2012). A molecular link between mitochondrial preprotein transporters and respiratory chain complexes. *Plant Signaling and Behavior*, 7(12), 1594–1597. <https://doi.org/10.4161/psb.22250>
82. Murphy, M. P., Leuenberger, D., Curran, S. P., Oppliger, W., & Koehler, C. M. (2001). The Essential Function of the Small Tim Proteins in the TIM22 Import Pathway Does Not Depend on Formation of the Soluble 70-Kilodalton Complex. *Molecular and Cellular Biology*, 21(18), 6132–6138. <https://doi.org/10.1128/mcb.21.18.6132-6138.2001>
83. Ndi, M., Marin-Buera, L., Salvatori, R., Singh, A. P., & Ott, M. (2018). Biogenesis of the bc1 Complex of the Mitochondrial Respiratory Chain. *Journal of Molecular Biology*, 430(21), 3892–3905. <https://doi.org/10.1016/j.jmb.2018.04.036>
84. Neupert, W. (1997). Protein Import Into Mitochondria. *Annual Review of Biochemistry*, 66(1), 863–917. <https://doi.org/10.1146/annurev.biochem.66.1.863>
85. Neupert, W., & Herrmann, J. M. (2007). Translocation of Proteins into Mitochondria Translocase: a membrane- embedded protein complex that mediates translocation of polypeptides from one side of the membrane to the other side. *Annual Review of Biochemistry*, 76, 723–749. <https://doi.org/10.1146/annurev.biochem.76.052705.163409>
86. Oliveira, A. N., & Hood, D. A. (2018). Effect of Tim23 knockdown in vivo on mitochondrial protein import and retrograde signaling to the UPRmt in muscle. *American Journal of Physiology - Cell Physiology*, 315(4), C516–C526. <https://doi.org/10.1152/ajpcell.00275.2017>
87. Opalińska, M., & Meisinger, C. (2014). Mitochondrial protein import under kinase surveillance. *Microbial Cell*, 1(2), 51–57. <https://doi.org/10.15698/mic2014.01.127>
88. Opaliński, Ł., Song, J., Priesnitz, C., Wenz, L. S., Oeljeklaus, S., Warscheid, B., Pfanner, N., & Becker, T. (2018). Recruitment of Cytosolic J-Proteins by TOM Receptors Promotes Mitochondrial Protein Biogenesis. *Cell Reports*, 25(8), 2036-2043.e5. <https://doi.org/10.1016/j.celrep.2018.10.083>
89. Osman, C., Voelker, D. R., & Langer, T. (2011). Making heads or tails of phospholipids in mitochondria. *Journal of Cell Biology*, 192(1). <https://doi.org/10.1083/jcb.201006159>
90. Palade, G. E. (1953). An Electron Microscope Study of The Mitochondrial Structure. *Journal of Histochemistry & Cytochemistry*, 1(22), 188–211. <https://doi.org/10.1177/1.4.188>

91. Pareek, G., Krishnamoorthy, V., & Silva, P. D. (2013). Molecular Insights Revealing Interaction of Tim23 and Channel Subunits of Presequence Translocase. *Molecular and Cellular Biology*, 33(23), 4641–4659. <https://doi.org/10.1128/MCB.00876-13>
92. Patergnani, S., Suski, J. M., Agnoletto, C., Bononi, A., Bonora, M., Marchi, E. De, Giorgi, C., Marchi, S., Missiroli, S., Poletti, F., Rimessi, A., Duszynski, J., Wieckowski, M. R., & Pinton, P. (2011). Calcium signaling around Mitochondria Associated Membranes ( MAMs ). *Cell Communication and Signalling*, 9(19)–10. <https://doi.org/10.1186/1478-811X-9-19>
93. Petrakis, N., Alcock, F., & Tokatlidis, K. (2009). Mitochondrial ATP-independent chaperones. *IUBMB Life*, 61(9), 909–914. <https://doi.org/10.1002/iub.235>
94. Pfanner, N. (2000). Protein sorting: Recognizing mitochondrial presequences. *Current Biology*, 10(11), 412–415. [https://doi.org/10.1016/S0960-9822\(00\)00507-8](https://doi.org/10.1016/S0960-9822(00)00507-8)
95. Pfanner, N., Craig, E. A., & Hönlinger, A. (1997). Mitochondrial Preprotein Translocase. *Annual Review of Cell and Developmental Biology*, 13(1), 25–51. <https://doi.org/10.1146/annurev.cellbio.13.1.25>
96. Pfanner, N., & Geissler, A. (2001). Versatility of the mitochondrial protein import machinery. *Nature Reviews Molecular Cell Biology*, 2(5), 339–349. <https://doi.org/10.1038/35073006>
97. Pfanner, N., & Meijer, M. (1997). Mitochondrial biogenesis: The Tom and Tim machine. *Current Biology*, 7(2), 100–103. [https://doi.org/10.1016/s0960-9822\(06\)00048-0](https://doi.org/10.1016/s0960-9822(06)00048-0)
98. Pfanner, N., Warscheid, B., & Wiedemann, N. (2019). Mitochondrial protein organization : from biogenesis to functional networks. *Nature Reviews Molecular Cell Biology*, 20(5), 267–284. <https://doi.org/10.1038/s41580-018-0092-0>
99. Pfanner, N., & Wiedemann, N. (2002). *Mitochondrial protein import: two membranes, three translocases* *Current Opinion in Cell Biology*, 14(4), 400–411. [https://doi.org/10.1016/S0955-0674\(02\)00355-1](https://doi.org/10.1016/S0955-0674(02)00355-1)
100. Pickles, S., Vigié, P., & Youle, R. J. (2018). Mitophagy and Quality Control Mechanisms in Mitochondrial Maintenance. *Current Biology*, 28(4), 170–185. <https://doi.org/10.1016/j.cub.2018.01.004>
101. Potting, C., Cerino, R., Pfeifer, M., Krastel, P., & Hoepfner, D. (2018). Stenomycin selectively inhibits TIM23- dependent mitochondrial protein import, *Nature Chemical Biology*, 13(12), 1239–1244. <https://doi.org/10.1038/nchembio.2493>
102. Rainbolt, T. K., Atanassova, N., Genereux, J. C., & Wiseman, R. L. (2013). Stress-regulated translational attenuation adapts mitochondrial protein import through Tim17A degradation. *Cell Metabolism*, 18(6), 908–919. <https://doi.org/10.1016/j.cmet.2013.11.006>
103. Ramesh, A., Peleh, V., Martinez-Caballero, S., Wollweber, F., Sommer, F., van der Laan, M., Schroda, M., Alexander, R. T., Campo, M. L., & Herrmann, J. M. (2016). A disulfide bond in the TIM23 complex is crucial for voltage gating and mitochondrial protein import. *Journal of Cell Biology*, 214(4), 417–431. <https://doi.org/10.1083/jcb.201602074>
104. Rampelt, H., Sucec, I., Bersch, B., Horten, P., Perschil, I., Martinou, J. C., Van Der Laan, M., Wiedemann, N., Schanda, P., & Pfanner, N. (2020). The mitochondrial carrier pathway transports non-canonical substrates with an odd number of transmembrane segments. *BMC Biology*, 18(1), 1–14. <https://doi.org/10.1186/s12915-019-0733-6>
105. Randall, K.S, Sheffield, W.P., Gordon, C.S., (1990). Mitochondrial precursor protein. *Journal of Biological Chemistry*, 265(19), 11069–11076.
106. Rao, S., Schmidt, O., Harbauer, A. B., Schönfisch, B., Guiard, B., Pfanner, N., & Meisinger, C. (2012). Biogenesis of the preprotein translocase of the outer mitochondrial membrane: Protein kinase A phosphorylates the precursor of Tom40 and impairs its import. *Molecular Biology of the Cell*, 23(9), 1618–1627. <https://doi.org/10.1091/mbc.E11-11-0933>

107. Rapaport, D. (2005). How does the TOM complex mediate insertion of precursor proteins into the mitochondrial outer membrane? *Journal of Cell Biology*, *171*(3), 419–423. <https://doi.org/10.1083/jcb.200507147>
108. Richter, F., Dennerlein, S., Nikolov, M., Jans, D. C., Naumenko, N., Aich, A., MacVicar, T., Linden, A., Jakobs, S., Urlaub, H., Langer, T., & Rehling, P. (2019). ROMO1 is a constituent of the human presequence translocase required for YME1L protease import. *Journal of Cell Biology*, *218*(2), 598–614. <https://doi.org/10.1083/jcb.201806093>
109. Rizzuto, R., De Stefani, D., Raffaello, A., & Mammucari, C. (2012). Mitochondria as sensors and regulators of calcium signalling. *Nature Reviews Molecular Cell Biology*, *13*(9), 566–578. <https://doi.org/10.1038/nrm3412>
110. Rutter, G. A., & Denton, R. M. (1988). Regulation of NAD<sup>+</sup>-linked isocitrate dehydrogenase and 2-oxoglutarate dehydrogenase by Ca<sup>2+</sup> ions within toluene-permeabilized rat heart mitochondria. Interactions with regulation by adenine nucleotides and NADH/NAD<sup>+</sup> ratios. *The Biochemical Journal*, *252*(1), 181–189. <https://doi.org/10.1042/bj2520181>
111. Saita, S., Shirane, M., & Nakayama, K. I. (2013). Selective escape of proteins from the mitochondria during mitophagy. *Nature Communications*, *4*, 1–14. <https://doi.org/10.1038/ncomms2400>
112. Sato, T. K., Kawano, S., & Endo, T. (2019). Role of the membrane potential in mitochondrial protein unfolding and import. *Scientific Reports*, *9*(1), 1–11. <https://doi.org/10.1038/s41598-019-44152-z>
113. Schendzielorz, A. B., Bragoszewski, P., Naumenko, N., Gomkale, R., Schulz, C., Guiard, B., Chacinska, A., & Rehling, P. (2018). Motor recruitment to the TIM23 channel's lateral gate restricts polypeptide release into the inner membrane. *Nature Communications*, *9*(1), 1–10. <https://doi.org/10.1038/s41467-018-06492-8>
114. Schendzielorz, A. B., Schulz, C., Lytovchenko, O., Clancy, A., Guiard, B., Ieva, R., van der Laan, M., & Rehling, P. (2017). Two distinct membrane potential-dependent steps drive mitochondrial matrix protein translocation. *Journal of Cell Biology*, *216*(1), 83–92. <https://doi.org/10.1083/jcb.201607066>
115. Schenkel, L. C., & Bakovic, M. (2014). Formation and regulation of mitochondrial membranes. *International Journal of Cell Biology*, *709*(18), 1-13. <https://doi.org/10.1155/2014/709828>
116. Schiller, D., Cheng, Y. C., Liu, Q., Walter, W., & Craig, E. A. (2008). Residues of Tim44 Involved in both Association with the Translocon of the Inner Mitochondrial Membrane and Regulation of Mitochondrial Hsp70 Tethering. *Molecular and Cellular Biology*, *28*(13), 4424–4433. <https://doi.org/10.1128/mcb.00007-08>
117. Schmidt, O., Harbauer, A. B., Rao, S., Eyrich, B., Zahedi, R. P., Stojanovski, D., Schönfisch, B., Guiard, B., Sickmann, A., Pfanner, N., & Meisinger, C. (2011). Regulation of mitochondrial protein import by cytosolic kinases. *Cell*, *144*(2), 227–239. <https://doi.org/10.1016/j.cell.2010.12.015>
118. Schmidt, O., Pfanner, N., & Meisinger, C. (2010). Mitochondrial protein import: From proteomics to functional mechanisms. *Nature Reviews Molecular Cell Biology*, *11*(9), 655–667. <https://doi.org/10.1038/nrm2959>
119. Sevrioukova, I. F. (2011). Apoptosis-inducing factor: Structure, function, and redox regulation. *Antioxidants and Redox Signaling*, *14*(12), 2545–2579. <https://doi.org/10.1089/ars.2010.3445>
120. Stan, T. (2000). Recognition of preproteins by the isolated TOM complex of mitochondria. *The EMBO Journal*, *19*(18), 4895–4902. <https://doi.org/10.1093/emboj/19.18.4895>
121. Steffen, J., & Koehler, C. M. (2014). The great escape: Mgr2 of the mitochondrial TIM23 translocon is a gatekeeper tasked with releasing membrane proteins. *Molecular Cell*, *56*(5), 613–614. <https://doi.org/10.1016/j.molcel.2014.11.022>

122. Stehling, O., & Lill, R. (2013). The role of mitochondria in cellular iron-sulfur protein biogenesis: Mechanisms, connected processes, and diseases. *Cold Spring Harbor Perspectives in Medicine*, 3(9), 1–17. <https://doi.org/10.1101/cshperspect.a011312>.
123. Stojanovski, D., Bohnert, M., Pfanner, N., Laan, M. Van Der, Schwarz, T. L., Stumpf, J. D., Saneto, R. P., William, C., Stojanovski, D., Bohnert, M., Gasparre, G., Porcelli, A. M., & Gray, M. W. (2014). Mechanisms of protein sorting in mitochondria mechanisms of protein sorting in mitochondria. *Cold Spring Harbor Perspectives in Biology*, 12(12), 1–18. <https://doi.org/10.1101/cshperspect.a011320>
124. Stojanovski, D., Guiard, B., Kozjak-Pavlovic, V., Pfanner, N., & Meisinger, C. (2007). Alternative function for the mitochondrial SAM complex in biogenesis of  $\alpha$ -helical TOM proteins. *Journal of Cell Biology*, 179(5), 881–893. <https://doi.org/10.1083/jcb.200706043>
125. Straub, S. P., Stiller, S. B., Wiedemann, N., & Pfanner, N. (2016). Dynamic organization of the mitochondrial protein import machinery. *Biological Chemistry*, 397(11), 1097–1114. <https://doi.org/10.1515/hsz-2016-0145>
126. Taylor, R. D., & Pfanner, N. (2004). The protein import and assembly machinery of the mitochondrial outer membrane. *Biochimica et Biophysica Acta - Bioenergetics*, 1658(1–2), 37–43. <https://doi.org/10.1016/j.bbabi.2004.04.017>
127. Ting, S., Schilke, B. A., Hayashi, M., & Craig, E. A. (2014). Architecture of the TIM23 Inner Mitochondrial Translocon and Interactions with the Matrix Import Motor. *Journal of Biological Chemistry*, 289(41), 28689–28696. <https://doi.org/10.1074/jbc.M114.588152>
128. Ting, S. Y., Schilke, B. A., Hayashi, M., & Craig, E. A. (2014). Architecture of the TIM23 inner mitochondrial translocon and interactions with the matrix import motor. *Journal of Biological Chemistry*, 289(41), 28689–28696. <https://doi.org/10.1074/jbc.M114.588152>
129. Tucker, K., & Park, E. (2019). Cryo-EM structure of the mitochondrial protein-import channel TOM complex at near-atomic resolution. *Nature Structural & Molecular Biology*, 26(12), 1158–1166. <https://doi.org/10.1038/s41594-019-0339-2>
130. van der Laan, M., Chacinska, A., Lind, M., Perschil, I., Sickmann, A., Meyer, H. E., Guiard, B., Meisinger, C., Pfanner, N., & Rehling, P. (2005). Pam17 Is Required for Architecture and Translocation Activity of the Mitochondrial Protein Import Motor. *Molecular and Cellular Biology*, 25(17), 7449–7458. <https://doi.org/10.1128/mcb.25.17.7449-7458.2005>
131. van der Laan, Martin, Hutu, D. P., & Rehling, P. (2010). On the mechanism of preprotein import by the mitochondrial presequence translocase. *Biochimica et Biophysica Acta - Molecular Cell Research*, 1803(6), 732–739. <https://doi.org/10.1016/j.bbamcr.2010.01.013>
132. Vander Heiden, M. G., Chandel, N. S., Li, X. X., Schumacker, P. T., Colombini, M., & Thompson, C. B. (2000). Outer mitochondrial membrane permeability can regulate coupled respiration and cell survival. *Proceedings of the National Academy of Sciences of the United States of America*, 97(9), 4666–4671. <https://doi.org/10.1073/pnas.090082297>
133. Verner, K. (1993). Co-translational protein import into mitochondria: an alternative view. *Trends in Biochemical Sciences*, 18(10), 366–371. [https://doi.org/10.1016/0968-0004\(93\)90090-A](https://doi.org/10.1016/0968-0004(93)90090-A)
134. Wagner, K., Gebert, N., Guiard, B., Brandner, K., Truscott, K. N., Wiedemann, N., Pfanner, N., & Rehling, P. (2008). The Assembly Pathway of the Mitochondrial Carrier Translocase Involves Four Preprotein Translocases. *Molecular and Cellular Biology*, 28(13), 4251–4260. <https://doi.org/10.1128/mcb.02216-07>
135. Weeber, E. J., Levy, M., Sampson, M. J., Anflous, K., Armstrong, D. L., Brown, S. E., David Sweatt, J., & Craigen, W. J. (2002). The role of mitochondrial porins and the permeability transition pore in learning and synaptic plasticity. *Journal of Biological*, 277(21), 18891–18897. <https://doi.org/10.1074/jbc.M201649200>
136. Weinhäupl, K., Lindau, C., Hessel, A., Wang, Y., Schütze, C., Jores, T., Melchionda, L., Schönfisch, B., Kalbacher, H., Bersch, B., Rapaport, D., Brennich, M., Lindorff-Larsen, K.,



- Wiedemann, N., & Schanda, P. (2018). Structural Basis of Membrane Protein Chaperoning through the Mitochondrial Intermembrane Space. *Cell*, 175(5), 1365-1379.e25. <https://doi.org/10.1016/j.cell.2018.10.039>
137. Weinhäupl, K., Wang, Y., Hessel, A., Brennich, M., Lindorff-Larsen, K., & Schanda, P. (2020). Architecture and subunit dynamics of the mitochondrial TIM9·10·12 chaperone. *BioRxiv*, 3(13). <https://doi.org/10.1101/2020.03.13.990150>
138. Wiedemann, N., & Pfanner, N. (2017). Mitochondrial Machineries for Protein Import and Assembly. *Annual Review of Biochemistry*, 86(1), 685–714. <https://doi.org/10.1146/annurev>
139. Wiedemann, N., Pfanner, N., & Chacinska, A. (2006). Chaperoning through the mitochondrial intermembrane space. *Molecular Cell*, 21(2), 145–148. <https://doi.org/10.1016/j.molcel.2006.01.001>
140. Wiedemann, N., Van Der Laan, M., Hutu, D. P., Rehling, P., & Pfanner, N. (2007). Sorting switch of mitochondrial presequence translocase involves coupling of motor module to respiratory chain. *Journal of Cell Biology*, 179(6), 1115–1122. <https://doi.org/10.1083/jcb.200709087>
141. Wrobel, L., Sokol, A. M., Chojnacka, M., & Chacinska, A. (2016). The presence of disulfide bonds reveals an evolutionarily conserved mechanism involved in mitochondrial protein translocase assembly. *Scientific Reports*, 27484(6), 1–14. <https://doi.org/10.1038/srep27484>
142. Wu, Z., Senchuk, M. M., Dues, D. J., Johnson, B. K., Cooper, J. F., Lew, L., Machiela, E., Schaar, C. E., DeJonge, H., Blackwell, T. K., & Van Raamsdonk, J. M. (2018). Mitochondrial unfolded protein response transcription factor ATFS-1 promotes longevity in a long-lived mitochondrial mutant through activation of stress response pathways. *BMC Biology*, 16(1), 1–19. <https://doi.org/10.1186/s12915-018-0615-3>
143. Wurm, C. A., & Jakobs, S. (2006). Differential protein distributions define two sub-compartments of the mitochondrial inner membrane in yeast. *Febs Letters*, 580(6), 5628–5634. <https://doi.org/10.1016/j.febslet.2006.09.012>
144. Yamano, K., Yatsukawa, Y. I., Esaki, M., Aiken Hobbs, A. E., Jensen, R. E., & Endo, T. (2008). Tom20 and Tom22 share the common signal recognition pathway in mitochondrial protein import. *Journal of Biological Chemistry*, 283(7), 3799–3807. <https://doi.org/10.1074/jbc.M708339200>
145. Yano, H., Baranov, S. V., Baranova, O. V., Kim, J., & Pan, Y. (2014). Inhibition of mitochondrial protein import by mutant huntingtin. *Nature Neuroscience*, 17(6), 822–831. <https://doi.org/10.1038/nn.3721>
146. Zeth, K. (2010a). Biochimica et Biophysica Acta Structure and evolution of mitochondrial outer membrane proteins of  $\beta$ -barrel topology. *BBA - Bioenergetics*, 1797(6–7), 1292–1299. <https://doi.org/10.1016/j.bbabi.2010.04.019>

## VIII. Acknowledgments

First of all, I would like to thank Prof. Dr. Martin Van der Laan for giving me the opportunity to work in the lab on different exiting projects. I liked working with him and I am grateful for all the inspiring discussions and the support I received.

Moreover, I would like to thank Prof. Johannes M. Herrmann for all the fruitful discussions during my Thesis Committee Meetings and for readily sharing knowledge.

In addition I would like to thank all current and past members of the Medical Biochemistry & Molecular Biology for creating a very nice work atmosphere and Center for Molecular Signaling (PZMS) for the utilizing the machines and service. I am grateful and thankful to Prof. Jean Paul di Rago for the collaborations in a project.

Furthermore, Thanks to my lab members Dr. Karina von der Malsburg, Dr. Alexander von der Malsburg, Dr. Stefan Schorr, Florian Wollweber, Amjad Aladawi, Sibylle Jungbluth, Katja Noll, Heike Haas, and Karina Parimann for being kind and helpful.

I would like to thank the IRTG1830 and Gabriele Amoroso for their support and advice during my time.

Last and most important I would like to thank my family, in-laws and Manish Kumar, my husband for their constant and unlimited support.

## **IX. Curriculum Vitae**

"The curriculum vitae was removed from the electronic version of the doctoral thesis for the reason of data protection."

"Aus datenschutzrechtlichen Gründen wird der Lebenslauf in der elektronischen Fassung der Dissertation nicht veröffentlicht."